Schizosaccharomyces pombe glucose/cAMP signaling requires the Hsp90/Git10 chaperone and the Git7 co-chaperone

Author: Manal Alaamery

Boston College Electronic Thesis or Dissertation, 2008

Boston College
The Graduate School of Arts and Sciences
Biology Department

Schizosaccharomyces pombe Glucose/cAMP Signaling Requires the Hsp90/Git10 Chaperone and the Git7 Co-chaperone

a dissertation

by

MANAL ALAAMERY

submitted in partial fulfillment of the requirements

for the degree of

Doctor of Philosophy

April 2008

ABSTRACT

Schizosaccharomyces pombe Glucose/cAMP Signaling Requires the Hsp90/Git10 Chaperone and the Git7 Co-chaperone

By Manal Alaamery

Advisor: Charles Hoffman

The fission yeast *Schizosaccharomyces pombe* senses environmental glucose through a cAMP-signaling pathway. Elevated cAMP levels activate protein kinase A (PKA) to inhibit transcription of genes involved in sexual development and gluconeogenesis, including the *fbp1*$^{+}$ gene, which encodes fructose-1,6-bisphosphatase. Glucose-mediated activation of PKA requires the function of nine *git* genes (*git*=glucose insensitive transcription), encoding adenylate cyclase, the PKA catalytic subunit and seven "upstream" proteins required for glucose-triggered adenylate cyclase activation. This thesis describes the cloning and characterization of the *git10*$^{+}$ gene, which is identical to *swo1*$^{+}$ and encodes the *S. pombe* Hsp90 chaperone protein. This discovery is consistent with the previous identification of the Git7 protein as a member of the Sgt1 Hsp90 co-chaperone family. Glucose repression of *fbp1*$^{+}$ transcription is impaired by both *hsp90*$^{-}$ *and git7*$^{-}$ mutant alleles, as well as by chemical inhibition of Hsp90 activity and temperature stress. Unlike the *swo1*$^{-}$ and *git7*$^{-}$ *ts* mutant alleles, the *git10-201* allele and *git7-93* allele support cell growth at 37º and show no cytokinesis defect, while severely reducing glucose repression of an *fbp1-lacZ* reporter, suggesting a separation-of-function

defect. A physical interaction between Git7 and Hsp90 in *S. pombe* was also detected and findings in this thesis suggest their involvement in the initial assembly of the cAMP complex.

DEDICATION

To Professor Haya Alrawaf, my mother in law, and true inspiration.

To the three most important men in my life, my father, my husband,

and my son Faris.

To the three most important women in my life, my mom, my sister

and my daughter, Aseel.

To the late Professor Shahabuddin who taught me

how science can be your soul.

ACKNOWLEDGEMENT

First I would like to thank my advisor, Professor Charles Hoffman. Charles has been my professor, mentor and like family to me. I thank him for his friendship, his patience, and for the many laughs we had. I would also like to thank him for giving me the opportunity to become a member of his lab. This gave me the chance of being around a group of excellent scientists.

Six years ago, I had little confidence that I will even make it through graduate school. Charlie kept pushing and asking the interesting questions. I kept thinking and trying to see the bigger picture. Charlie's knowledge and continuous mentoring guided me through. I was able to solve the challenges and overcome the obstacles. His humble style in teaching and guiding undoubtedly changed my way of thinking. I think I am a better scientist because of him. I could never have asked for a better mentor.

I am also very grateful to my committee members for giving me time from their busy schedules. I would like to thank Professor Junona Moroianu for being supportive from day one of my rotation in her lab. She continued her support until my last day in BC and I hope will continue it further. I also would like to thank Dr. Anne Stellwagen for her help and valuable discussions during our lab meetings; discussions that I believe were very valuable in shaping my thesis. I would also like to thank Professor Jeffrey Chuang for helping in the PDE project, and also Hideo from his lab. I would also like to thank Professors Kenneth Williams and Marc Gubbels for being generous and giving me their time to read my thesis and for being on my committee.

The Hoffman lab has been an enjoyable learning environment. I am grateful to Dr. Douglas Ivey and Dr. Lili Wang who provided me with support, training, and friendship during my early years as a graduate student. I would also like to thank Didem Demirbas,

a Hoffman lab colleague, and a great friend. Didem's continuous scientific challenges helped me develop my ideas further. She truly has all the ingredients of a great scientist. She is a true friend and I have been privileged to have her as part of my life.

I am blessed to have a wonderful group of friends who have been there for me through my joys and tough moments: Katie, Marisa, Robin, Tomasz, Arleide, Steven, Deb, Chrissy, Howard, Mikey, Ozge, Karie, Jayme, Julian, Fay, Aaron, Matt, Derek, Kevin, Maria, Maia, Guliz, Jerome, Jennifer, Chenjia, Mark, Kiebish, Melanie, Richard, Pascal, Pooja, Rajeeve, Amaal, Nasreen, Bandar, and of course Nevine. They have always been there when I needed them. Without them my PhD experience would not be special.

I have also had the good fortune of having an incredible supportive friend, Kristin. I cannot imagine my life without having her in it. She is definitely another sister to me. Knowing her was the best thing that happened to me during my PhD.

I would also like to thank Fahdah, whose friendship meant so much to me. She is a unique individual whom I have learned a great deal from. Thank you!

I would also like to thank Dr. Danielle Taghian for being an extraordinary friend, nurturing me during my difficult times. I would also like to thank Dr. Michael Piatelli for reading my first paper and telling me that it is a wonderful story. His encouragement and continuous support made me put behind the painful moments that come with research and focus instead on the bright side of things.

In addition, I would like to thank Dr. Annette Parks and Dr. Nivedita Sahoo who made significant contributions to my scientific development. Dr. Annette Parks in particular always provided thoughtful feedback and helpful suggestions in a diplomatic way. You are an awesome friend and a great teacher.

There is no way to adequately acknowledge my parents, Abdulrahman and Hessa, and my in-laws Faris and Haya, for their love, support, and patience. From them, I learned the value of hard work and understood the joy of discovering new things. In addition, I would like to thank my brothers, Motaz and Fahad, for believing in me. A special thank to my dearest sister Rania, for her endless love support, and prayers. This effort would not have been possible without her continuous encouragement.

In addition I would like to thank Anas, my love, my husband, and most importantly my best friend. His undying love, encouragement, and excitement have no boundaries. Twelve years ago, when we met, I had no expectation of what a beautiful future I would have with him. My success is all owed to him. Our life together, with our kids, our friends, our shared ambitions and dreams, is priceless.

I would also like to offer a million thanks to Anatalia Ladga who made all of this possible. Without her, there was no way I would be who I am today. In addition, I would like to thank my kids, Faris and Aseel, who had to endure late nights and lost weekends.

I am indebted to the Biology Department of Boston College. To Peter Marino for always being willing to help and for putting up with my annoying requests right up until the last minute of this thesis. Also, I would like to thank Colette for lightening up my day with her humorous comments. She always put a smile on my face before I stepped out of her office.

I thank the National Institute of Health (NIH) for funding the Hsp90 project and making this work possible. I would also like to thank the Ministry of Higher Education (MHE) in Saudi Arabia for the great scholarship that supported me during my studies.

I would also like to thank the Broad Institute of MIT and Harvard screening facility program, especially Dr. Lynn VerPlank for being helpful, giving me valuable suggestions and for making the screening process an enjoyable and unforgettable experience.

Finally, I would like to thank Dean Candace Hetzner for her kindness and support throughout my stay at BC, and for giving me the opportunity to be the doctoral students representative on the GSAS commencement. She definitely made my last days at BC memorable.

TABLE OF CONTENTS

DEDICATION ..... **I**

ACKNOWLEDGEMENT ..... **II**

TABLE OF CONTENTS ..... **VI**

THESIS LIST OF FIGURES ..... **IX**

APPENDIX ONE FIGURES ..... **X**

APPENDIX TWO FIGURES ..... **XI**

APPENDIX THREE FIGURES ..... **XI**

THESIS LIST OF TABLES ..... **XI**

CHAPTER ONE **1**

INTRODUCTION **1**

1.1. SIGNAL TRANSDUCTION 2
1.2. CYCLIC AMP PATHWAY 3
1.3. CYCLIC AMP SIGNALING IN *SCHIZOSACCHAROMYCES POMBE* 4
1.4. HSP90 FUNCTION AND SIGNALING 10
1.4. HSP90 ROLE IN EVOLUTION, CANCER, AND IMMUNITY 17
1.5. HSP90 STRUCTURE AND THE CHAPERONE CYCLE 18
1.6. HSP90 FUNCTIONS IN THE CONTEXT OF SGT1 STRUCTURE 24
1.7. FOCUS OF RESEARCH 31

CHAPTER TWO **33**

MATERIALS AND METHODS **33**

2.1. MATERIALS 34
2.1.1. Growth Medium 34
2.1.2. Yeast 34
2.1.3. Bacteria 39
2.1.4. Enzymes 39
2.2. METHODS 39
2.2.1. Strain mating and tetrad dissection 39
2.2.2. β-galactosidase assays of *fbp1-lacZ* expression 40
2.2.3. X-Gal Filter Lift 41
2.2.4. PCR walking 41
2.2.5. DNA sequencing 42
2.2.6. Cloning and Plasmid Constructions 42
2.2.7. Epitope-tagging of Hsp90 43
2.2.8. Protein extraction for Western blot analysis 43
2.2.9. Co-immunoprecipitation 43
2.2.10. Western and immunoblotting 44
2.2.11. Tandem Affinity Purification (TAP) 45
2.2.12. Spot Plating assay 46

2.2.13. Starvation-independent mating test 46
2.2.14. Glucose uptake assay 47
2.2.15. Cyclic AMP extraction 47
2.2.16. Protein extraction for cAMP 48
2.2.17. Plasmid rescue from yeast (Smash and Grab) 48
2.2.18. *Escherichia coli* transformation 48
2.2.19. Yeast transformation 49
2.2.20. Microscopy 49

CHAPTER THREE 51

CLONING AND CHARACTERIZING *GIT10*$^+$ 51

3.1. GENETIC MAPPING AND CLONING OF THE *S. POMBE GIT10*$^+$ GENE 52
3.2. HSP90 IS REQUIRED FOR NUTRIENT REGULATION OF SEXUAL DEVELOPMENT 60
3.3. GENETIC, ENVIRONMENTAL, AND CHEMICAL INSULTS TO HSP90 ACTIVITY DEREPRESS *FBP1-LACZ* EXPRESSION 65
3.4. PHENOTYPIC DIFFERENCES BETWEEN *SWO1*$^-$ AND *GIT10*$^-$ ALLELES OF *HSP90*$^+$ 70
3.5. SEQUENCE ANALYSIS OF *SWO1*$^-$ AND *GIT10*$^-$ ALLELES 80
3.6. HSP90 LOCALIZATION IN *S.POMBE* 85

CHAPTER FOUR 88

HSP90 WORKS TOGETHER WITH GIT7 IN *SCHIZOSACCHAROMYCES POMBE* 88

4.1. GIT7 INTERACTS WITH HSP90 AND REQUIRES FUNCTIONAL HSP90 89
4.1.1. Sensitivity of *git7* mutants to a specific inhibitor of Hsp90 89
4.1.2. Association of Git7 with Hsp90 in *Schizosaccharomyces pombe* 94
4.1.3. Git7 requires a functional Hsp90 to maintain cell wall integrity, normal septation and proper cAMP signaling 95
4.2. HSP90 AND GIT7 ACT IN THE ASSEMBLY OF THE CAMP SIGNALING COMPLEX 105
4.2.1. Hsp90 and Git7 are not regulated by glucose unlike other proteins of cAMP Pathway 105
4.2.2. Significant delay between inhibition of Hsp90 and defect in glucose signaling 108

CHAPTER FIVE 118

SUMMARY AND FUTURE DIRECTIONS 118

5.1. GIT10 ENCODES AN HSP90 PROTEIN INVOLVED IN THE CAMP PATHWAY 119
5.2. A NOVEL LINK BETWEEN GLUCOSE AND HEAT SENSING APPEARS TO INVOLVE HSP90 123
5.3. HSP90 AND GIT7 TRANSIENTLY INTERACT IN *S. POMBE* 127
5.4. GIT7 IS AN HSP90 CO-CHAPERONE 129
5.5. A MODEL OF THE ROLES OF HSP90 AND GIT7 FUNCTION IN THE CAMP PATHWAY 134

APPENDIX ONE 143

THE DISCOVERY OF NOVEL HUMAN PDE7A INHIBITORS USING YEAST AS A CELL-BASED SYSTEM FOR HIGH THROUGHPUT SCREENING 143

1. INTRODUCTION 144
1.1. Cyclic AMP 144
1.2. Phosphodiesterases 144
1.3. PDE7 145
1.4. PDE7A 145

1.5. Using *Schizosaccharomyces pombe* to screen for PDE inhibitors 148
1.6. Focus of research 149
2. MATERIALS AND METHODS 152
2.1. Growth Medium 152
2.2. Yeast 152
2.3. Strain mating and tetrad dissection 152
2.4. β-galactosidase assays of *fbp1-lacZ* expression 153
2.5. PDE7A sequencing 153
2.6. PCR 154
2.7. Cyclic AMP and protein extraction 154
2.8. PDE7A transformation and screen for positive integration 155
2.9. Microscopy 155
2.10. Screening process 156
2.11. Bioinformatics 156
3. RESULTS 159
3.1. Construction of strains that express human PDE7A 159
3.2. PDE7A optimization 164
3.3. Strain expressing PDE7A responds partially to IBMX but not to rolipram 172
3.4. Screening and Hits analysis 175
3.5. PDE7A specific inhibitors restore 5FOA^R growth 180
3.6. PDE 7A specific inhibitor elevate cAMP levels 187
CONCLUSION 190
4.1. Summary 190
4.2. Future directions 191

APPENDIX TWO 193

SCREENING FOR HUMAN PDE7A ACTIVATORS USING A YEAST CELL-BASED SYSTEM 193

1. INTRODUCTION 194
2. SCREENING PROCESS 194
3. RESULTS 195
3.1. Strain optimization 195
3.2. Strain Screening and Hit's 195
3.2.1. Experiment 1091.0133 Hits 199
3.2.2. Experiment 1091.0134 Hits 199
DISCUSSION 209

APPENDIX THREE 210

OPTIMIZATION OF DIFFERENT STRAINS TO BE USED FOR HIGH THROUGHPUT SCREENING 210

1. INTRODUCTION 211
2. STRAIN OPTIMIZATION 211
2.1. Strain CHP1156 optimization 211
2.2. Strain CHP1155 optimization 212
2.3. Strain CHP1132 and CHP1142 optimization 212
3. CONCLUSION 213

REFERENCES 218

THESIS LIST OF FIGURES

Figure 1. *Schizosaccharomyces pombe* cAMP signaling pathway 8
Figure 2. Comparison of the structures of human and yeast Hsp90 12
Figure 3. Hsp90 complex network 15
Figure 4. Hsp90, co-chaperones and clients act on different cellular processes 19
Figure 5. Hsp90 structure and Hsp90 ATPase cycle 22
Figure 6. Hsp90 Clamp mechanism 25
Figure 7. Schematic of Sgt1 protein structure 27
Figure 8. Two translational fusions and their associated phenotypes 37
Figure 9. Git10 cloning process 53
Figure 10. Complementation of *git10-201* mutation by plasmid-expressed *git10*$^{+}$. 56
Figure 11. Complementation of *git10-201* mutation by plasmid expressed *git10-V5* 58
Figure 12. Test if *git10*/*hsp90* can act as a high-copy suppressor of mutations in 61
other genes in the glucose-sensing cAMP pathway 61
Figure 13. Homothallic *git10-201* cells conjugate and sporulate in nutrient-rich medium 63
Figure 14. Prolonged heat stress derepresses *fbp1-lacZ* transcription 68
Figure 15. Chemical inhibition of Hsp90 derepress *fbp1-lacZ* transcription 71
Figure 16. Temperature-dependent growth of *hsp90*$^{+}$, *swo1-26, swo1-21*, and *git10-201* strains. 73
Figure 17. Temperature-dependent morphology of *hsp90*$^{+}$, *swo1-26, swo1-21*, and *git10-201* strains. 76
Figure 18. Cell morphology of *hsp90*$^{+}$, *swo1-26, swo1-21*, and *git10-201* strains at 30°C on YEA. 78
Figure 19. Alignment of Hsp90 proteins from *S. pombe*, *S. cerevisiae*, and *C. elegans* 81
Figure 20. Crystal structure of the central domain of *S. cerevisiae* Hsp82 83
Figure 21. Subcellular localization of Git10/Hsp90 86
Figure 22. Temperature-dependent growth of wt, *git7-235*, *git7-27*, *git7-93*, *swo1-26*, *swo1-21*, and
***git10-201* strains 90**
Figure 23. The *git7* mutants and *hsp90* mutants display severe drug sensitivity 92
Figure 24. Git7 and Hsp90 interact in *Schizosaccharomyces pombe* 96
Figure 25. Cells display morphological defects in Hsp90 and Git7 mutants under elevated
geldanamycin or temperature, but not in *git7-93* and *wt* strains 99

Figure 26. Cells display no morphological defects in *git2* deletion strain under elevated geldanamycin concentration 103
Figure 27. Hsp90 protein levels are not regulated by glucose; Git1 and Git2 are regulated by glucose conditions 106
Figure 28. Hsp90 inhibition affects the stability of cAMP components after 18 hours of drug addition 110
Figure 29. The abundance of Git1 and Git2 was not affected by brief exposure of GA 113
Figure 30. Cyclic AMP response to glucose in the presence of GA 116
Figure 31. Git10 in cAMP signaling pathway encodes an Hsp90 protein 120
Figure 32. Stress may redirect Hsp90 from acting in the cAMP pathway to acting upon targets that are critical to survival of heat stress. 125
Figure 33. Schematic of Git7 protein structure 131
Figure 34. Three models proposed to test the function of Hsp90 in cAMP pathway 136
Figure 35. Git7 and Git10/Hsp90 are required for the assembly of the cAMP complex 140

APPENDIX ONE FIGURES

Figure 1. Human PDE7A binding to IBMX 146
Figure 2. cAMP pathway in *S. pombe* 150
Figure 3. PDE7A screening process 157
Figure 4. Human PDE7A integration process to *S.pombe* 160
Figure 5. Human PDE7A integrants are able sporulate under starvation conditions 162
Figure 6. PDE inhibitors screening concept 165
Figure 7. Optimization conditions of strain CHP1169 168
Figure 8. Test different PDE7 genetic background 170
Figure 9. The PDE7A is partially sensitive IBMX and resistant to rolipram 173
Figure 10. PDE7A screening results 176
Figure 11. Most of PDE7A hits were identified from the commercial libraries 178
Figure 12. PDE7 specific inhibitors 181
Figure 13. PDE7A specific inhibitors restore $5FOA^R$ growth 183
Figure 14. Comparing PDE7A specific inhibitors effect in 5FOA medium 185
Figure 15. Comparing PDE7A specific inhibitors effect on cAMP levels 188

APPENDIX TWO FIGURES

Figure 1. Optimization of strain CHP1171 ..... **197**
Figure 2. Experiment 1091.0133 Hits **200**
Figure 3. Experiment 1091.0134 Hits **202**
Figure 4. Experiment 1091.0135 Hits **205**

APPENDIX THREE FIGURES

Figure 1. Strains optimizations with 1x cell density **214**
Figure 2. Strain optimizations with 2X cell density **216**

THESIS LIST OF TABLES

Table 1. Strain list **35**
Table 2. Glucose repression of *fbp1-lacZ* expression as a function of growth temperature **66**

CHAPTER ONE

INTRODUCTION

INTRODUCTION

1.1. Signal Transduction

Signal transduction allows a cell to interact with its environment and it is how the cell converts a specific external or internal signal to a chain of cellular reactions. This results in a particular action or response that is crucial to the cell's existence. The initiation of a signal often starts with an external stimulus first interacting with a receptor on the surface of the cell. This receptor can then initiate the production of a second messenger, which will subsequently amplify and transmit the signal to targets. As a result of the signaling, a negative or positive response results in these target proteins being either inhibited or activated. The signal sometimes results in an alteration in gene expression, which is ultimately responsible for different but very specific outcomes.

For instance, the binding of certain hormones to specific receptors on the surface of a cell triggers the production of cyclic AMP (cAMP) within the cell (Coppe and Steer, 1978). Cyclic AMP is a second messenger, which will initiate the internal signaling cascade. Other second messengers include cyclic GMP, $InsP_3$ and calcium (CLAPHAM 1995; COPPE and STEER 1978; DIVECHA and IRVINE 1995; PFISTER 1989). In general, these second messengers serve to amplify the external signal and bring about the final effect of the signal.

1.2. Cyclic AMP Pathway

Cyclic AMP is a small molecule that has a very important role in both prokaryotes and eukaryotes. It is synthesized from adenosine triphosphate (ATP) by an enzyme called adenylate cyclase and is degraded by another enzyme called cAMP phosphdiesterase.

The concentration of cAMP in the cell is critical for different cellular processes. The strength of the transduced signal is controlled by cAMP concentrations, which in turn is determined by a balance in the production and the degradation of cAMP. It is very important to have the right amount of cAMP at the right time in the right place; any change in this process can result in aberrant cell behavior. For example impaired cAMP signaling contributes to the pathophysiology of cardiovascular, neurological, metabolic and inflammatory disorders (CAI *et al.* 2001; MOORE and WILLOUGHBY 1995; MOVSESIAN and BRISTOW 2005). Recently, direct monitoring of rapid subcellular cAMP dynamics has been utilized to gain a better understanding of disease mechanisms (WILLOUGHBY and COOPER 2008).

A significant role of cAMP is to activate protein kinase A (PKA) which will then affect the transcription of specific genes (BEEBE 1994). Amazingly, cAMP regulation is an ancient mechanism that is highly conserved from bacteria to humans (DAS *et al.* 2007; KAMENETSKY *et al.* 2006).

However, our understanding of the diverse biological effects of cAMP regulation is still in its infancy. Uncovering how cAMP signal translates into a specific gene expression change is crucial to enable the control of defective regulation that may contribute to disease (SANDS and PALMER 2008). Since cAMP signaling is present in simpler single cell organisms, these organisms serve as convenient models for studying cAMP signaling pathways.

1.3. Cyclic AMP signaling in *Schizosaccharomyces pombe*

Glucose signaling pathways regulate gene expression in both prokaryotic and eukaryotic cells, and have been well studied in a variety of model organisms. The fission yeast *Schizosaccharomyces pombe* monitors glucose to regulate a wide range of biological processes such as sexual development and metabolism. Unlike *Saccharomyces cerevisiae*, which senses glucose through a number of signaling pathways, glucose detection in *Schizosaccharomyces pombe* is primarily through a cAMP-signaling pathway (HOFFMAN 2005a; HOFFMAN 2005b).

In *S. cerevisiae* and *S. pombe*, glucose-cAMP signaling is very similar with only a few key differences. In general, both have a G-protein receptor that activates a G-protein, which in turn activates adenylate cyclase (HOFFMAN 2005a; IVEY and HOFFMAN 2005). In *S. cerevisiae,* glucose signaling also involves Ras proteins (COLOMBO *et al.* 1998; FUKUI *et al.* 1986; MBONYI *et al.* 1988; MINTZER and FIELD 1994). In contrast, the *S.*

pombe Ras homolog plays no role in adenylate cyclase activation (FUKUI *et al.* 1986; HOFFMAN and WINSTON 1991).

Our lab has focused on the transcriptional regulation of the glucose-repressed *fbp1*$^{+}$ gene, which encodes the gluconeogenic enzyme fructose-1,6-bisphosphatase in *S. pombe* (VASSAROTTI and FRIESEN 1985). Previously, we identified mutations in genes that confer constitutive *fbp1*$^{+}$ transcription (HOFFMAN and WINSTON 1990). These *g*lucose *i*nsensitive *t*ranscription (*git*) genes encode the components of a PKA pathway (HOFFMAN 2005b), which acts antagonistically to a stress-activated MAPK (SAPK) pathway required for *fbp1*$^{+}$ transcription (STETTLER *et al.* 1996; STIEFEL *et al.* 2004).

The *S. pombe* cAMP signaling genes have been identified by using genetic screens to find mutants defective in glucose repression of transcription of the gene *fbp1* (HOFFMAN 2005b; HOFFMAN and WINSTON 1991). One of the imperative genes was identified to be *git2*$^{+}$/*cyr1*$^{+}$ which encodes adenylate cyclase (HOFFMAN and WINSTON 1991). The *S. pombe cyr1*/*git2* adenylate cyclase gene was cloned by different groups by hybridization using the *S. cerevisiae CYR1* gene. On the contrary to *S. cerevisiae*, *S. pombe* adenylate cyclase is not essential and not regulated by Ras protein (FUKUI *et al.* 1986; HOFFMAN and WINSTON 1991; MAEDA *et al.* 1990; YAMAWAKI-KATAOKA *et al.* 1989; YOUNG *et al.* 1989). The function of adenylate cyclase is to produce the second messenger cAMP from ATP to activate PKA, whose catalytic subunit is encoded by the *pka1*$^{+}$/*git6*$^{+}$ gene (JIN *et*

al. 1995; MAEDA *et al.* 1990; YU *et al.* 1994) and whose regulatory subunit is encoded by the *cgs1*$^{+}$ gene (DEVOTI *et al.* 1991).

The *git6/pka1* was cloned by its ability to suppress the dominant-negative mutation of the *S. cerevisiae RAS2* gene (YU *et al.* 1994). The loss of the catalytic activity of Pka1p mimics a starvation signal allowing the cell to conjugate and sporulate even in the presence of abundant nutrients. On the other hand, mutations in genes that elevate PKA activity inhibit cell conjugation. This led to the identification of *cgs1* which encodes the regulatory subunit of PKA and *cgs2* that encodes phosphodiesterase (DeVoti et al. 1991), as mutations in these genes suppress the lethal haploid meiosis conferred by a *pat1*$^{-}$ mutation.

Seven additional *git* genes are required for adenylate cyclase activation and form at least two functionally distinct groups. Four genes encode the Git3 G protein-coupled receptor (WELTON and HOFFMAN 2000) and its cognate heterotrimeric G protein composed of the Gpa2 Gα (ISSHIKI *et al.* 1992; NOCERO *et al.* 1994), the Git5 Gβ (LANDRY *et al.* 2000), and the Git11 Gγ (LANDRY and HOFFMAN 2001). Overexpression of Gpa2 suppresses the defect in *fbp1* transcriptional repression caused by *git3* or *git5* mutations. These findings suggest that Gpa2 functions downstream from Git3 and Git5 (LANDRY *et al.* 2000) (Figure1). In addition, using a two-hybrid assay we found that Git3 interacts with Gpa2 and this interaction was facilitated by the Git5 Gβ (D.A. Kelly and C.S. Hoffman,

unpublished results (HOFFMAN 2005b). The Git3 GPCR and Git5-Git11 Gβγ dimer are required for Gpa2 Gα activation, and can be bypassed by mutations that activate Gpa2 (WELTON and HOFFMAN 2000), which directly binds and activates adenylate cyclase (IVEY and HOFFMAN 2005).

Interestingly, unlike the other *git genes*, mutations in *git7*, *git10*, and *git1* cannot be suppressed by an activated allele of *gpa2* (WELTON and HOFFMAN 2000). Therefore, they either function independently from Gpa2 to activate adenylate cyclase or are required for Gpa2-mediated activation of adenylate cyclase by stabilizing or assembling a functional complex (Figure1). Git1 contains a C2 domain, which in some proteins binds phospholipids, and two munc domains (MHD1 and MHD2) that might also bind phospholipids (KOCH *et al.* 2000). Genetics and biochemical studies indicate that *git1* is required for the activation of adenylate cyclase (BYRNE and HOFFMAN 1993). In addition co-immunoprecipitation experiments have detected physical interactions between Git1 and Git2/ adenylate cyclase (KAO *et al.* 2006).

Figure 1. *Schizosaccharomyces pombe* cAMP signaling pathway

The Git3 protein detects glucose and transfers the signal to the heterotrimeric G proteins, which will in turn activate Git2 adenylate cyclase, which will produce cAMP. Three other proteins Git7, Git10, and the Git1 are also required for the activation of Git2. Elevation of cAMP levels results in activation of PKA. This action will affect the transcription of specific genes like *fbp1* in *Schizosaccharomyces pombe.*

Figure 1.

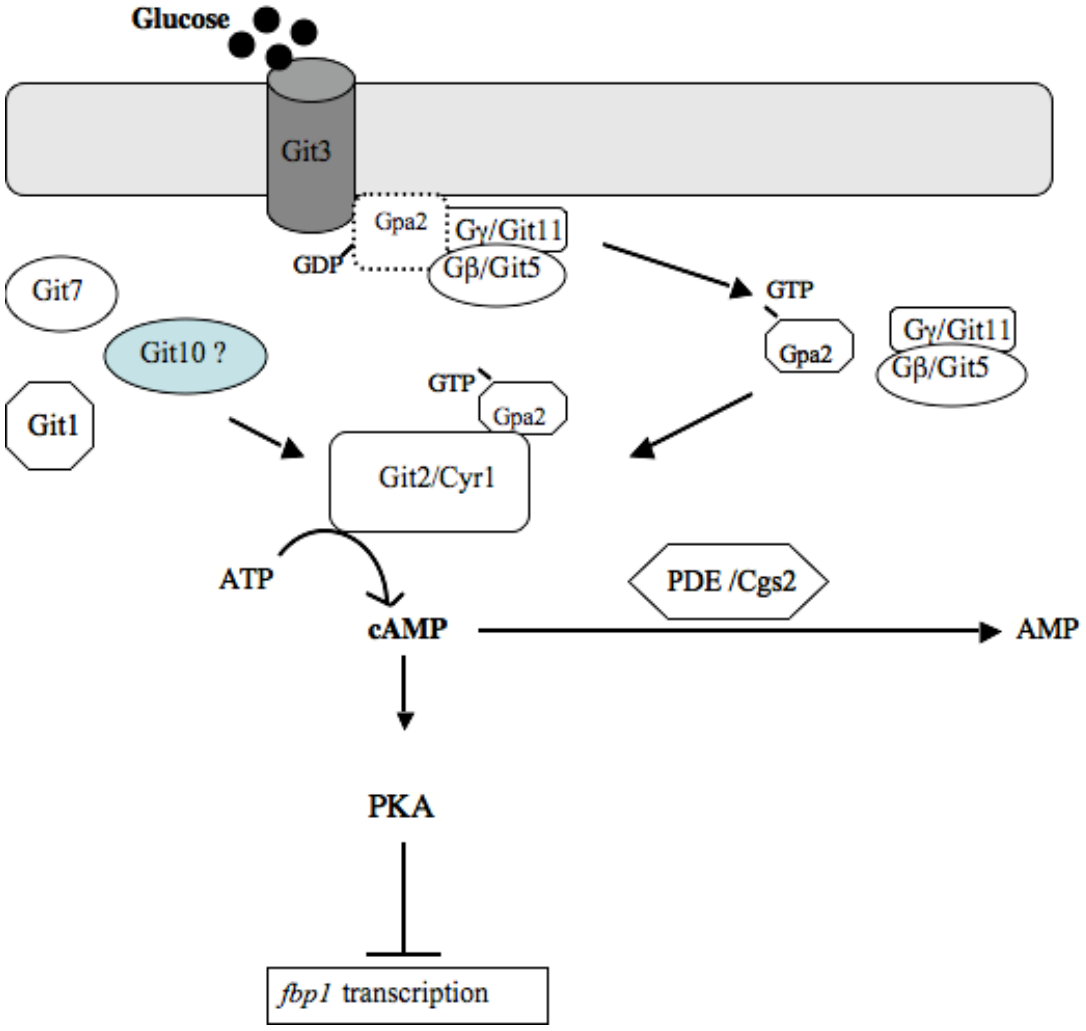
Glucose
Git3
Gpa2
Gγ/Git11
GDP
Gβ/Git5
Git7
Git10 ?
Git1
GTP
Gpa2
Gγ/Git11
Gβ/Git5
GTP
Gpa2
Git2/Cyr1
ATP
cAMP
PDE /Cgs2
AMP
PKA
fbp1 transcription

Git7 is a member of the Sgt1 protein family, whose *Saccharomyces cerevisiae* ortholog SGT1 was originally identified as a multicopy suppressor of *skp1* mutation. SGT1 has been implicated in adenylate cyclase function (DUBACQ *et al.* 2002). It is also essential and appeared to be important for septation and maintaining cell wall integrity (DUBACQ *et al.* 2002; SCHADICK *et al.* 2002) and kinetochore assembly (KITAGAWA *et al.* 1999).

The goal of this thesis project was to identify and characterize *git10*, the one remaining *git* gene that plays an important role in *fbp1* repression. Through a mapping approach, I discovered that *git10* encodes Hsp90, a heat shock protein that is a member of the 90 kD protein family found in many eukaryotes, including the budding yeast *S. cerevisiae*, plants, and mammals (BARDWELL and CRAIG 1987; LINDQUIST and CRAIG 1988b; SPENCE and GEORGOPOULOS 1989). The *git10/hsp90* gene was previously identified as *swo1*, a gene that when mutated suppresses the mitotic effect of overexpression of *wee1* kinase, which negatively regulates mitotic entry (ALIGUE *et al.* 1994).

1.4. Hsp90 function and signaling

Hsp90 is one of the most abundant cellular proteins under normal conditions and is highly expressed in response to different kinds of stress including heat, osmotic stress (SATHIYAA *et al.* 2001; SPEES *et al.* 2002), and toxic stresses (SNYDER *et al.* 2001; WIEGANT *et al.* 1998). Hsp90 is an essential molecular chaperone, a molecule which is greatly conserved from bacteria to mammals (BARDWELL and CRAIG 1987; LINDQUIST

and CRAIG 1988a; SPENCE and GEORGOPOULOS 1989). The high sequence homology and conserved structure of Hsp90 suggest that its function might also be preserved across species. Using the molecular biology toolkit (MBT), a protein workshop software (MORELAND *et al.* 2005) I was able to show how remarkably closely the structure of human and *Saccharomyces cerevisiae* Hsp90 resemble each other due to high Hsp90 conservation (Figure 2).

Another Hsp90 isoform that has been reported is Hsp90N, which is involved in the cellular transformation process (GRAMMATIKAKIS *et al.* 2002). In addition Hsp90 paralogs includes Grp94, a glucose regulated protein and the mitochondrial Trap1/Hsp75 (CSERMELY *et al.* 1998; NEMOTO *et al.* 1996). In *S. cerevisiae* there are two isoforms Hsp82, a heat shock induced chaperone, and Hsc82 a constitutively expressed protein (ALIGUE *et al.* 1994; BORKOVICH *et al.* 1989). Both in *S. cerevisiae* and in *S. pombe*, Hsp90 is essential for cell viability.

Hsp90's function is highly complex. To understand this complexity, several groups have tried to uncover the Hsp90 network in yeast and mammalian systems using proteomic and genomic approaches (FALSONE *et al.* 2005; ZHAO *et al.* 2005).

Figure 2. Comparison of the structures of human and yeast Hsp90

Comparison of the structures of human and yeast Hsp90 to show how closely they resemble each other due to high Hsp90 conservation. **(A)** The N-terminal domain of human Hsp90 (1yet) binding to Geldanamycin (GA). **(B)** The N-terminal domain of *Saccharomyces cerevisiae* Hsp90 (1a4h) binding to Geldanamycin (GA). Images were created using MBT protein workshop (MORELAND *et al.* 2005) available on protein data bank (PDB) website. Human crystal structure data was obtained from (STEBBINS *et al.* 1997) and yeast structural data from (PRODROMOU *et al.* 1997).

Figure 2.

A.

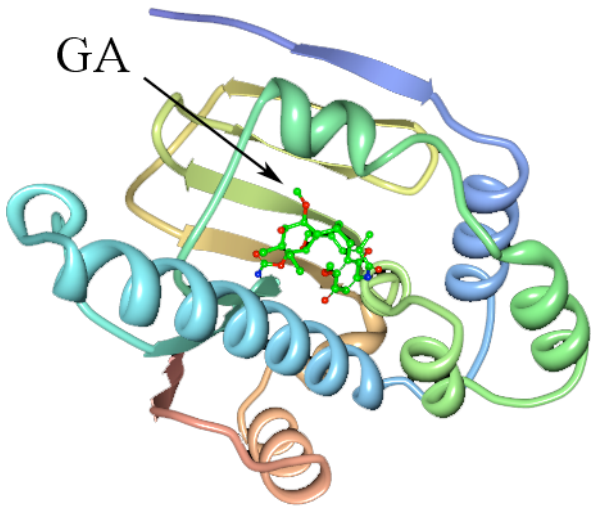

B.

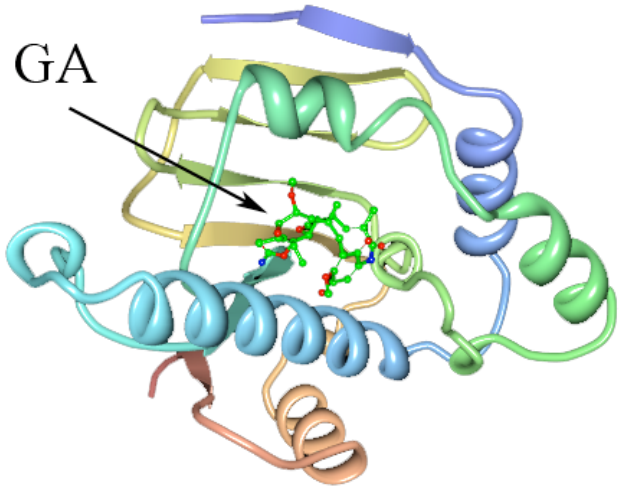

It is an unusual chaperone in that most of its identified substrates are signal transduction proteins (PEARL and PRODROMOU 2000; POWERS and WORKMAN 2006; ZHANG and BURROWS 2004). The Hsp90 protein networks suggest that Hsp90 plays a central role affecting multiple pathways and cellular processes, such as signaling of steroid hormone receptors and protein kinases (NOLLEN and MORIMOTO 2002; RICHTER and BUCHNER 2001), membrane trafficking (BIJLMAKERS and MARSH 2000; FAN *et al.* 2006; SAKISAKA *et al.* 2002) and the cytoskeletal network (PAI *et al.* 2001); (KORCSMAROS *et al.* 2007) (Figure 3). Therefore, the number of client proteins identified for Hsp90 has been increasing gradually.

Hsp90 regulates cellular functions in different ways. Hsp90 can help in folding newly synthesized proteins and also facilitate the maturation of many proteins to a stable confirmation (CSERMELY *et al.* 2007; KORCSMAROS *et al.* 2007; MILLSON *et al.* 2005; ZHAO *et al.* 2005; ZHAO and HOURY 2007). In addition, Hsp90 function in complex with various co-chaperones that regulate its function. The different co-chaperones can direct Hsp90 to different sets of substrates/targets (ZHAO and HOURY 2005). Therefore, Hsp90 is a crucial element for a target protein to function in different signaling pathways. However, the structural flexibility that is needed for these substrates to carry out diverse cellular functions may render them less stable and make them more susceptible to damage if Hsp90 was compromised (YOUNG *et al.* 2001).

Figure 3. Hsp90 complex network

Hsp90 is involved with protein-protein interactions, the cytoskeletal network, and membrane trafficking (KORCSMAROS *et al.* 2007). Signaling through Hsp90 links these pathways to each other. See Picard list http://www.picard.ch/downloads/Hsp90interactors.pdf.

Figure 3.

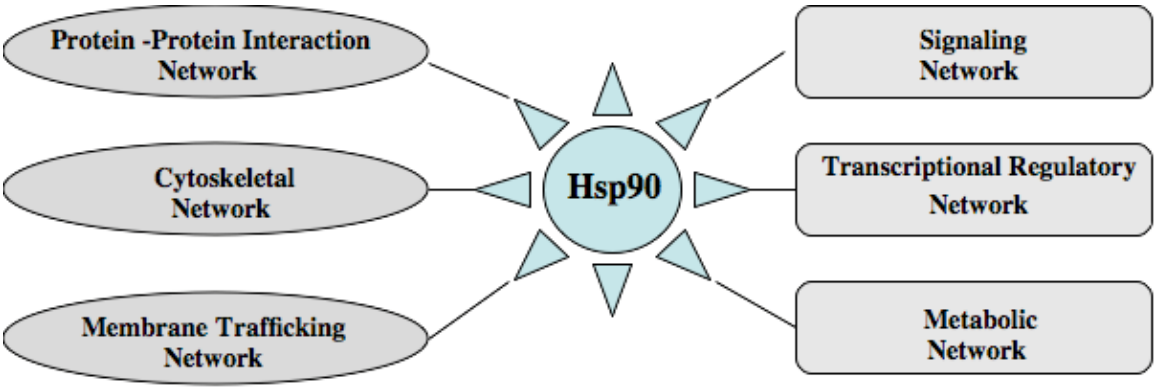
Protein -Protein Interaction Network
Cytoskeletal Network
Membrane Trafficking Network
Hsp90
Signaling Network
Transcriptional Regulatory Network
Metabolic Network

As a result, a compromised Hsp90 will result in the destabilization of client proteins and induce their degradation.

1.4. Hsp90 role in evolution, cancer, and immunity

In fruit fly and in plants Hsp90 demonstrates an important role in evolution by masking mutations. It acts as a buffering device to maintain the wild type phenotype. The Hsp90 impaired by either mutations or by pharmacological inhibitors led to developmental abnormalities. The Lindquist lab established that these developmental abnormalities phenotypes were due to reduced Hsp90 function. They also showed that elevated temperature could produce Hsp90-dependent phenotypes. The reason for that remarkable effect may be that Hsp90 has a crucial role in stabilizing proteins that are involved in a intricate signaling pathway (MITCHELL-OLDS and KNIGHT 2002; RUTHERFORD 2003; RUTHERFORD and LINDQUIST 1998).

On the other hand, Hsp90 inhibition is sometimes beneficial. Recent research has revealed a distinctive medically important role of Hsp90 in cancer (CHIOSIS G *et al.* 2004; GOETZ *et al.* 2003; MALONEY A and P. 2002). Hsp90 is overexpressed in cancer cells and required for the stability and function of signaling proteins that promote cancer cell growth (ISAACS *et al.* 2003; NATHAN and LINDQUIST. 1995; NECKERS 2007; PRATT and TOFT. 1997; WHITESELL and LINDQUIST 2005). In a murine model system, Hsp90 was concentrated in tumor tissue while being unaltered in other tissues (BANERJI *et al.*

2005; EISEMAN *et al.* 2005; NECKERS 2007; VILENCHIK *et al.* 2004; XU *et al.* 2003). Therefore, Hsp90 is a potential anticancer drug target. For example, geldanamycin is a specific Hsp90 inhibitor that blocks the ATP binding site of Hsp90, thus impairing its chaperone activity, which will limit a variety of cell signaling pathways and cell growth (OBERMANN *et al.* 1998; SCHNEIDER *et al.* 1996).

Hsp90 also plays a central role in innate immunity in higher eukaryotes. In plants, it has been shown that Hsp90, SGT1, and RAR1 together regulate the stability of R proteins, a family of proteins that is important in disease resistance (AZEVEDO *et al.* 2002; BOTER *et al.* 2007; LIU *et al.* 2004; TAKAHASHI *et al.* 2003; THAO *et al.* 2007). Recently, it has also been shown that Hsp90 plays an important role in the immune response in mammalians. This process involves an Hsp90 co-chaperone Sgt1, together they activate the immune response by inducing the Nod-like receptor proteins (NLR) to form an inflammasome complex (MAYOR *et al.* 2007). Since the immune response networks in plants and mammals share some general components, Hsp90-Sgt1 signaling might be a conserved mechanism that regulates the immune response and ensures disease resistance (Figure 4).

1.5. Hsp90 structure and the Chaperone Cycle

Hsp90 possesses three domains: an N-terminal ATP-binding domain, a central regulatory domain involved in client protein-binding, and a C-terminal dimerization domain (Figure 5A) (PEARL and PRODROMOU 2006).

Figure 4. Hsp90, co-chaperones and clients act on different cellular processes

Hsp90 and its co-chaperones act on a wide range of client proteins kinases, transcription factors, and others to control different cellular processes (JACKSON *et al.* 2004; KORCSMAROS *et al.* 2007).

Figure 4.

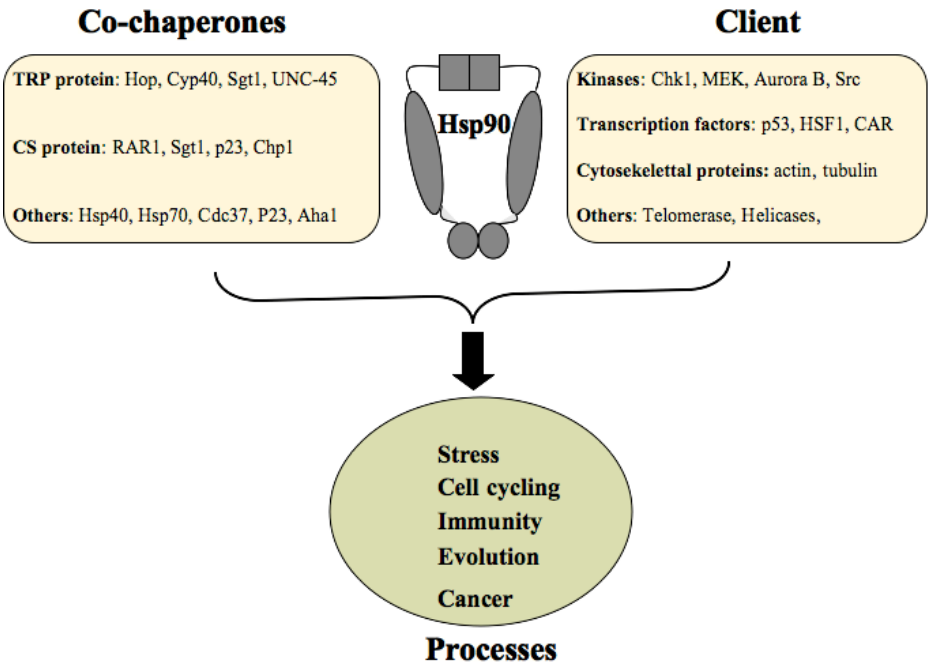
Co-chaperones
TRP protein: Hop, Cyp40, Sgt1, UNC-45
CS protein: RAR1, Sgt1, p23, Chp1
Others: Hsp40, Hsp70, Cdc37, P23, Aha1
Hsp90
Client
Kinases: Chk1, MEK, Aurora B, Src
Transcription factors: p53, HSF1, CAR
Cytosekelettal proteins: actin, tubulin
Others: Telomerase, Helicases,
Stress
Cell cycling
Immunity
Evolution
Cancer
Processes

Emerging evidence suggests the importance of the middle domain of Hsp90 and sheds light on its role in the activation of the N-terminal ATP-binding domain. In *S. cerevisiae*, it has been shown that Hsp90 middle domain interacts with Aha1, a co-chaperone that stimulates ATP hydrolysis and enhances the efficiency of its client protein activity either indirectly or directly (FONTANA J *et al.* 2002; MEYER *et al.* 2003; SATO *et al.* 2000). A recent report showed that the middle domain could also play a role in discriminating between different types of client proteins (HAWLE *et al.* 2006).

The N-terminus had been identified by structural studies and biochemical studies to be the ATP binding site of Hsp90 and can be also blocked by Geldanamycin (GA), a specific Hsp90 inhibitor (BUCHNER 1999; STEBBINS *et al.* 1997). On the other hand, the C-terminus of Hsp90 also has an important role since truncations of this region resulted in unviable yeast cells (LOUVION *et al.* 1996; MINAMI *et al.* 1994) and also abolished ATP hydrolysis (PRODROMOU *et al.* 2000). These results imply that the N-terminal domain of Hsp90, which is important for ATP hydrolysis (RICHTER *et al.* 2002), is enhanced by the C-terminal dimerization (TERASAWA *et al.* 2005). Conformational changes of Hsp90 when bound to ADP or ATP is important to the function of the chaperone cycle which includes the transition process between the open and the closed structure (Figure 5B) (CSERMELY *et al.* 1993; GRENERT *et al.* 1997; SULLIVAN *et al.* 1997).

Figure 5. Hsp90 structure and Hsp90 ATPase cycle

(A) Hsp90 contains three domains: (N) the N-terminal (ATP) binding domain, (M) the middle or -protein binding domain, (C) the C-terminus or dimerization domain.

(B) The inactive form of Hsp90 is the open/relaxed structure. ATP binding activates Hsp90 and induces conformational changes, creating a closed structure. Adapted from (PRODROMOU *et al*. 2000; TERASAWA *et al.* 2005)

Figure 5.

A.

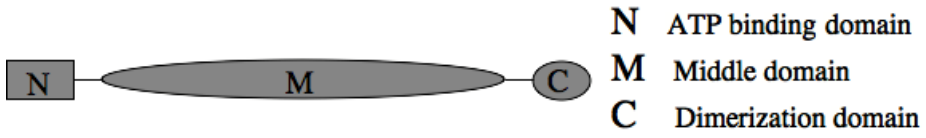
N
M
C
N ATP binding domain
M Middle domain
C Dimerization domain

B.

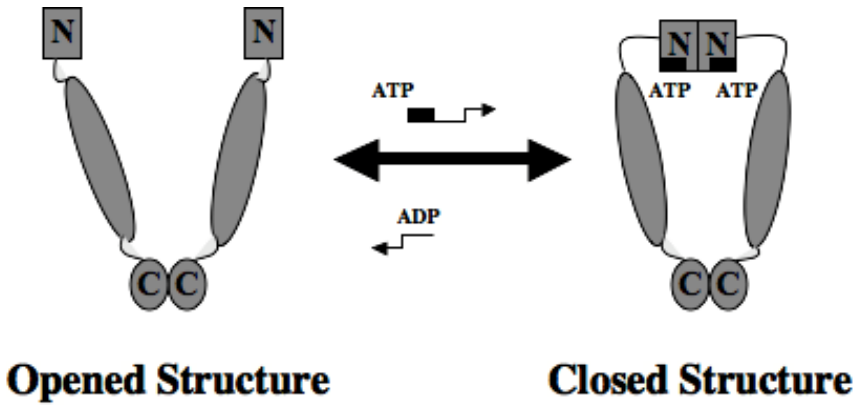
N
N
C C
ATP
ADP
N N
ATP ATP
C C
Opened Structure
Closed Structure

The ADP-bound Hsp90 form, which is the open structure, is capable of capturing the client proteins (Figure 6A). ATP binding will induce conformation changes, resulting in a closed state (Figure 6B) that will result in client protein encapsulation (RICHTER and BUCHNER 2006). There is also evidence that a wide range of co-chaperones play an important role in the loading (Figure 6A) and releasing (Figure 6C) mechanisms of Hsp90 in a client-specific manner (BUCHNER 1999; KELLERMAYER and CSERMELY 1995; PEARL and PRODROMOU 2006).

Natural inhibitors, geldanamycin produced from *Streptomyces hygroscopicus* (DEBOER *et al.* 1970) and the antifungal antibitotic radicicol produced by *Humicola fuscoatra* (SOGA *et al.* 2003) bind to the ATP conserved pocket resulting in compromised ATPase activity (PRODROMOU *et al.* 1997; SCHULTE *et al.* 1999; STEBBINS *et al.* 1997). Blocking the ATP site locks Hsp90 in the ADP confirmation thereby inducing client degradation (Figure 6D).

1.6. Hsp90 functions in the context of Sgt1 structure

Sgt1 is found in humans (LEE *et al.* 2004; STEENSGAARD *et al.* 2004), *Arabidopsis thaliana* (AZEVEDO *et al.* 2002), *Saccharomyces cerevisiae* (KITAGAWA *et al.* 1999), and recently in *S. pombe,* designated *git7* (SCHADICK et al. 2002). Sgt1p contains three important domains (Figure 7).

Figure 6. Hsp90 Clamp mechanism

(A) Hsp90 in the open state can capture the client protein. **(B)** ATP binding induces Hsp90 conformational changes resulting in the closed state. The closed structure facilitates client activation and/or assembly with another protein. **(C)** Some co-chaperones will accelerate the ATPase reaction, which results in client disassociations. **(D)** Geldanamycin (GA) blocks the ATP binding site, which will result in client destabilization and degradation (BAGATELL and WHITESELL 2004; MEYER *et al.* 2003; PEARL and PRODROMOU 2006; RICHTER and BUCHNER 2006).

Figure 6.

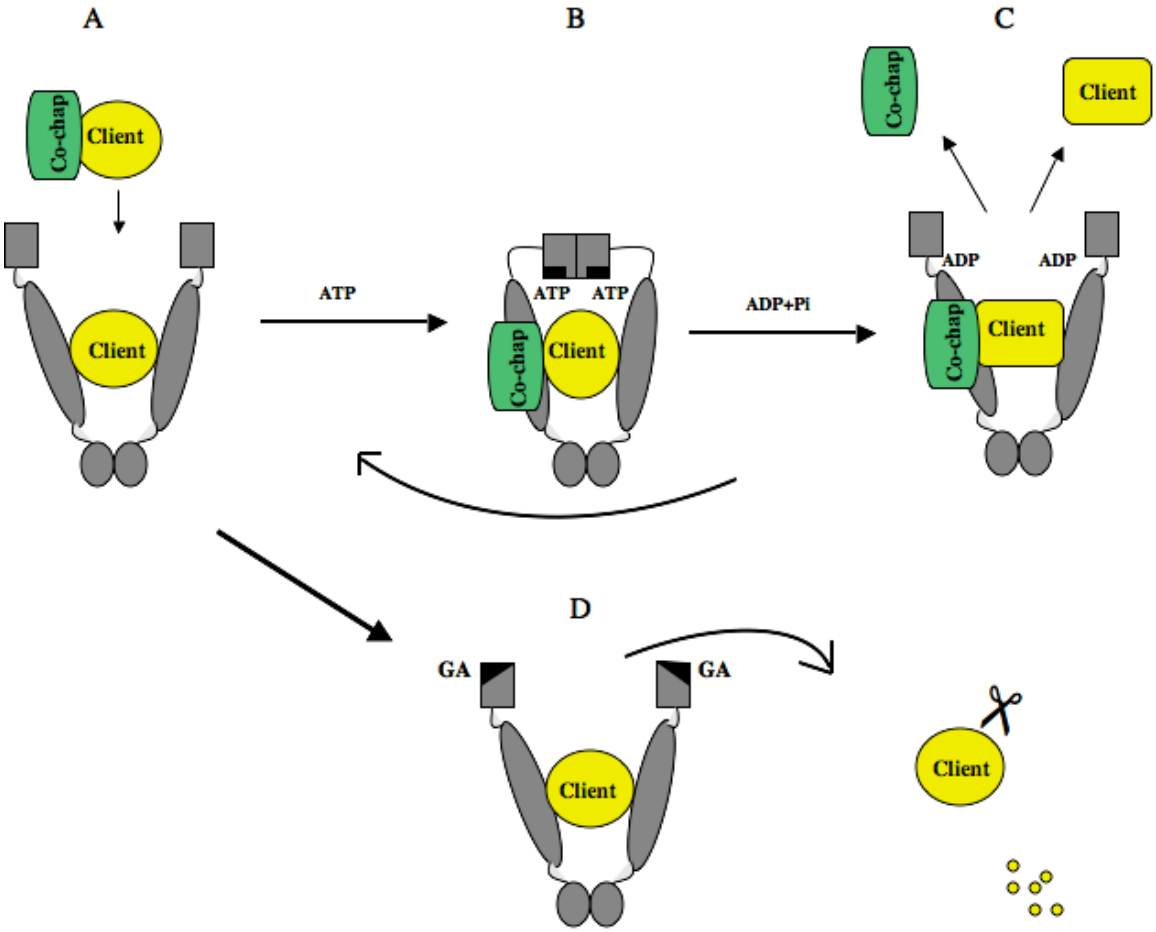
A
B
C
Co-chap
Client
Client
ATP
ATP
ATP
Co-chap
Client
ADP+Pi
Co-chap
Client
ADP
ADP
Co-chap
Client
D
GA
GA
Client
Client

Figure 7. Schematic of Sgt1 protein structure

Schematic of Sgt1 protein structure showing the three domains: TRP, CS, and SGS and the binding site of Hsp90. In addition it shows some phenotypes associated with Sgt1 mutants in humans (LEE *et al*. 2004) and *Saccharomyces cerevisiae* (BANSAL *et al.* 2004; DUBACQ *et al*. 2002) compared to its ortholog Git7 in *Schizosaccharomyces pombe (*SCHADICK et al. 2002). Geldanamycin is a drug that inhibits Hsp90 function. TRP: tetratricopeptide repeat domain. CS: CHORD domain. SGS: Sgt1 specific domain.

Figure 7.

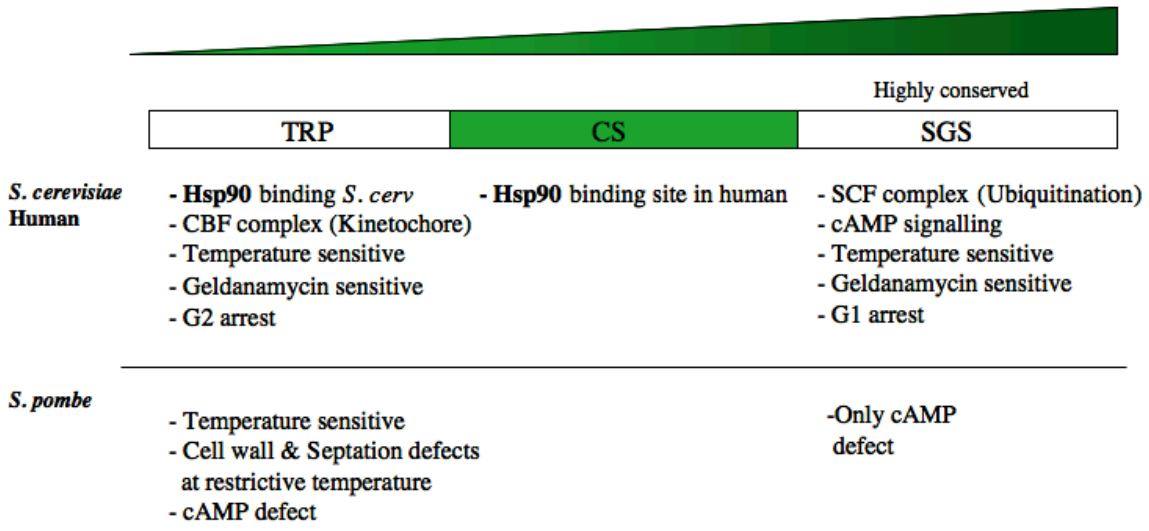
Highly conserved
TRP
CS
SGS
S. cerevisiae
Human
- Hsp90 binding S. cerv
- CBF complex (Kinetochore)
- Temperature sensitive
- Geldanamycin sensitive
- G2 arrest
- Hsp90 binding site in human
- SCF complex (Ubiquitination)
- cAMP signalling
- Temperature sensitive
- Geldanamycin sensitive
- G1 arrest
S. pombe
- Temperature sensitive
- Cell wall & Septation defects at restrictive temperature
- cAMP defect
-Only cAMP defect

The N-terminus contains a tetratricopeptide repeat domain (TRP) (LAMB *et al.* 1995) which is conserved from humans to yeast (KORDES *et al.* 1998). Proteins that contain the TRP motif were found to be involved in protein folding, protein–protein interactions, and cell cycle and transcription regulation (BLATCH and LASSLE 1999).

Mutations in this domain alter normal cellular processes due to disruption of protein interactions. This domain was found to interact transiently with Hsp90 in *S. cerevisiae* and *A. thaliana* (BANSAL *et al.* 2004; TAKAHASHI *et al.* 2003) an interaction that is essential for the formation of the Centromere Binding Factor 3 (CBF3), and the kinetochore complex (LINGELBACH and KAPLAN 2004).

Sgt1 works as a linker to connect Hsp90 to Skp1 which results in CBF3 complex formation by activating Ctf13. Therefore Sgt1 may function as a co-chaperone that recruits specific clients to Hsp90 (CATLETT and KAPLAN 2006). In plants the Hsp90 interaction with the TRP domain of Sgt1 was found to be important in disease resistance (TAKAHASHI *et al.* 2003). In *S. pombe*, *git7-27* and the *git7-235* alleles, which contain single missense mutations in the region encoding the amino terminus of Git7 demonstrates defective phenotype in cAMP signaling, cell wall integrity and septation (SCHADICK *et al.* 2002).

The middle domain of Sgt1, referred to as the CHORD (CS) domain, is also conserved among species. Proteins that contain this region were found to interact with Hsp90 (AZEVEDO *et al.* 2002; DUBACQ *et al.* 2002). In contrast to *S. cerevisiae*, human Sgt1 binds Hsp90 through the CS domain (LEE *et al.* 2004). Structural analysis using NMR and mutational analyses of the CS domain of Sgt1 in *Arabidopsis thaliana* showed that the CHORD II domain of RAR1 and the N-terminus domain of HSP90 interact with opposite faces of the CS domain of Sgt1. The Sgt1 function in Rx resistance is specifically dependent on its interaction with Hsp90, demonstrating that the role of Sgt1 may be to recruit chaperone activity to multi protein complexes (BOTER *et al.* 2007).

The C-terminus of Sgt1 contains the SGS domain, which stands for Sgt1 specific domain. This domain is the most evolutionarily conserved region within the protein across different species; therefore it might carry a conserved function (AZEVEDO *et al.* 2002). Mutations in this region showed defects in SCF (Skp1p/Cdc53p–Cullin–F-box) machinery and the cAMP pathway. These mutants were also sensitive to geldanamycin, which indicates Hsp90 involvement in these processes. For example in *S. cerevisiae,* the *sgt1-5* allele, which is a mutation in the C-terminus was defective in SCF ubiquitination, in adenylate cyclase activity and was sensitive to geldanamycin (BANSAL *et al.* 2004; KITAGAWA *et al.* 1999).

In *S. cerevisiae* Sgt1 physically interacts with the yeast adenylate cyclase Cyr1p/Cdc35p (DUBACQ *et al.* 2002). However, Sgt1 involvement in cAMP signaling was observed but SGT1/Git7 and Cyr1/Git2 interactions were not found in *S. pombe* (Wang, unpublished data). Interestingly cells expressing *git7-93,* which has duplication in the C-terminal coding region, display a defect in cAMP pathway and not in any other functions associated with other *git7* mutant alleles. Thus, this region is specifically involved in cAMP pathway (SCHADICK *et al.* 2002).

1.7. Focus of research

Prior to this study, genes that were responsible for mutants defective in glucose repression of *fbp1* transcription were all cloned with the exception of *git10*. The initial aim is to clone and characterize the *git10* gene. I will describe here the cloning process and provide evidence that it encodes a heat shock protein Hsp90 that plays an important role in cAMP pathway (ALAAMERY and HOFFMAN 2008).

I have determined for the first time that the induction of *fbp1* transcription during heat stress acts through Hsp90, suggesting a novel link between temperature sensing and nutrient sensing through a PKA pathway in *S. pombe*.

Before this study, Git7 a member of the Sgt1 protein family had been shown to be important for septation, cell wall integrity and proper cAMP signaling in *S. pombe*

(SCHADICK et al. 2002). I demonstrated that Git7's function in maintaining cell wall integrity requires functional Hsp90. Furthermore; I showed that Swo1/Hsp90 and Git7 proteins interact suggesting their presence in the same complex. These findings establish a connection between Hsp90 and Git7 that have never been previously revealed in *S. pombe.* In other systems, the interaction between Git7 and Hsp90 is important in the transient assembly of protein complexes.

Finally, I analyzed the effect of compromising Hsp90 on key players of the cAMP pathway. This analysis indicates that Hsp90 is involved in assembling the cAMP-signaling complex.

CHAPTER TWO

MATERIALS AND METHODS

MATERIALS AND METHODS

2.1. MATERIALS

2.1.1. Growth Medium

Yeast was grown and maintained using several types of media. Yeast extract agar (YEA) and yeast extract liquid (YEL) are the standard media supplemented with 0.2% casamino acids (GUTZ *et al.* 1974). Defined medium EMM (MP Biochemicals) was supplemented with required nutrients at 75 mg/L, except for L-leucine, which was at 150 mg/L. Sensitivity to 5-fluoro-orotic acid (5FOA) was determined on SC solid medium containing 0.4 g/L 5-fluoro-orotic acid 5FOA and 8% glucose as previously described (HOFFMAN and WINSTON 1990). LB medium (1% tryptone, 0.5% yeast extract, 1% NaCl) was used to grow *E. coli*.

2.1.2. Yeast

Table 1 lists the yeast strains used in this study. Most of the strains in this thesis carried the *fbp1::ura4*$^{+}$ and *ura4::fbp1-lacZ* reporters (Figure 8). Both are translational fusions integrated at the *fbp1*$^{+}$ and *ura4*$^{+}$ loci, respectively, as described by Hoffman and Winston (HOFFMAN and WINSTON 1990). Strains were grown at 30°C unless otherwise indicated.

Table 1. Strain list

Strain	Genotype
FWP17	*mat2-102 ura4-294 lys1-131*
FWP72	h^- *fbp1::ura4*$^+$ *ura4::fbp1-lacZ leu1-32*
FWP87	h^+ *fbp1::ura4*$^+$ *ura4::fbp1-lacZ leu1-32*
CHP27	h^+ *fbp1::ura4*$^+$ *ura4::fbp1-lacZ leu1-32 ade6-M210 his7-366 git7-27*
CHP465	h^- *fbp1::ura4*$^+$ *ura4::fbp1-lacZ leu1-32 ade6-M210 git7-235*
CHP567	h^+ *fbp1::ura4*$^+$ *ura4::fbp1-lacZ leu1-32 ade6-M210 git10-201*
CHP573	h^- *fbp1::ura4*$^+$ *ura4::fbp1-lacZ leu1-32 ade6-M210 his7-366 git10-201*
CHP894	h^- *fbp1::ura4*$^+$ *ura4::fbp1-lacZ leu1-32 lys1-131 cdc1-P13 git10-201*
CHP981	h^- *fbp1::ura4*$^+$ *ura4::fbp1-lacZ leu1-32 ade6-M210 swo1-26*
CHP979	h^+ *fbp1::ura4*$^+$ *ura4::fbp1-lacZ leu1-32 ade6-M210 his7-366 swo1-26*
CHP989	h^+ *fbp1::ura4*$^+$ *ura4::fbp1-lacZ leu1-32 swo1-21*
PR164	h^- *ura4-D18 leu1-32 swo1-21*
PR165	h^- *ura4-D18 leu1-32 swo1-25*
CHP362	h^{90} *leu1-32 ade6-M210 lys1-131*
CHP558	h^{90} *fbp1::ura4*$^+$ *leu1-32 ade6-M216 git2-1::LEU2*
CHP486	h^{90} *leu1-32 lys1-131 git5-1::his7*

CHP483 h^{90} *ura4::fbp1-lacZ* *leu1-32* *ade6-M216*

MAP1 h^{90} *fbp1::ura4*$^{+}$ *ura4::fbp1-lacZ* *leu1-32* *git10-201*

MAP10 - *fbp1::ura4*$^{+}$ *ura4::fbp1-lacZ* *git2-Myc::kan* *git1-V5::leu*$^{+}$ *git7-93*

MAP12 - *fbp1::ura4*$^{+}$ *ura4::fbp1-lacZ* *git2-Myc::kan* *git1-V5::leu*$^{+}$

Figure 8. Two translational fusions and their associated phenotypes

(A) Two constructed under the *fbp1* promoter, used for selecting mutations that are defective in repression of *fbp1* transcription. **(B)** Strains carrying *fbp1-ura4* and *fbp1-lacZ* fusions are Ura$^-$, 5FOA-resistant, and express little β-galactosidase activity when grown under repressing conditions (8% glucose).

Figure 8.

A.

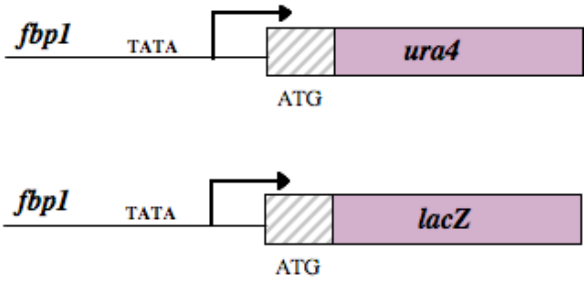

B.

	Phenotype under repressed conditions		
Genotype	5-FOA	Ura	β-galactosidase
Wild type	5-FOA^{R}	Ura^{-}	Low β-gal
git^{-} mutant	5-FOA^{S}	Ura^{+}	High β-gal

2.1.3. Bacteria

ElectroTen-Blue or XL1-Blue electroporation-competent cells (Stratagene, La Jolla, CA) or TOP10 chemical-competent cells were used to amplify plasmids (Invitrogen, San Diego). Bacterial transformants were selected on (100 mg/L) ampicillin resistance LB plates.

2.1.4. Enzymes

Restriction endonuclease enzymes, ligation enzymes, and their buffers were purchased from New England Biolabs (NEB, Ipswich, MA). Protocols for digestion reactions were performed using NEB catalog. NEB cutter software was also used to visualize the restriction digestion patterns (VINCZE *et al.* 2003). AccuPrime *Taq* DNA polymerase was purchased from Invitrogen (Carlsbad,CA). *PfuTurbo* DNA polymerase was purchased from Stratagene (La Jolla, CA). Lastly, the Failsafe PCR kit was purchased from (Epicentre Technologies, Madison, WI).

2.2. METHODS

2.2.1. Strain mating and tetrad dissection

Stains were patched on YEA solid media prior to mating. The freshly streaked strains were then mated on malt-extract agar (MEA) for 24 to 48 h at 30˚C. In the case of

homothallic stains, they were pregrown at 37˚C before mating. Asci formed on MEA were transferred using a dissection needle to YEA 3% glucose rich plate. Selected zygotic asci were then incubated at 37˚C for at least 2 h to facilitate the breakage of the cell wall and the release of spores. Tetrads were then needle dissected on the plate and moved away from each other to ease the scoring process. Plates were then incubated at 30 ˚C for 3 days and then scored.

2.2.2. β-galactosidase assays of *fbp1-lacZ* expression

Cells were cultured for 18 h under repressing conditions (8% glucose) in yeast extract at the indicated temperatures (YEL) or PM for transformants. Subcultures were grown to exponential phase $1x10^7$ cells/mL. Soluble protein extracts were prepared by glass bead in breaking buffer (0.1 M Tris pH 8, 20% glycerol, 1mM DTT) and PSMF (40mM). The assay was performed using Z buffer according to in current molecular biology protocol. Ortho-nitrophenyl-β-galactoside (ONPG) was used to start the reaction and Na_2CO_3 (1 M) solution was used to stop the reaction when a yellow color appeared. Samples were read at OD_{420}. Total soluble protein was measured by BCA assay (Pierce Chemical Co) to calculate β-galactosidase-specific activity (NOCERO *et al.* 1994).

2.2.3. X-Gal Filter Lift

This assay was used to confirm the present of the *lacZ* reporter in the strain. Strains for testing were patched on YEA or solid selective medium and grown for 24 to 48 h before testing. Cells were replica-plated directly onto a 0.2µm BioTrace NT nitrocellulose membrane filter (Pall Life Sciences, East Hills, NY). The filter that absorbed the cells was then submerged into liquid nitrogen for 60 s to lyse the cells. Afterwards, the filter was moved from liquid nitrogen and allowed to thaw for 2 min. The filter with the cells was laid on a blotting paper saturated with 2.5 mL of Z buffer mixed with 150 µl of 5-bromo-4-chloro-3-indolyl-beta-D-galactopyranoside (X-gal) (20 mg/mL). The cells were incubated at 30˚C for 15 min or until a color developed. Stains that carried *lacZ* reporter turned blue.

2.2.4. PCR walking

Polymerase chain reactions (PCR) were performed using the high Fidelity PCR kit for enzyme *Pfu* according to the manufacturer's instruction. PCR walking method was preformed on cosmid SPAC926 to cover the region where *git10*$^{+}$ gene was mapped to by using the following primers:

[Git10-1F (5'CTGGAAACCTGACGCGGGTA3') and Git10-1R (5'CTTTGCAACGTA

CTTCTACTCGC3')], [Git10-2F(5'CCGTACTTCTTACGGCG CTC3') and Git10-2R(5' GCTGAAAAGCATGCTCCCGA 3')], [Git10-3F (5'CCGTACTTCTTACGGCG CT C3') and Git10-3R(5'CAAATTTTATACGGCCCGC3')], [Git10-4F (5'GAATTCCAAA ACGCGGGC3') and Git10-4R (5'TAAGCCAAATTCCGAACGG3')], [Git10-5F (5'AA AATTTCTGACCGCTCGG3') and Git10-5R (5'GCGTTTGCTGTACGAGAGGG 3')], [Git10-6F(5'CTTCCATAACGTCTTCTACACGC3') and Git10-6R (5'TCATCAACGT ATACGTTCGGG3')], [Git10-7F (5'TGAGCCATAATAGCCCGAACG3') and Git10-7R (5'ACAAATGCAATGCGCCTAAC3')], [Git10-8F (5'AACTGCAGTGATCGGAC GGG3') and Git10-8R (5'GGGTTACATTTACGCTCTACGC3')], [Git10-9F (5'ATGG CTAGAAAAGGGACGGC3') and Git10-9R (5'GCAAACCCTTCACGAGTGTC 3')].

2.2.5. DNA sequencing

Mutant alleles of *hsp90*$^{+}$ gene (*swo1-21*, *swo1-25, swo1-26, and git10-201*) were PCR amplified from *S. pombe* strains and the PCR products were directly sequenced using custom oligonucleotides (Integrated DNA Technologies). DNA sequencing was performed using the CEQ DTCS-Quick Start kit (Beckman Coulter).

2.2.6. Cloning and Plasmid Constructions

The *S. pombe* genomic DNA insert from cosmid SPAC926 was amplified by PCR using custom oligonucleotides that divided the insert into nine segments (see Figure 9) and

cloned using pNMT41 TOPO cloning vector (Invitrogen) according to the manufacturer's instructions.

2.2.7. Epitope-tagging of Hsp90

hsp90-for (5'ATGTCGAACACAGAAACTTTCAAG3') and *hsp90*-revTAG (5' ATCGACTTCCTCCATCTTGCTC3') were used in a PCR reaction on wild type *S. pombe* genomic DNA to amplify the *hsp90*$^{+}$ ORF. The resultant PCR product, lacking the *hsp90*$^{+}$ STOP codon, was cloned into the TOPO cloning vector pNMT41 vector (Invitrogen) creating plasmid pMAR3, which expresses Hsp90 with a C-terminal V5 (SOUTHERN *et al.* 1991) tag followed by a hexahistidine tag (Hsp90-V5his6).

2.2.8. Protein extraction for Western blot analysis

Strains were grown in YEL 3% glucose to log phase $1x10^{7}$ cells/mL. Protein extracts were prepared on ice by TCA precipitation as described by Volland. (VOLLAND *et al.* 1994)

2.2.9. Co-immunoprecipitation

S. pombe strains MAP12, MAP10, CHP456, and CHP27 were grown to exponential phase and broken in lysis buffer (50 mM Tris-HCl [pH 7.5], 0.2% Triton X-100, 300 mM NaCl, protease inhibitor) by grinding in liquid nitrogen. A total of 800 µl of cell lysate was incubated with 2.5 µl of α-Sgt1 (donated by the Ken Kaplan lab) for 1 h at 4°C on a

rotator. 50 µl of Protein G Sepharose 4 Fast Flow (Amersham Pharmacia) was added in a 1:1 ratio with lysis buffer and incubated on a rotator for 2 h at 4°C. Precipitated immune complexes were isolated by microcentrifugation for 20 seconds. The pellets were washed six times with lysis buffer. Pellets were resuspended in 30 µl of Laemmli buffer and heated for 3 min at 95°C. Beads were pelleted by centrifugation for 20 seconds, and the supernatants were removed for analysis.

2.2.10. Western and immunoblotting

Protein extracts were separated by 4%-15% SDS-PAGE gradient gel (Biorad; Hercules, CA) and transferred to a polyvinylidene difluoride membrane (PVDF) (Millipore; Temecula, CA). Membranes were blocked for 3 h at room temperature in 5% nonfat milk powder dissolved in Tris-saline-Tween-20 buffer (TBST). The PVDF membrane was washed three times with 1 X (TBST). Immunodetection of V5-tagged and Myc–tagged proteins were performed using monoclonal mouse α-V5 (Invitrogen) and monoclonal mouse α-*myc* (Santa Cruz Biotechnology). Then, peroxidase-labeled goat α-mouse IgG secondary antibody (Kirkegaard & Perry Laboratories) was used as secondary antibodies to recognize mouse primary antibodies. Actin protein was detected using mouse polyclonal IgG (JLA20) against actin and peroxidase-conjugated goat α-mouse IgG was used as a secondary antibody. Gpa2 was detected using α-*S. pombe* Gpa2 antibody while peroxidase-conjugated goat α-rabbit IgG served as a secondary antibody. The Hsp90 was detected by using α-Hsp90 (K41220) primary mouse antibody. Then, peroxidase-labeled

goat α-mouse IgG was used as secondary antibodies to recognize mouse primary antibodies. Samples were visualized using LumiGLO Enhanced chemiluminescence (Kirkegaard & Perry Laboratories; KPL) following manufacturer's directions.

2.2.11. Tandem Affinity Purification (TAP)

Strains CHP993 (*git7-235*), and CHP998 (*git10-201*) both carrying a TAP-tagged adenylate cyclase were grown overnight in 1 L of YEL 8% glucose to log phase. Cells were then collected by filtration and ground with the filter in liquid nitrogen and glass beads. The lysate was transferred to a 50 mL falcon tube and centrifuged in a table centrifuge for 5 minutes at 3500 rpm. Then the supernatant was transferred to a Nalgene tube and centrifuged for 1 h using the 70Ti rotor at 38,000 rpm. Then, 800 μl of IgG /sepharose in NP-40 buffer (1:1) was added to the clear lysate and incubated for 2 h at 4° C on a rotating platform. Then, the lysate the beads were poured into a Biorad Poly Chromatography column.The beads were washed with 30 mL IPP150 buffer and by TEV cleavage buffer. Then, the TEV was added and the column was closed at the top and bottom and incubated for 2 h at 16°C. After 2 h of incubation with TEV, the eluate was drained to a new column with 1 mL of TEV CB. CBB buffer was then added to the TEV supernatant with 6 μl of 1M $CaCl_2$ and 300 μl of calmodulin resin and incubated for 1 h at 4°C. Beads were then washed twice with CBB 0.1% NP-40 and once with CBB 0.02% NP-40. Samples were then eluated in 1 mL CEB and 0.02% NP-40 and split in half. Both halves were TCA precipitated and washed first with cold acetone and (0.05 N) HCl and

then with only acetone. Supernant was removed and pellets were dried using speed vacuum. The first half was analyzed by running the samples in SDS-PAGE and then silver-stained using a Biorad kit. The other half was analyzed using sent for mass spectrometry analysis.

2.2.12. Spot Plating assay

Spot tests on *hsp90*$^{+}$, *swo1-26, swo1-21*, and *git10-201* strains were preformed at 25ºC, 28ºC, 30ºC, and 37ºC. Strains FWP72 (wild type), CHP567 (*git10-201*), CHP989 (*swo1-21*), CHP979 (*swo1-26*), were cultured to 1 x 10^7 cells/mL in YEL liquid medium. Cells then were washed with YEL medium and adjusted to 2 x 10^7 cells/mL along with five 10-fold serial dilutions. Five microliters of each culture were spotted on a YEA plate and grown for 3 days at the indicated temperature before photographing.

2.2.13. Starvation-independent mating test

To test if homothallic *git10-201* cells can conjugate and sporulate in rich medium, homothallic (h^{90}) strains CHP362 (*git10*$^{+}$), CHP558 (*git2*Δ), CHP486 (*git5*Δ), and MAP1 (*git10-201*) were grown to exponential phase in PM liquid medium (8% glucose) at 37°C (to inhibit conjugation), diluted to 10^6 cells/mL in PM liquid medium in the presence or absence of 5 mM cAMP, and incubated overnight at 30°C without shaking. Cells were then observed under the microscope and images were captured.

2.2.14. Glucose uptake assay

Glucose uptake was determined using quantitative glucose (GO) assay kit (Sigma, MO). By using glucose oxidase, the glucose in medium was oxidized to gluconic acid and hydrogen peroxide, which then reacted with o-dianisidine in the presence of peroxidase to form a colored product. Sulfuric acid was then added to form a more stable product. The absorbance of the color was measured at 540 nm. The glucose level in YEL was measured using the supernatant. The pellet from the same sample was also used for β-galactosidase analysis.

2.2.15. Cyclic AMP extraction

Cells were collected by air vacuum into micropore glass filters (Fisher). Filters were then submerged in 1 mL of (1 M) formic acid and vortexed for 30 sec to break the cell walls. After removing the filters, the samples were centrifuged for 10 min at 14,000 RPM. Four hundred microliters of supernatant was lyophilized using a speed vacuum for 4 h. Finally, the pellets were resuspended in 80 μl of (0.1 M) HCl (BYRNE and HOFFMAN 1993). Assay was performed using cAMP Direct Kit (Assay Designs).

2.2.16. Protein extraction for cAMP

Cells were pelleted and washed with cold water. The cell pellet then was resuspended in 500 μl of 0.2 N NaOH. Half of the suspension was transferred into a microcentrifuge tube with 0.4 g glass beads. The tubes were then vortexed for 3 min to break the cells. The samples were boiled for 3 min followed by centrifugation for at 14,000 RPM for 2 min to remove cell debris. Protein quantification was preformed using the BCA kit.

2.2.17. Plasmid rescue from yeast (Smash and Grab)

Smash and Grab protocol was used to rescue plasmid from yeast (HOFFMAN and WINSTON 1987). Cells were grown in selective liquid medium for overnight. Then cultures were pelleted, resuspended, and vortexed with glass beads, 0.2 mL phenol-chloroform, and 0.2 mL of Smash and Grab buffer made as described by Hoffman and Winston (HOFFMAN and WINSTON 1987). The cells were then centrifuged for 5 min and the supernatant containing the isolated plasmid was transferred to a new tube.

2.2.18. *Escherichia coli* transformation

Escherichia coli transformations were done using Ten-Blue or XL1-Blue electroporation-competent cells (Stratagene).

2.2.19. Yeast transformation

Cells were grown in YEL overnight to early log phase $5x10^6$. Cells were pelleted and washed twice with cold water and (LiAc/TE) buffer. Pellets were resuspended in 100 µl LiAc/TE and mixed with 1 µl boiled salmon testes DNA and 5-10 µl of the sample DNA. The samples were kept for 10 min in room temperature before adding 260 µl of (40% PEG, 100 mM LiOAc, 10 mM Tris-HCl pH 7.5) buffer. Samples were then incubated at 30°C for 1 h. The samples then were heat shocked for 5 min at 42°C after adding 43 µl of DMSO to the samples. Finally, cells in different dilutions were plated on selective medium (BÄHLER *et al.* 1998). Transformation was also, performed by growing yeast on YEA medium for overnight at 30°C. Cells were then collected directly on the plate and resuspended in PLATE (40% PEG; 10 mM Tris HCl, 100 mM LiOAc; 1mM EDTA). Next, 100 µl of the mixture was used for each transformation with 1 µl boiled salmon testes DNA and 5-10 µl of the sample DNA. The samples were incubated at 30°C for 24 h before they were plated on selective medium.

2.2.20. Microscopy

The images of cells were captured using a Zeiss microscope with an Orca-ER CCD camera. The microscope –camera are connected to a computer equipped with Openlab software. Strains were grown in appropriate liquid media to $2\text{-}4x10^6$ cells/mL, then cells were fixed with paraformaldehyde as previously described (HAGAN and HYAMS 1988)

with some modification. Yeast cell walls were digested with 0.5 mg/mL 100T Zymolyase. The Hsp90 V5-tagged protein was detected by using α-V5 primary mouse antibody (Invitrogen) diluted 1:100 in PEMBAL. The endogenous Hsp90 protein was detected by using α-Hsp90 (K41220) primary mouse antibody diluted 1:100 in PEMBAL. Both were visualized using secondary antibody Alexa Fluor 488-labeled goat α-mouse (Molecular Probes) diluted 1:50 in PEMBAL overnight in the dark. The Fluorescence Alexa Fluor 488-labeled antibodies signals were visualized under fluorescein isothiocyanate (FITC) filter. Localization of Hsp90 was captured using a Nikon confocal microscope system with a Nikon Eclipse inverted microscope and EZC1 Software system. Hoechst 33342 was also used to stain the nuclei. Septum was stained using calcofluor. Both were visualized under 4', 6-diamidino-2-phenylindole (DAPI) filter.

CHAPTER THREE

CLONING AND CHARACTERIZING *git10*$^{+}$

This chapter is published as a research article in Genetics, Vol. 178, 1927-1936, April 2008

CLONING AND CHARACTERIZING *git10*$^+$

3.1. Genetic mapping and cloning of the *S. pombe git10*$^+$ gene

Git$^-$ mutant strains display 5FOA-sensitive (5FOA^S) growth due to their inability to glucose repress the *fbp1-ura4*$^+$ reporter (HOFFMAN and WINSTON 1990). To date, nine *git* genes have been shown to play a significant role in *fbp1*$^+$ repression, with only *git10*$^+$ remaining to be cloned. Due to the large number of multicopy suppressors encountered when screening plasmid libraries during attempts to clone genes in this pathway (DAL SANTO *et al.* 1996; HOFFMAN and WINSTON 1991; JIN *et al.* 1995; WANG *et al.* 2005b), a genetic mapping approach to identify the *git10*$^+$ gene was performed.

Chromosomal mapping of *git10-201* by benomyl-induced haploidization of an *h*$^-$/*mat2-102* diploid strain (ALFA *et al.* 1993) was carried out with strains FWP17 and CHP573 (Table 1). This technique allows the formation of haploids from a diploid strain in the absence of meiotic recombination, such that the alleles on each of the three parental chromosomes form individual linkage groups. All 5FOA-sensitive haploids produced this way possessed chromosome 2 from CHP573, containing the *fbp1-ura4*$^+$ reporter, as well as chromosome 1 from CHP573, presumably possessing *git10-201* (data not shown). The *git10-201* allele was further mapped by tetrad dissection, in a cross of strain FWP87 with strain CHP894.

Figure 9. Git10 cloning process

(A) The *git10*$^{+}$ gene maps between *lys1* and *cdc1*$^{+}$. The genetic mapping data suggested that *git10*$^{+}$ is present on cosmid SPAC926. **(B)** PCR amplification of SPAC926 was divided into nine fragments and then these fragments were TOPO-cloned into plasmids that were used to transform *S. pombe* strain CHP567.

Figure 9.

A.

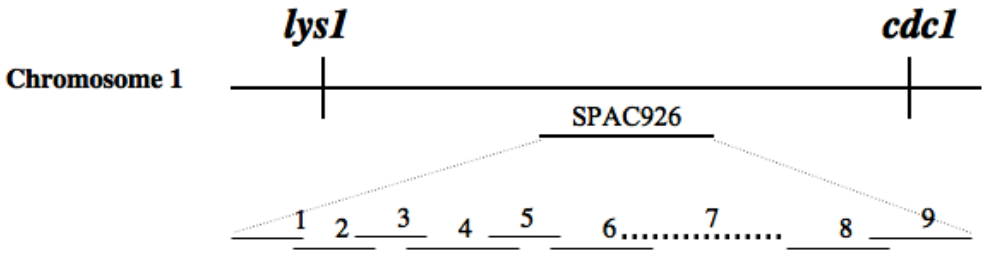
lys1
cdc1
Chromosome 1
SPAC926
1
2
3
4
5
6
7
8
9

B.

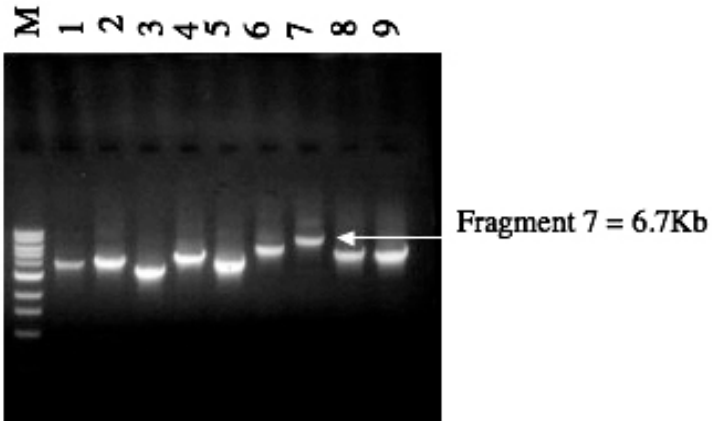
M
1
2
3
4
5
6
7
8
9
Fragment 7 = 6.7Kb

The *git10*$^{+}$ gene maps between *lys1*$^{+}$ (23.2 cM with a PD:TT:NPD ratio of 45:39:0) and *cdc1*$^{+}$ (30.4 cM with a PD:TT:NPD ratio of 38:45:1). The *lys1*$^{+}$ and *cdc1*$^{+}$ genes are 54.8 cM from each other with a PD:TT:NPD ratio of 22:56:6.

The genetic mapping data suggested that *git10*$^{+}$ is present on cosmid SPAC926 (one of an ordered set of cosmids used in the *S. pombe* genome sequencing project (Figure 9) (WOOD *et al.* 2002). Insert DNA from SPAC926 was divided into nine fragments by PCR amplification and TOPO-cloning into a plasmid suitable for transformation of *S. pombe*. Plasmids from this set of clones were used to transform *S. pombe* strain CHP567 (*git10-201*) to Leu^{+} and transformants were tested for restoration of 5FOA-resistance to indicate complementation of the *git10*$^{-}$ defect. Plasmids pMAR1 and pMAR2, which carry fragment number 7, base pairs 2308 to 9026 in either orientation with respect to the vector, were the only clones to confer 5FOA-resistance (Figure 10A). These transformants also glucose-repress *fbp1-lacZ* expression as judged by β-galactosidase assays (Figure 10B). Plasmids pMAR1 and pMAR2 contain two genes, one of which is *hsp90*$^{+}$/*swo1*$^{+}$. Digestion with *Nru*I followed by ligation removed a 1.4 kb fragment internal to the *hsp90*$^{+}$ open reading frame and produced plasmids pMAR1A and pMAR2B, which lost the ability to suppress the *git10-201* mutation (Figure 10). Thus, *hsp90*$^{+}$ appears to be responsible for suppression of the *git10-201* mutant allele.

Figure 10. Complementation of *git10-201* mutation by plasmid-expressed *git10*$^{+}$.

(A) CHP567 (*git10-201*) cells were transformed to Leu^{+} with pNMT41 (empty vector), pMAR1 (*git10*$^{+}$), pMAR1A (*git10*Δ*236-1607*), pMAR2 (*git10*$^{+}$ cloned in the opposite orientation to that of pMAR1), pMAR2B (*git10*Δ*236-1607* cloned in the opposite orientation to that of pMAR1A). The *git10*Δ*236-1607* contains a partial dropout of the *git10* ORF. The two independent transformants of each plasmid indicated in the Figure were spotted on EMM–leu and then replica plated after 2 days to EMM–leu and 5FOA plates. Plates were photographed after three days incubation at 30ºC. **(B)** ß-galactosidase activity was determined as described in MATERIALS AND METHODS. The values represent the average ± standard deviation of at least two independent transformants.

Figure 10.

A.

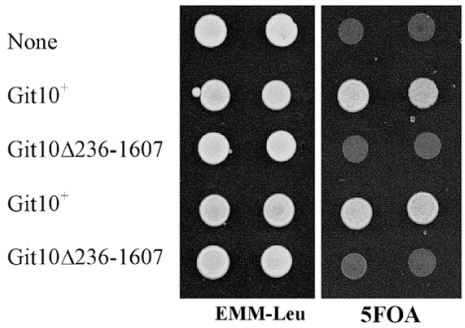

B.

Host Genotype	Plasmid	Plasmid product	β-gal activity
git10-201	pNMT41	None	691±104
git10-201	pMAR1	Git10^{+}	51± 17
git10-201	pMAR1A	Git10Δ*Nru*I	272± 17
git10-201	pMAR2	Git10^{+}	41± 25
git10-201	pMAR2B	Git10Δ *Nru*I	526±146

Figure 11. Complementation of *git10-201* mutation by plasmid expressed *git10-V5*

Plasmid pMAR3 carries only the *hsp90* ORF, while plasmids pMAR1 and pMAR2 carry larger segments of the chromosomal DNA that include the $hsp90^{+}$ gene. Plasmid pMAR3 complements the *git10-201* mutation whereas pNMT41 (empty vector) does not. Transformants were spotted on EMM–leu and then replica plated after 2 days to EMM–leu and 5FOA plates. Plates were photographed after three days incubation at 30ºC.

Figure 11.

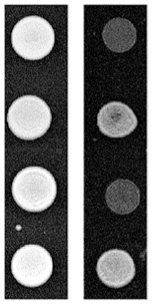

EMM -Leu 5FOA

Host Genotype	Plasmid	Plasmid product
git10-201	pNMT41	None
git10-201	pMAR3	Git10^{+}V5his6
git10-201	pNMT41	None
git10-201	pMAR3	Git10^{+}V5his6

To confirm that *hsp90*$^{+}$ is *git10*$^{+}$, plasmid pMAR3 was constructed to express an epitope-tagged form of Hsp90 (see Materials and Methods). CHP567 (*git10-201*) transformants carrying pMAR3 are 5FOA-resistant (Figure 11) proving that *hsp90*$^{+}$ is able to suppress the *git10-201* mutation. In contrast, transformation by pMAR3 fails to suppress the PKA pathway mutations *git1*$^{-}$, *git2*$^{-}$ (*cyr1*$^{-}$), *git7*$^{-}$ or *pka1*$^{-}$ (Figure 12).

3.2. Hsp90 is required for nutrient regulation of sexual development

Wild type *S. pombe* requires either a glucose or a nitrogen starvation signal to initiate mating and meiotic entry (STETTLER *et al.* 1996). Consequently, mutations in genes required for glucose/cAMP signaling allow cells to mate and sporulate even in a nutrient-rich medium (ISSHIKI *et al.* 1992; JIN *et al.* 1995; KAO *et al.* 2006; LANDRY and HOFFMAN 2001b; LANDRY *et al.* 2000; MAEDA *et al.* 1990; SCHADICK *et al.* 2002; WELTON and HOFFMAN 2000). Consistent with a role in this pathway, the *git10-201* allele of *hsp90*$^{+}$ allows homothallic (h^{90}) cells to mate in a glucose-rich medium, as evidenced by presence of meiotic asci (Figure 13). This starvation-independent mating is similar to that conferred by deletion of the adenylate cyclase gene (*git2*$^{+}$) or the Gß subunit gene (*git5*$^{+}$; Figure 13). Addition of 5 mM cAMP to the medium suppresses conjugation in all three mutant strains (Figure 13). This starvation-independent, cAMP-suppressible defect in the regulation of sexual development is another indication that Hsp90 plays a role in the *S. pombe* glucose/cAMP signaling pathway.

Figure 12. Test if *git10*/*hsp9*0 can act as a high-copy suppressor of mutations in other genes in the glucose-sensing cAMP pathway

Plasmid pMAR3 was expressed into strains carrying mutations in *git1*$^{+}$, *git2*$^{+}$, *git7*$^{+}$, *git10*$^{+}$, and *pka1*$^{+}$. All of these transformants remain 5-FOA-sensitive. On the contrary, plasmid pMAR3 was able to suppress the *git10-201* mutation.

Figure 12.

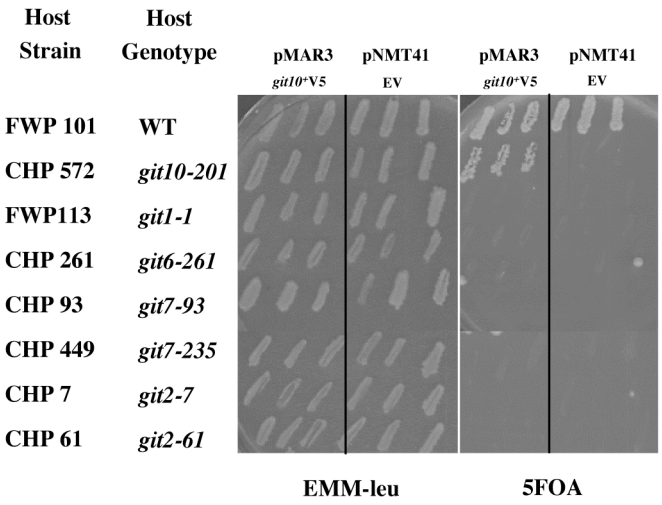
Host Strain
Host Genotype
pMAR3 git10+V5
pNMT41 EV
pMAR3 git10+V5
pNMT41 EV
FWP 101 WT
CHP 572 git10-201
FWP113 git1-1
CHP 261 git6-261
CHP 93 git7-93
CHP 449 git7-235
CHP 7 git2-7
CHP 61 git2-61
EMM-leu
5FOA

Figure 13. Homothallic *git10-201* cells conjugate and sporulate in nutrient-rich medium

Homothallic *git10-201* cells conjugate and sporulate in nutrient-rich medium, similar to other cAMP pathway mutants. Homothallic (h^{90}) strains CHP362 (*git10*$^{+}$), CHP558 (*git2*Δ), CHP486 (*git5*Δ), and MAP1 (*git10-201*) were grown to exponential phase in PM liquid medium (8% glucose) at 37°C (to inhibit conjugation), diluted to 10^6 cells/ml in PM liquid medium in the presence or absence of 5 mM cAMP, and incubated overnight at 30°C without shaking. Starvation-independent conjugation and sporulation, which is suppressible by addition of cAMP, is observed in all three mutant strains.

Figure 13.

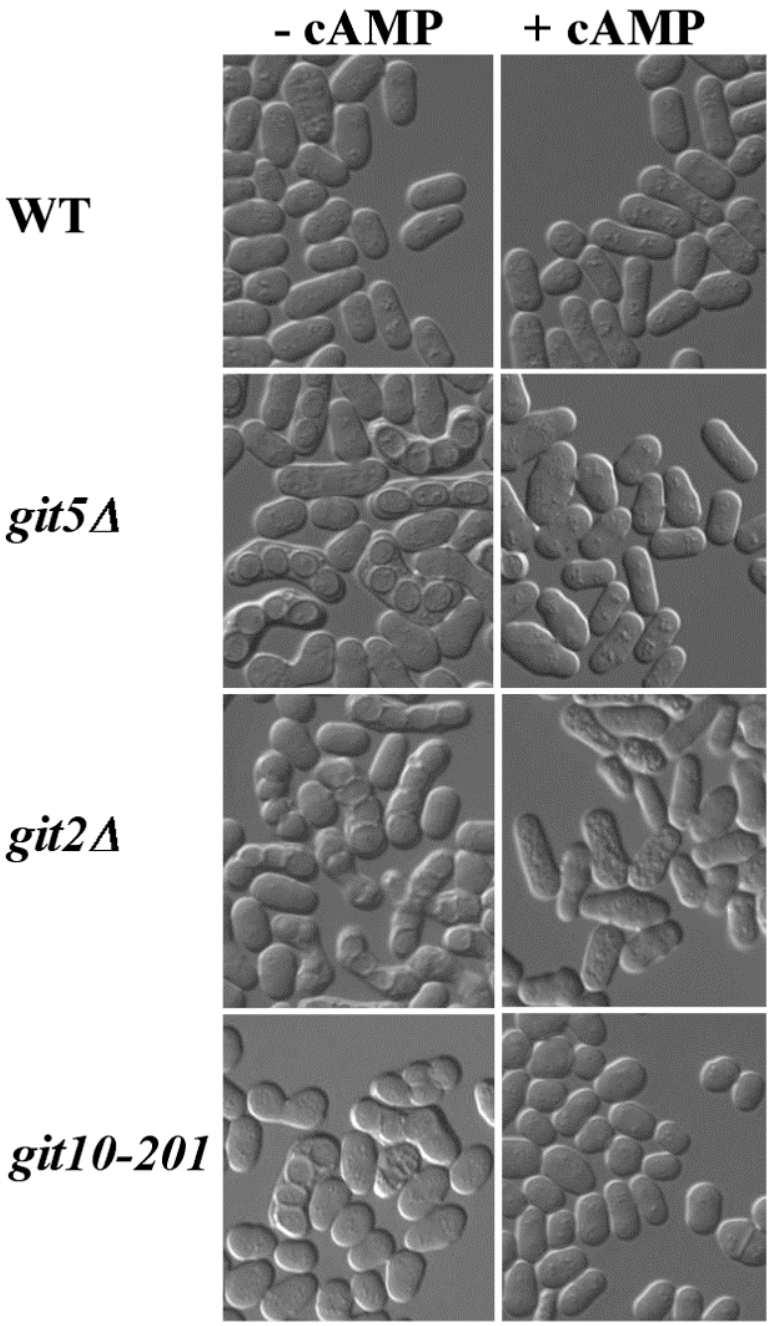

Furthermore, a mutation in any gene required for glucose-cAMP signaling will result in a defect in the glucose repression of *fbp1-lacZ* expression and 5FOA sensitive phenotype (ISSHIKI *et al.* 1992; LANDRY and HOFFMAN 2001; LANDRY *et al.* 2000; MAEDA *et al.* 1990; WELTON and HOFFMAN 2000). Therefore, a mutation in *git10/hsp90* ORF should confer a Git$^-$ mutant phenotype, an elevated *fbp1-lacZ* expression in cells grown under glucose-rich conditions (Figure 10B) and 5FOA sensitive growth due to constitutive expression of the *fbp1-ura4*$^+$ reporter (Figure 10A). These results demonstrate that *git10/hsp90* is required for the cAMP-dependent regulation of conjugation, as well as *fbp1* transcriptional regulation.

3.3. Genetic, environmental, and chemical insults to Hsp90 activity derepress *fbp1-lacZ* expression

To investigate the role of Hsp90 in the regulation of *fbp1*$^+$ transcription, ß-galactosidase activity expressed from the *fbp1-lacZ* reporter was measured in wild type, *git10*$^-$, and *swo1*$^-$ mutant strains grown at various temperatures (Table 2). Both the *swo1-21* and *swo1-26* alleles confer a temperature-dependent defect in *fbp1-lacZ* repression, in addition to a temperature-sensitive growth defect.

Table 2. Glucose repression of *fbp1-lacZ* expression as a function of growth temperature

		ß-galactosidase activity				
Strain	***hsp90* allele**	**25º**	**27º**	**30º**	**32º**	**37º**
FWP87	wild type	15±5	11± 0	10 ±6	12 ± 4	392±6
CHP567	*git10-201*	154±20	252 ±26	626±30	661±157	1336±131
CHP981	*swo1-26*	54±3	144 ±5	517±55	Inviable	Inviable
CHP989	*swo1-21*	157±12	377±8	605±105	Inviable	Inviable

ß-galactosidase activity was measured in cells growing in YEL medium under glucose-repressing conditions (8% glucose) for 18 hours at the indicated temperature. The values given represent specific activity average ± standard deviation from two or three independent cultures.

The *git10-201* allele also confers a temperature-dependent defect in *fbp1-lacZ* repression, however these cells remain viable when cultured at 37ºC. Surprisingly, wild type cells display a partial defect in *fbp1-lacZ* repression when cultured at 37ºC, suggesting that temperature stress of wild type cells leads to a reduction in PKA activity, and not simply the activation of the Spc1/Sty1 MAPK required for $fbp1^{+}$ transcription.

The effect of temperature stress on *fbp1-lacZ* repression was further examined in a time-course experiment in which wild type cells were cultured at 30ºC or 40ºC, a temperature that does not support growth of *S. pombe*, but at which cells remain viable for several days (C.A. Hoffman and C.S. Hoffman, unpublished results). Increased ß-galactosidase activity in response to temperature stress can be detected within one hour (data not shown), although it remains modest even after six hours of incubation (Figure 14A). By 24 hours, however, the ß-galactosidase activity rises to 547 ± 80 units, demonstrating that prolonged exposure to heat stress is required for significant $fbp1^{+}$ derepression. As the glucose levels in the media remain above 7.5% in all cultures, the increased *fbp1-lacZ* expression is due to heat stress and not glucose starvation (Figure 14B).

To independently test whether Hsp90 is required for $fbp1^{+}$ regulation, I examined the effect of chemical inhibition of Hsp90 on *fbp1-lacZ* expression by exposing cells to the Hsp90 inhibitor geldanamycin (WHITESELL *et al.* 1994).

Figure 14. Prolonged heat stress derepresses *fbp1-lacZ* transcription.

(A) Wild type strain FWP77 was pregrown to exponential phase at 30º and then subcultured at 30º or 40º in YEL medium under glucose-repressing conditions. ß-galactosidase activity was measured at the times indicated. The values given represent specific activity average ± standard deviation from two or three independent cultures. **(B)** Glucose levels of the same samples were measured.

Figure 14.

A.

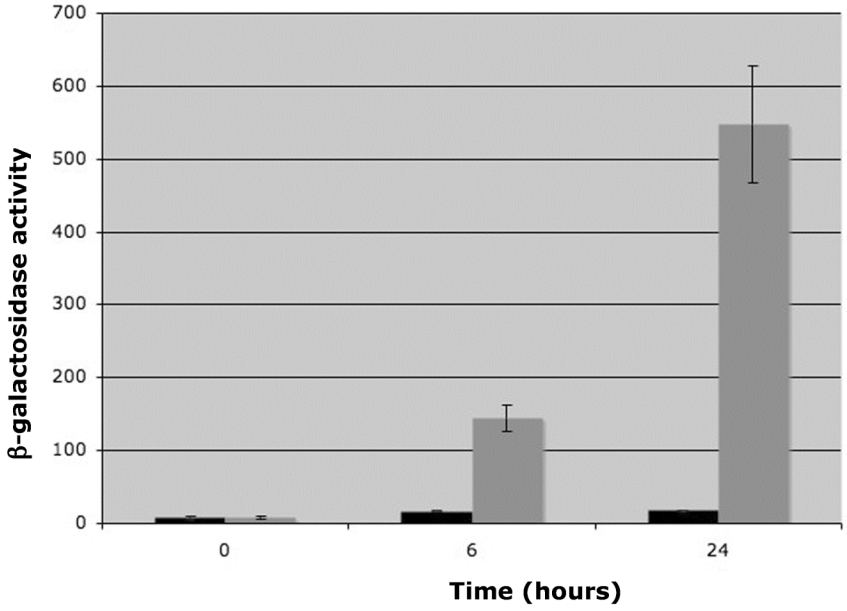

B.

		30°C	
	0h	**6h**	**24h**
β galactosidase activity	8±2	17±2	18±1
Glucose level (%)	7.5±0	7.6±0.2	7.6±0.3
		40°C	
		6h	**24h**
β galactosidase activity		144±18	547±80
Glucose level (%)		7.6±0.2	7.5±0.1

ß-galactosidase activity was measured from wild type strain FWP77 cells grown at 30ºC for 18 hours in the presence or absence of geldanamycin (2 μg/ml, 5 μg/ml, 10 μg/ml). There was a clear dose-dependent derepression of *fbp1-lacZ* expression, although the levels of expression did not reach those detected in cells subjected to prolonged heat stress (Figure 15).

3.4. Phenotypic differences between *swo1*$^-$ and *git10*$^-$ alleles of *hsp90*$^+$

In the course of assaying ß-galactosidase activity from *swo1*$^-$ and *git10*$^-$ strains, I confirmed previous observations that indicated that the *swo1*$^-$ alleles confer temperature sensitive growth (ALIGUE *et al.* 1994), while the *git10-201* allele does not.

For a more rigorous comparison, I carried out spot tests on *hsp90*$^+$, *swo1-26, swo1-21*, and *git10-201* strains to examine growth on rich medium at 25º, 28º, 30º, and 37ºC. Both *swo1*$^-$ mutants display a severe temperature-sensitive growth defect, even at 30ºC, while the *git10-201* mutants only displays a slow growth phenotype at 37ºC rather than a loss of cell viability (Figure 16).

Figure 15. Chemical inhibition of Hsp90 derepress *fbp1-lacZ* transcription

ß-galactosidase activity was measured in cells growing in 8% glucose YEL medium for 18 hours in the presence of the Hsp90 inhibitor geldanamycin at the indicated concentrations. The values given represent specific activity average ± standard deviation from two or three independent samples.

Figure 15.

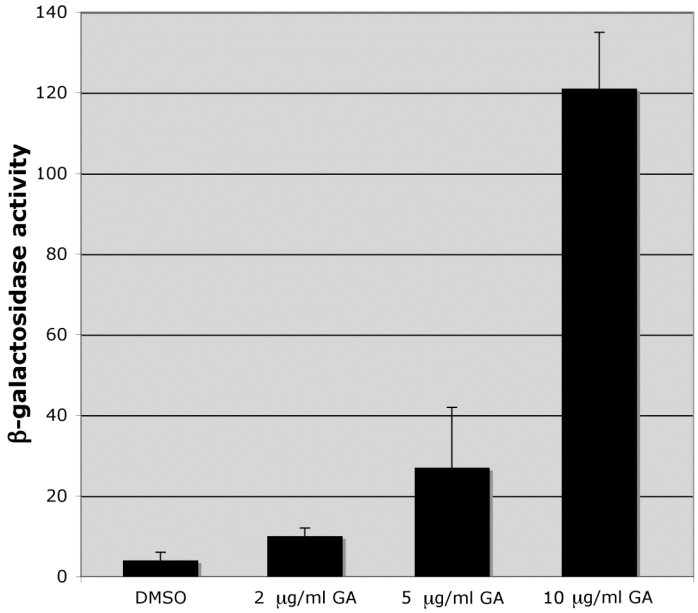
β-galactosidase activity
140
120
100
80
60
40
20
0
DMSO
2 μg/ml GA
5 μg/ml GA
10 μg/ml GA

Figure 16. Temperature-dependent growth of *hsp90*$^{+}$, *swo1-26, swo1-21*, and *git10-201* strains

Spot tests were carried out on YEA rich medium at 25º, 28º, 30º, and 37ºC. Strains FWP72 (wild type), CHP567 (*git10-201*), CHP989 (*swo1-21*), CHP979 (*swo1-26*), were cultured to 1 x 10^7 cells/ml in YEL liquid medium. Cells were washed with YEL medium and adjusted to 2 x 10^7 cells/ml and subjected to five 10-fold serial dilutions. Five microliters of each culture was spotted to a YEA plate and grown for 3 days at indicated temperature before photographing.

Figure 16.

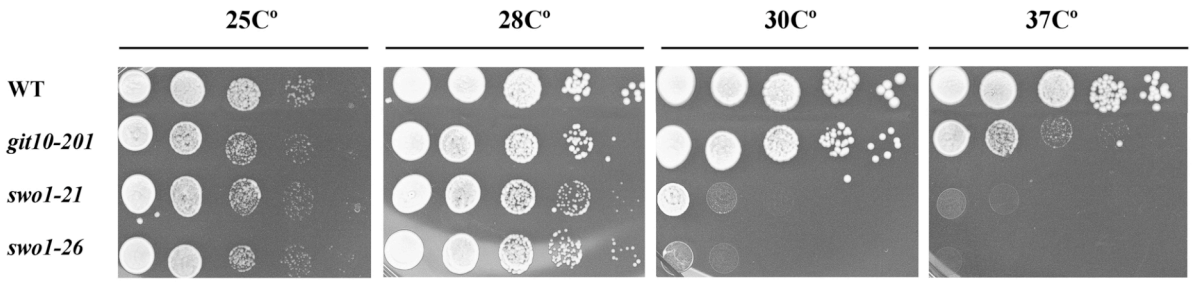

Microscopic examination of *hsp90*$^{+}$, *swo1*$^{-}$ and *git10-201* strains growing at 28º, 30º, and 37ºC was carried out to examine the nature of the temperature-dependent growth defect. After 24 hours growth on EMM defined medium, the *swo1-21* strain displayed abnormal cells that were lysed or binucleate or with misplaced nuclei in cultures grown at 30°C and 37°C (Figure 17). The *swo1-26* strain appeared normal at 30ºC, while most cells had improperly placed nuclei at 37º. These results contrast somewhat with those from the spot test of a *swo1-26* strain at 30ºC (Figure 16), and appears to be a medium-specific effect with these cells displaying a more severe growth defect on YEA rich medium than on EMM defined medium as seen in Figure 18.

No growth defects were observed in wild type or *git10-201* cells at any temperature (Figure 16,17), distinguishing the cAMP pathway defect caused by the *git10-201* mutation from the cell growth defects caused by the *swo1-21* and *swo1-26* mutations.

Figure 17. Temperature-dependent morphology of *hsp90*$^{+}$, *swo1-26, swo1-21*, and *git10-201* strains. Strains were precultured at 28ºC and then transferred to EMM defined medium and grown for 24 hours at 28, 30, and 37°C. Cells were heat-fixes and stained with Hoechst 33342 and Calcofluor. Images were visualized and captured using a Zeiss Axioplan2 microscope with an Orca-ER CCD camera and Openlab software. The *swo1-21* strain displayed lysed or binucleate cells at 30ºC (Red Arrows). The *swo1-26* 30ºC cells had improperly placed nuclei at 37ºC (Red Arrowheads). The *git10-201* cells appeared normal.

Figure 17.

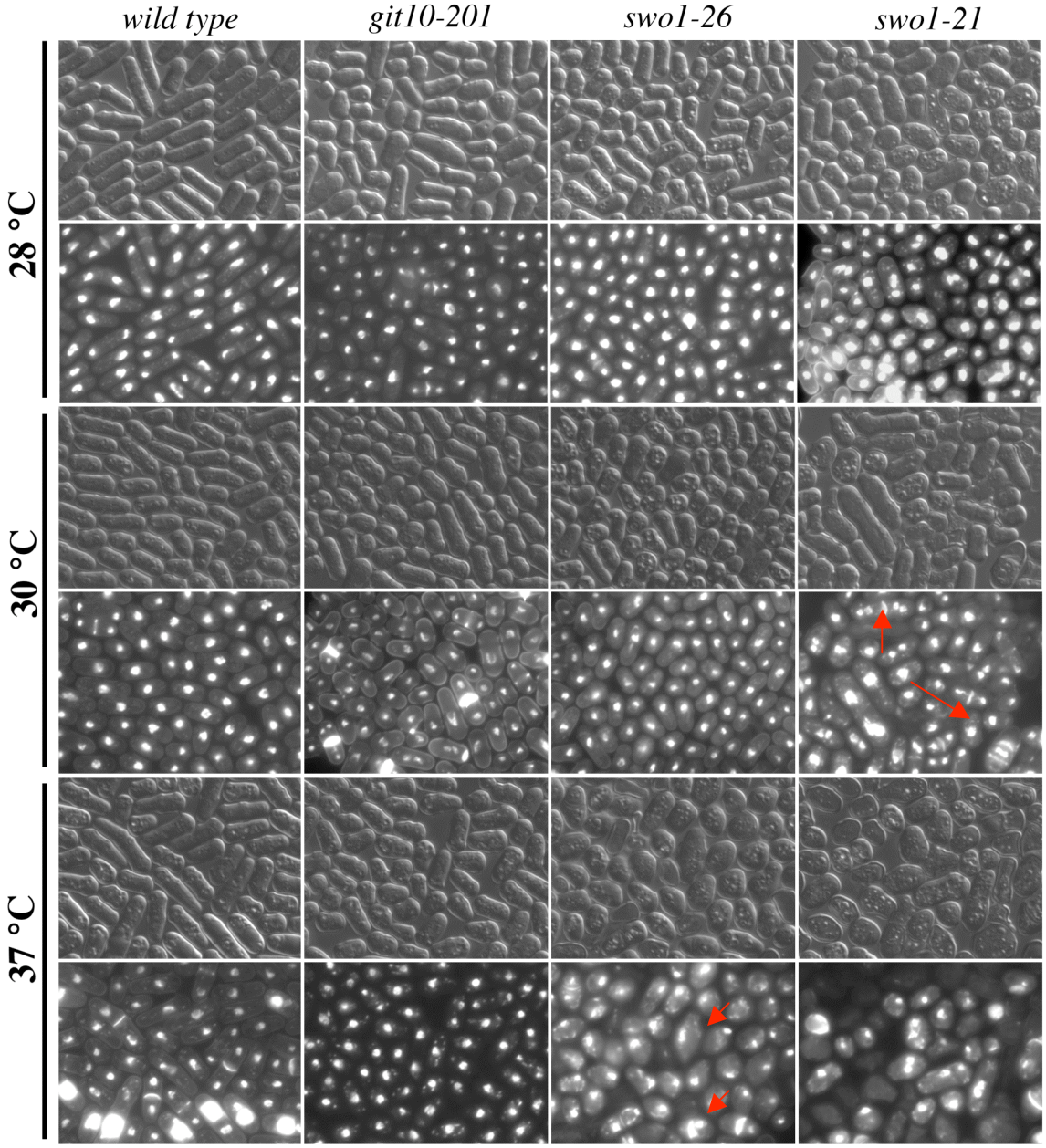

Figure 18. Cell morphology of *hsp90*$^{+}$, *swo1-26, swo1-21*, and *git10-201* strains at 30°C on YEA

The same strains as shown in Figure 16 were precultured at 28ºC and then transferred to YEA instead of defined medium (EMM) and grown for 24 hours at 28°C, 30°C. Cells were heat-fixed and stained with Hoechst 33342 and Calcofluor. Hsp90 mutant strains appeared normal at 28°C (data not shown) but show defects at 30°C. These cells display more severe growth defect (Arrowheads) on YEA rich medium than on EMM defined medium.

Figure 18.

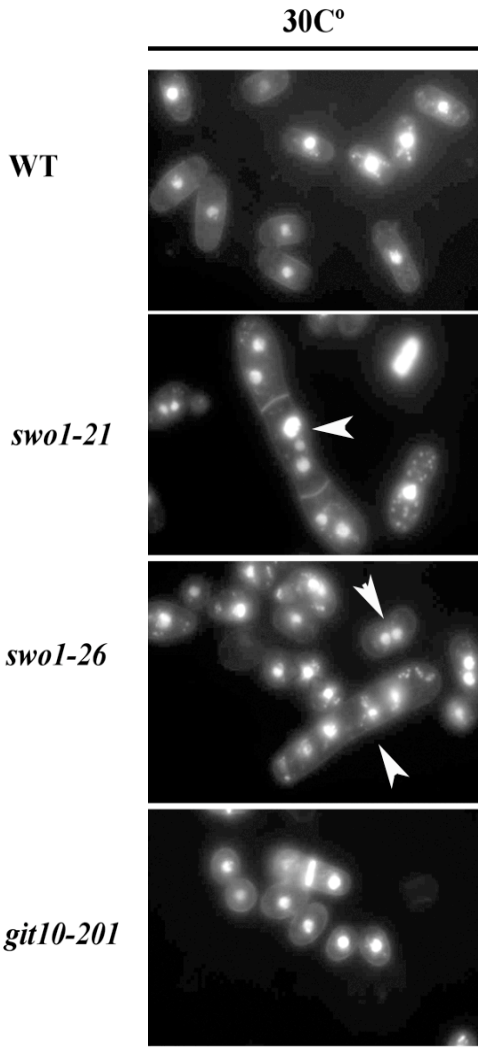

3.5. Sequence analysis of *swo1*$^-$ and *git10*$^-$ alleles

The sequence of the entire *hsp90*$^+$ open reading frame was determined from strains carrying the *swo1-21*, *swo1-25*, *swo1-26*, and *git10-201* alleles. The *swo1-25* and *swo1-26* alleles carry the same mutation, changing residue 84 from glycine to cysteine, while the mutation in *swo1-21* changes residue 654 from leucine to arginine. The *git10-201* allele changes residue 338 from leucine to proline (Figure 19). Thus, the *swo1-25* and *swo1-26* alleles affect the N-terminal ATP-binding domain, the *swo1-21* allele affects the C-terminal dimerization domain, and the *git10-201* allele affects the central, client protein-binding domain.

The locations of these mutations are consistent with the observations that the *swo1*$^-$ mutant alleles appear to be general reduction-of-function alleles, while the *git10-201* mutation appears to confer only a modest growth defect, but a significant defect in glucose/cAMP regulation of *fbp1*$^+$ transcription. A similar separation-of-function allele of an Hsp90 gene *daf-21* has been observed in the cGMP signaling pathway of the nematode *Caenorhabditis elegans* (BIRNBY *et al.* 2000). The *daf-21* mutation as seen in Figure 19 and Figure 20 is a missense mutation that alters a residue in the Hsp90 central domain not far from the residue altered by the *S. pombe git10-201* mutation.

Figure 19. Alignment of Hsp90 proteins from *S. pombe*, *S. cerevisiae*, and *C. elegans*

The *S. pombe* Hsp90 protein (accession number CAB54152) was aligned using ClustalW (THOMPSON *et al.* 1994) with the *S. cerevisiae* Hsc82 protein (accession number CAA89919), *C.elegans* DAF-21 (accession number NP_506626), human Hsp90α (accession number NP_005339), and displayed using BOXSHADE 3.21. Identical residues are shaded in black, while conserved residues are shaded in gray. Amino acid changes associated with the *swo1-21*, *swo1-26*, and *git10-201* mutant alleles are also indicated, as well as that of the *C. elegans daf-21* mutation.

Figure 19.


S. pombe
S. cerevisiae
C. elegans
Human
C (swo1-26)
K (daf-21)
P (git10-201)
R (swo1-21)

Figure 20. Crystal structure of the central domain of *S. cerevisiae* Hsp82

Hsp82 (accession number AAA02813) showing the location of the residues altered by the *S. pombe git10-201* mutation and the *C. elegans daf-21* mutation. The two altered residues are on the same surface of the Hsp90 central domain. The graphic image was created using Pymol (DeLano Scientific).

Figure 20.

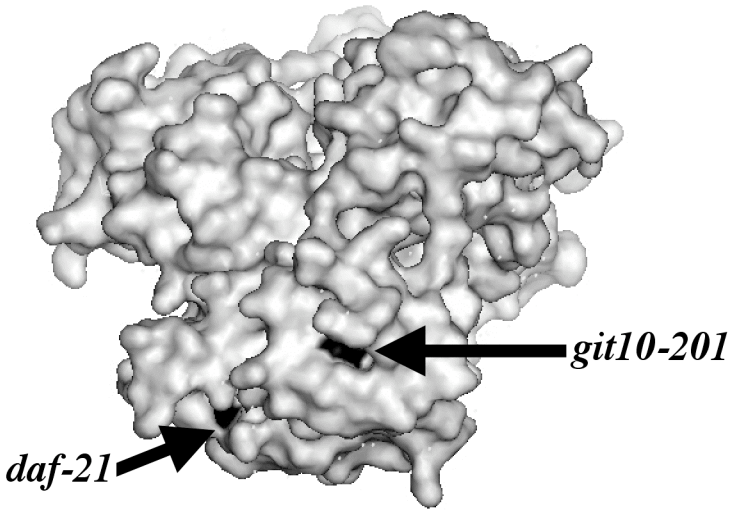

The similarity between these two mutations and their associated phenotypes suggest that Hsp90 plays a similar role in both *S. pombe* and *C. elegans* cyclic nucleotide signaling pathways to regulate metabolic pathways in response to temperature and nutritional conditions (See summary and future directions).

3.6. Hsp90 localization in *S.pombe*

I examined Hsp90 localization using indirect immunofluorescence microscopy on cells carrying plasmid pMAR3 (nmt41-Hsp90-V5) and cells carrying an empty vector. The signal was detected using α Hsp90 antibody (K41220) against the Hsp90-V5 and the endogenous Hsp90 (Figure 21). Cytoplasmic punctate was observed throughout the cytoplasm of the cell. This is not surprising as Hsp90 is likely to be one of the most abundant proteins in *S. pombe.*

The localization of endogenous Hsp90 appears the same as Hsp90-V5 although the endogenous signal was less intense than the expressed form of Hsp90. These results suggest that the immunofluorescent signal using that was observed is real and the Hsp90 antibody (K41220) is recognizing Hsp90 specifically since the signal was induced when Hsp90 was overexpressed. Previous studies in our lab showed similar cytoplasmic punctate pattern of other components of the glucose/cAMP pathway including Git1 (KAO *et al.* 2006), Git2 (Wang, unpublished data), and Git7 (SCHADICK *et al.* 2002) but not Git3 (Chandler, unpublished data).

Figure 21. Subcellular localization of Git10/Hsp90

DIC and fluorescent images of cells expressing tagged Hsp90 to detect the overexpressed Hsp90-V5 as indicated. Endogenous Hsp90 was detected using Hsp90 antibodies (K41220). The overexpressed Hsp9-V50 was detected using αV5 antibodies. Empty vector (EV) and αV5 antibodies was used as a control.

Figure 21.

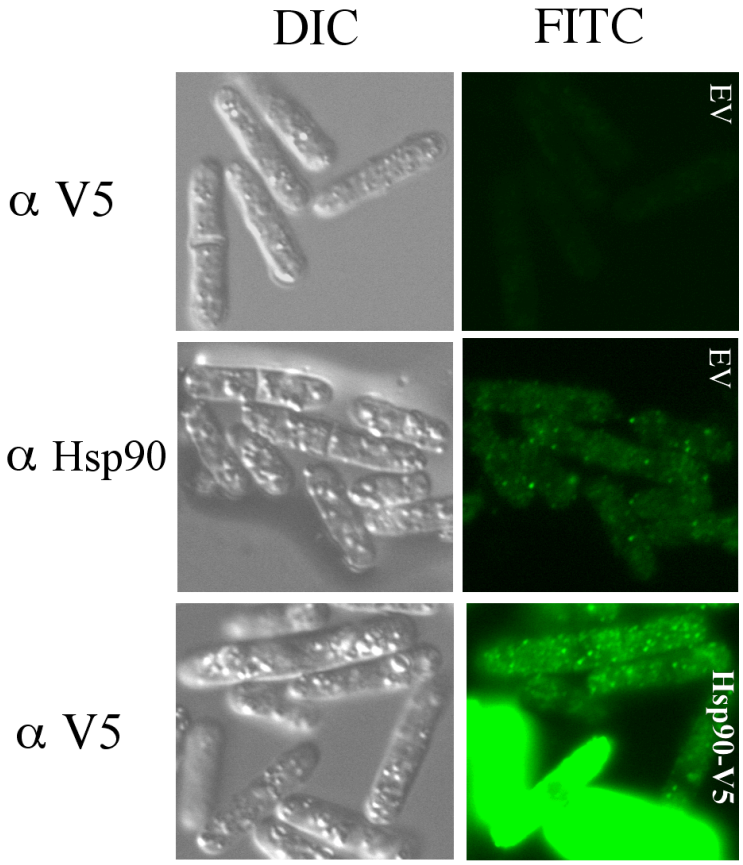

CHAPTER FOUR

Hsp90 Works Together with Git7 in *Schizosaccharomyces pombe*

Hsp90 Works Together with Git7 in *Schizosaccharomyces pombe*

4.1. Git7 Interacts With Hsp90 and Requires Functional Hsp90

4.1.1. Sensitivity of *git7* mutants to a specific inhibitor of Hsp90

In the previous chapter, I showed that *git10*/*hsp90* is identical to *swo1*$^{+}$, which encodes the *S. pombe* Hsp90 protein. This discovery shed light on the earlier identification of the Git7 protein as a member of the Sgt1 family in *S. cerevisiae* (SCHADICK *et al.* 2002). Git7 and Hsp90 are both found to be important in proper cAMP signaling in *S. pombe*. Mutations in any of these genes causes elevated levels of *fbp1*gene transcription in cells grown in the presence of glucose (HOFFMAN and WINSTON 1990; HOFFMAN and WINSTON 1991). To investigate whether the function of Git7 involves Hsp90, I used a pharmacological approach to understand the role of Hsp90 and Git7. I monitored the growth of wild-type, Git7 mutants, and Hsp90 mutants on YEA plates in the presence of a low (2 μg/ml) to high dose (10 μg/ml) of geldanamycin (GA), or Dimethyl sulfoxide (DMSO) and observed their ability to form colonies at the permissive temperature. The same temperature sensitive Git7 mutants, *git7-27*, *git7-235*, as well Hsp90 temperature sensitive mutants *swo1-21*, *swo1-26* (Figure 22, 23) displayed drug sensitivity even under low doses of geldanamycin.

Figure 22. Temperature-dependent growth of wt, *git7-235*, *git7-27*, *git7-93*, *swo1-26*, *swo1-21*, and *git10-201* strains

The *git7-235* and *swo1*$^-$ mutants display a severe temperature sensitive growth phenotype. The *git7-93* mutant grows well at 37ºC, while the *git10-201* mutant shows only a partial reduction in growth at 37ºC. Spot tests were carried out on YEA rich medium at the indicated temperature. Strains FWP72 (wild type), CHP465 (*git7-235),* CHP27 (*git7-27*), CHP800 (*git7-93),* CHP567 (*git10-201*), CHP989 (*swo1-21*), and CHP979 (*swo1-26*) were cultured to 1 x 10^7 cells/ml in YEL liquid medium. Cells were washed with YEL medium and adjusted to 2 x 10^7 cells/ml and subjected to five 10-fold serial dilutions. Five microliters of each culture was spotted to a YEA plate and grown for 3 days at the indicated temperature before photographing.

Figure 22.

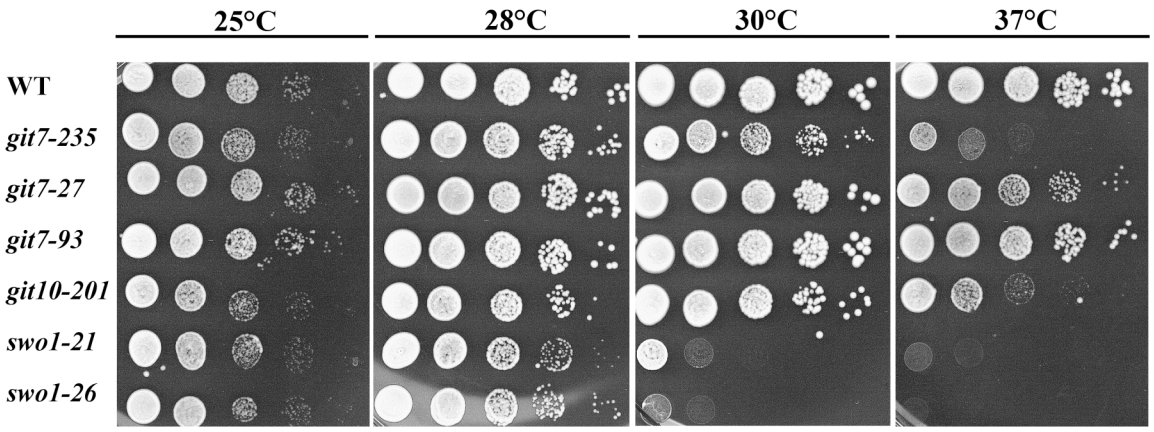
25°C
28°C
30°C
37°C
WT
git7-235
git7-27
git7-93
git10-201
swo1-21
swo1-26

Figure 23. The *git7* mutants and *hsp90* mutants display severe drug sensitivity

git7 mutants and *hsp90* mutants show geldanamycin sensitivity whereas, *git7-93* mutant grows well even in the presence of high concentration of geldanamycin (GA). Spot tests were carried out on YEA rich medium containing (2 µg/ml), (5 µg/ml), and (10 µg/ml) of geldanamycin (GA), or Dimethyl sulfoxide (DMSO) at the permissive temperature (28ºC). Strains FWP72 (wild type), CHP465 (*git7-235),* CHP27 (*git7-27*), CHP800 (*git7-93),* CHP567 (*git10-201*), CHP989 (*swo1-21*), CHP979 (*swo1-26*) were cultured to 1 x 10^7 cells/ml in YEL liquid medium. Cells were washed with YEL medium and adjusted to 2 x 10^7 cells/ml and subjected to five 10-fold serial dilutions (left to right). Five microliters of each culture was spotted to a YEA plate and grown for 3 days at the indicated temperature before photographing.

Figure 23.

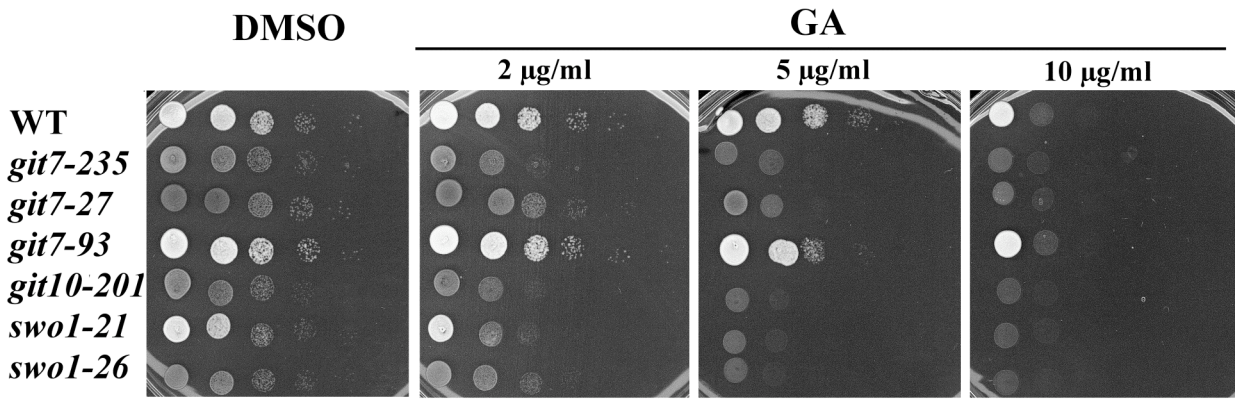
DMSO
GA
2 µg/ml
5 µg/ml
10 µg/ml
WT
git7-235
git7-27
git7-93
git10-201
swo1-21
swo1-26

These results are consistent with the previous finding in *Saccharomyces cerevisiae* where *sgt1* temperature-sensitive mutants showed sensitivity to geldanamycin (BANSAL *et al.* 2004; DUBACQ *et al.* 2002). Surprisingly, a strain carrying the *git7-93* allele, which contains duplication in the C-terminal coding region showed neither temperature sensitivity nor a geldanamycin supersensitive effect (Figure 22, 23).

4.1.2. Association of Git7 with Hsp90 in *Schizosaccharomyces pombe*

The Git7 protein is a member of the *Saccharomyces cerevisiae* Sgt1 protein family. Recent studies show that Sgt1 interacts with Hsp90 in *S. cerevisiae* (KITAGAWA *et al.* 1999) in *Arabidopsis* (TAKAHASHI *et al.* 2003) and in humans (LEE *et al.* 2004). The structures of Git7/Sgt1 proteins and Hsp90 are highly conserved and their functions are essential for viability in yeast and plants. It was also suggested that Sgt1 might act as an Hsp90 co-chaperone in *S. cerevisiae* (DUBACQ *et al.* 2002; SCHADICK *et al.* 2002)

To test if Hsp90 and Git7 interact in *S. pombe,* I carried out an immunoprecipitation experiment in *wt, git7-235*, *git7-27*, *git7-93,* and in *git10-201* strains using α-Sgt1 antibodies that have been shown to cross-react with Git7 (CHARLTON, 2005). The specificity of the immunoprecipitation was confirmed by western blot analysis. Previous efforts to precipitate Hsp90 and Git7 have been unsuccessful (CHARLTON, 2005). Therefore, the immunoprecipitation protocol was repeated with some modification. One important alteration was performing protein extraction in liquid nitrogen instead of using

the Bead Beater (See Material and Methods).

Although, little to no interaction between Hsp90 and Git7 was observed in the wild type strain, I was able to demonstrate the presence of Hsp90 in the Git7 immunoprecipitates in *git7* mutants and *git10-201*. The interaction was modest in *git7-93*, and greater in *git7-27* strain. A significant interaction was observed between Git7 and Hsp90 in *git7-235* strain which has a mutation in the N-terminus and in *git10-201*/*hsp90-201* strain which has a mutation in the middle domain of Hsp90 (Figure 24; See summary and future directions).

4.1.3. Git7 requires a functional Hsp90 to maintain cell wall integrity, normal septation and proper cAMP signaling

Previous analysis showed that Git7 has additional essential functions that are unrelated to cAMP signaling. The *git7* temperature sensitive mutants developed cytokinetic defects when incubated at the restrictive temperature (SCHADICK *et al.* 2002). This led to test if Git7 needs Hsp90 to be able to carry out these functions properly. Therefore, I tested whether the previous cytokinetic defect of the *git7* mutants was due specifically to the need of functional Hsp90.

Figure 24. Git7 and Hsp90 interact in *Schizosaccharomyces pombe*

Immunoblot of protein extracts probed with Hsp90 antibodies (K41220) from α-Sgt1 immunoprecipitation. Cells were grown under repressing conditions (3% glucose). Protein extracts were prepared from strains MAP12 (*wt*), CHP465 (*git7-235)*, CHP27 (*git7-27*), MAP10 (*git7-93)* and CHP567 (*git10-201)* by grinding cells in liquid nitrogen as described in the Material and Methods. Approximately 30 µl of protein extracts were loaded into a 4%-15 SDS-PAGE gradient gel. Crude extracts, along with fractions that bound or failed to bind an α-Sgt1 antibodies, were probed with Hsp90 antibodies and visualized at approximately 90 kDa. Note that Git7 protein detection in the bound lane was hindered due to the fact that Git7 is approximately 43 kDa in size and runs at the same mobility of the IgG heavy chain.

Figure 24.

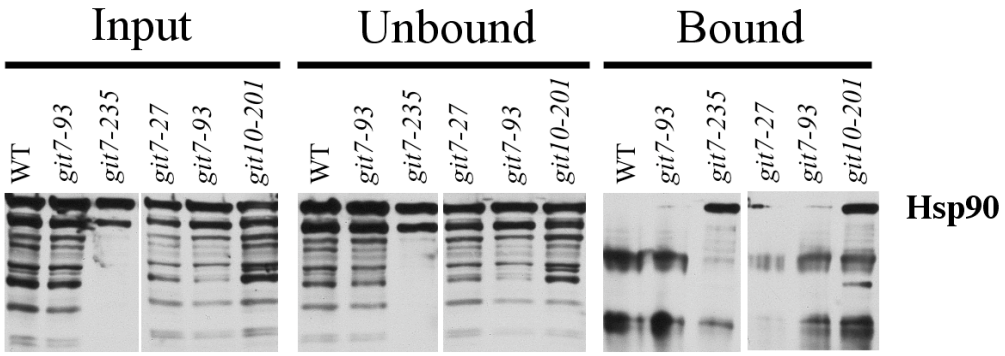
Input
Unbound
Bound
WT
git7-93
git7-235
git7-27
git7-93
git10-201
WT
git7-93
git7-235
git7-27
git7-93
git10-201
WT
git7-93
git7-235
git7-27
git7-93
git10-201
Hsp90

This test was possible by using geldanamycin (GA), a specific Hsp90 inhibitor. Wild type cells, Git7 mutants, and Hsp90 mutants were grown under the permissive temperature (28ºC) in the presence of (GA) (Figure 25A). For comparison, the same strains were also grown at restrictive temperatures (30ºC, 37ºC) (Figure 25B). The cells were fixed by heat and stained with Hoechst 33342 and Calcofluor to visualize the nuclei and septa, respectively. Interestingly, the same cytokinesis defects that were detected in Git7 and Hsp90 temperature sensitive mutants at restrictive temperatures were seen in these cells treated with the geldanamycin at permissive temperatures. The wild-type strain showed mononucleate cells, while the *git7-235, git7-27, swo1-21* and *swo1-26* strains contained mainly multinucleate cells and a multiseptum phenotype in the presence of the drug, which is consistent with the temperature dependent phenotype.

Consistent with *git7-93* being a separate-of-function allele, *git7-93* exhibited no defect in the presence of geldanamcyin. In contrast, *git7-235* showed a severe defect of elongated multinucleated cells in the presence of geldanamycin. This phenotype was also observed at elevated temperatures (Figure 25A,B). The *git10-201* strain showed moderate temperature sensitivity and only moderate sensitivity to geldanamycin (Figure 22, 23).

Figure 25. Cells display morphological defects in Hsp90 and Git7 mutants under elevated geldanamycin or temperature, but not in *git7-93* and *wt* strains

(A) Geldanamycin-dependent morphology of *wt*, *git7-27*, git7-*235*, *git7-93*, *swo1-26, swo1-21*, and *git10-201* strains. Strains were grown in the presence of geldanamycin at the permissive 28°C for 18 hours. **(B)** Temperature-dependent morphology of *wt*, *git7-27*, git7-*235*, *git7-93*, *swo1-26, swo1-21*, and *git10-201* strains. Strains were precultured at 28º and then transferred and grown for 18 hours at 28°C, 30°C and 37°C. Cells were heat-fixed and stained with Hoechst 33342 and Calcofluor. Red arrows indicate multinucleate cells. Red arrowheads indicate multi septum cells.

Figure 25. (A)

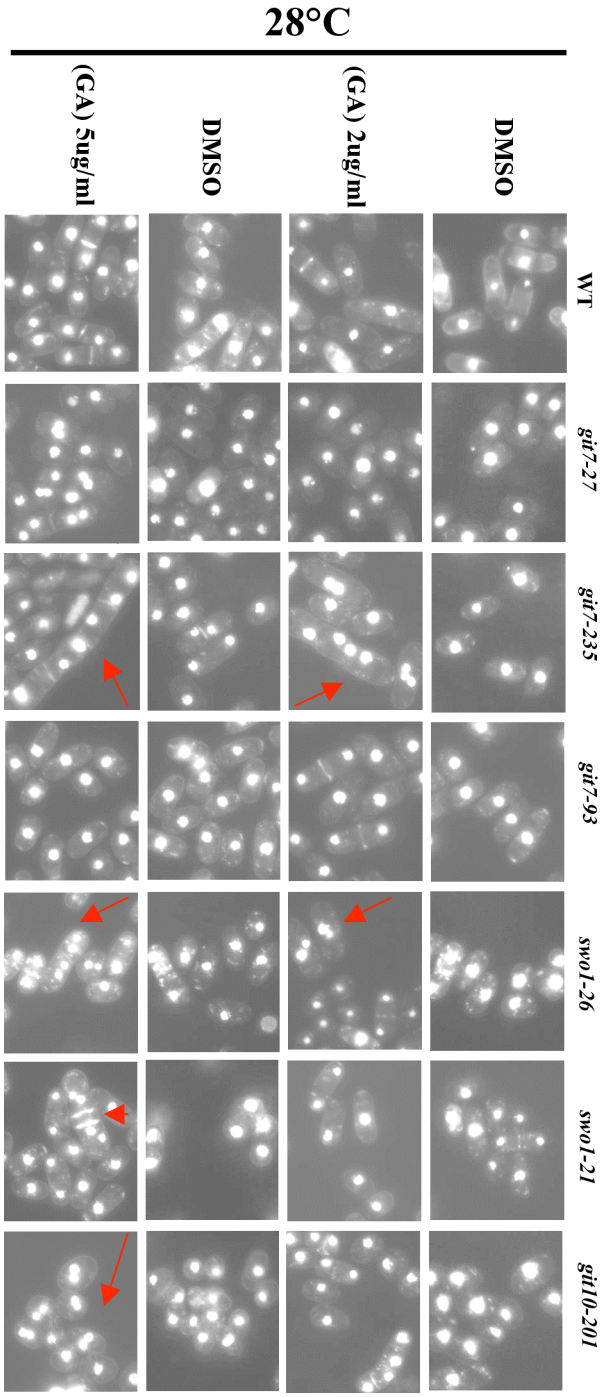
28°C
WT
git7-27
git7-235
git7-93
swo1-26
swo1-21
git10-201
DMSO
(GA) 2ug/ml
DMSO
(GA) 5ug/ml

(B)

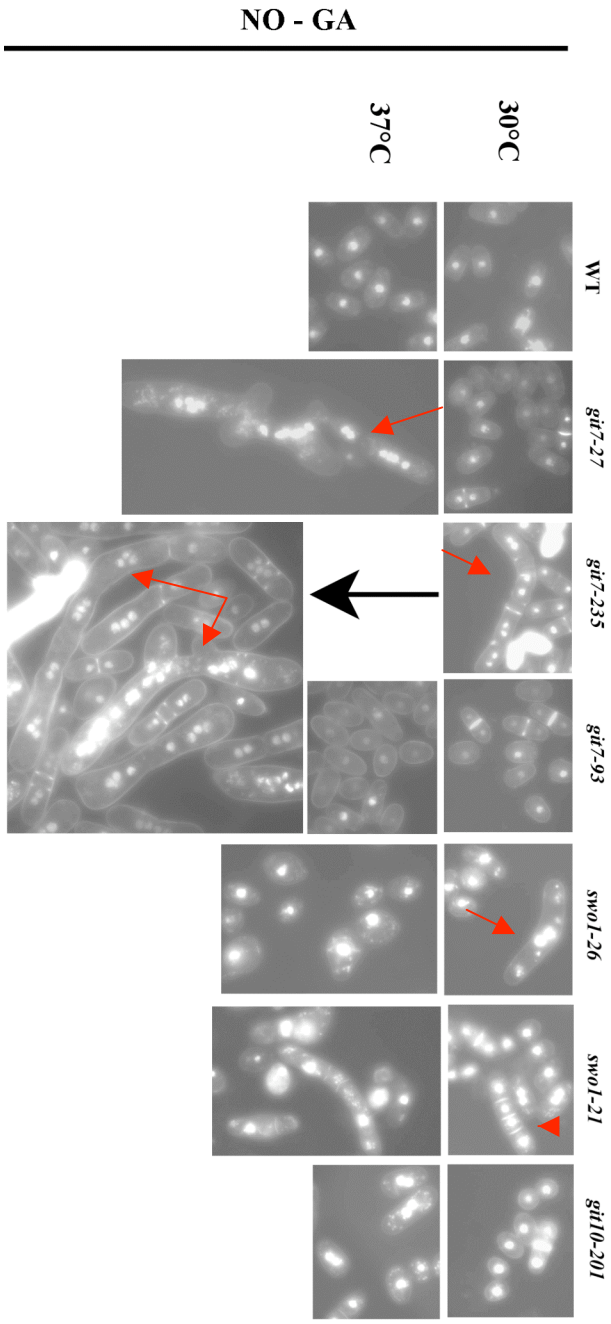
NO - GA
30°C
37°C
WT
git7-27
git7-235
git7-93
swo1-26
swo1-21
git10-201

The *git7 ts* alleles (*git7-27* and *git7-235*) and *swo-1* alleles of *hsp90* confer a cell septation and a temperature/geldanamycin sensitive phenotype not observed in *git7-93* strain and seen mildly in *git10-201* (Figure 25A,B) suggesting that both Git7 and Hsp90 have a separate and independent role from cAMP. Cells lacking adenylate cyclase did not show abnormal morphology even under high concentration of geldanamycin consistent with the idea that cAMP defect is not the cause of the septation defect (Figure 26).

Figure 26. Cells display no morphological defects in *git2* deletion strain under elevated geldanamycin concentration

Cells display no morphological defects in *git2* deletion (FWP190) or wild type (FWP72) strains under elevated geldanamycin concentration whereas (CHP567) *git10-201* strain displayed multinucleate cells at high concentration of geldanamycin. Strains were precultured in 8% glucose YEL medium at 30ºC and then transferred and grown for 26 hours at 30°C in the presence of geldanamycin. Cells were heat-fixed and stained with Hoechst 33342 and Calcofluor.

Figure 26.

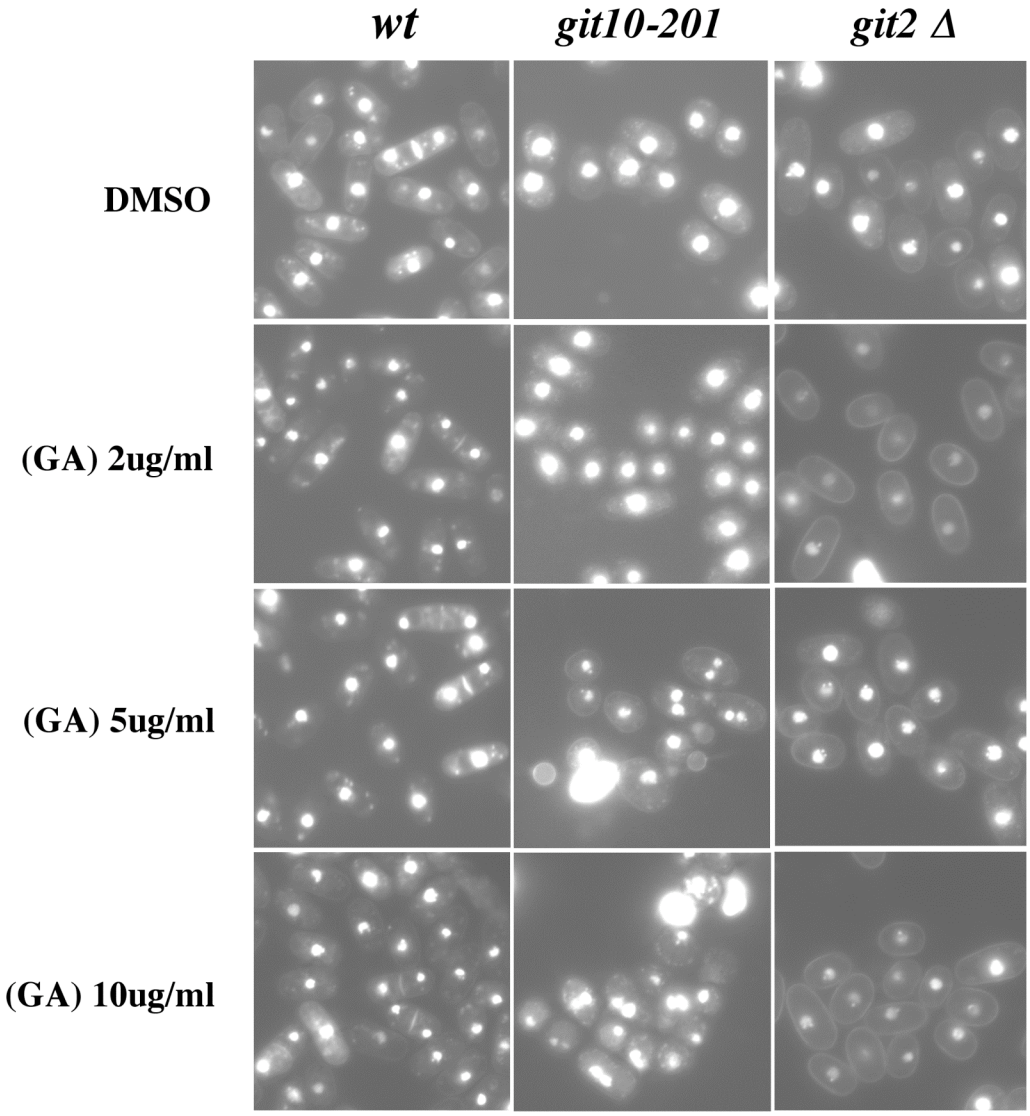

4.2. Hsp90 and Git7 Act in the Assembly of the cAMP Signaling Complex

4.2.1. Hsp90 and Git7 are not regulated by glucose unlike other proteins of cAMP Pathway

Glucose concentration had no effect on Hsp90 and Git7 protein abundance, unlike Git1 and Git2 (Protein proven to be part of the cAMP core complex). MAP5 strain expressing GFP-tagged Hsp90, V5-tagged Git1 and Myc-tagged Git2 were cultured in YEL 0.1% glucose (derepressing) and YEL 8% glucose (repressing conditions).

Protein extraction and immunoblot analysis showed no significant change of Hsp90 abundance in either condition, whereas Git1 and Git2 were significantly affected (Figure 27). Similar to Hsp90, Git7 levels do not appear to be regulated by glucose (CHARLTON, 2005). Despite that a mutation in either the *git7* or *hsp90* genes can result in high β-galactosidase activity for an *fbp1-lacZ* reporter, Hsp90 and Git7 protein levels were not regulated by the glucose conditions. In contrast, Git1 and Git2 protein levels were regulated by glucose conditions (Figure 27). Grandy, 2004 from Hoffman lab had also demonstrated that glucose addition to starved cells causes approximately a twelve-fold decrease in the transcription of *git1* and a thirteen-fold decrease of *git2* after thirty minutes of glucose addition (GRANDY, 2004).

Figure 27. Hsp90 protein levels are not regulated by glucose; Git1 and Git2 are regulated by glucose conditions

Immunoblot analysis of protein extracts obtained from a MAP5 a wild type strain harboring GFP-tagged Hsp90, V5-tagged Git1, and Myc-tagged Git2. Cells were grown under glucose-repressing/glucose rich (R) or derepressing/glucose starved (D) conditions. Actin was used as a loading control.

Figure 27.

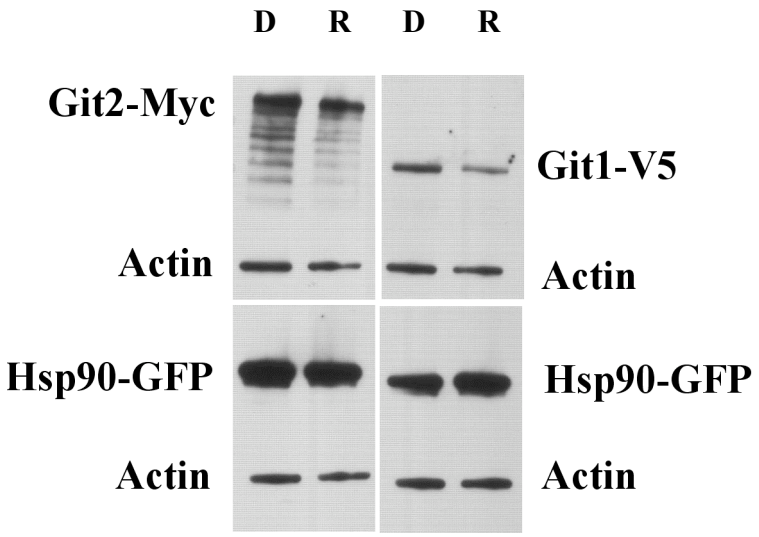
D
R
D
R
Git2-Myc
Git1-V5
Actin
Actin
Hsp90-GFP
Hsp90-GFP
Actin
Actin

Therefore, glucose might directly affect the core component of the cAMP complex (Git1 and Git2), but not proteins required for complex assembly (Hsp90 and Git7; See summary and future directions).

4.2.2. Significant delay between inhibition of Hsp90 and defect in glucose signaling

I have already proven that Hsp90 and Git7 work together in *S. pombe*. In order to understand the role of these proteins in cAMP pathway, I wanted to test the involvement of Hsp90 in the stabilization of key players in cAMP pathway and to investigate Hsp90's possible involvement in the assembly of cAMP complex. Hsp90 is a chaperone that is involved in stabilizing multiple signaling complexes in the cell. The form of Hsp90 required for chaperone activity is the ATP-bound form that allows regulation of the stability of proteins, and permits their activation in signaling cascades. In contrast, when Hsp90 is in the Hsp90-ADP form, its clients will be targeted to the proteasome for degradation. Geldanamycin (GA) is a drug that binds the N-terminal ATP-binding site of Hsp90 and will lock Hsp90 into the inactive form (ADP form). This will result in inhibiting Hsp90 normal function and subjecting its targets to degradation (Figure 6). Therefore, this drug has been widely used to study the role of Hsp90 in modulating the function of signaling proteins, and to aid in Hsp90 client discovery.

In Chapter 3 (Figure 15) I demonstrated that GA treatment affected *fbp1-lacZ* expression. When I examined the effect of geldanamycin (GA) (2, 5, 10 μg/ml) on *fbp1-lacZ*

expression after 18 hours there was a clear dose-dependent derepression of *fbp1-lacZ* expression, although the levels of expression did not reach the levels of that detected in cAMP/glucose mutants. To further test this observation at the protein level, I tested the effect of disrupting Hsp90 using GA on some key players in the glucose/cAMP pathway. After exposing a strain (MAP5) that carries tagged forms of Git1, Git2, and Hsp90 to GA for 18 h, cells were harvested and total protein was extracted by a TCA precipitation method (see Materials and Methods). By conducting immunoblot analyses against the endogenous Git1-V5, Git2-Myc, Gpa2, Hsp90 –GFP and Actin I determined whether the Git1, Git2, or Hsp90 protein levels were affected by GA treatment (Figure 28). In a dose-dependent manner, GA significantly reduced Git1, Git2 and Gpa2 protein levels. In contrast, Hsp90 and Actin levels were not affected (Figure 28). These results demonstrate that functional Hsp90 is important for cAMP signaling since components of this signaling pathway were notably affected.

Therefore I investigated how long it would take GA to have an effect on Git1, and Git2 after drug treatment. MAP5 strain was grown in 3% glucose YEL medium for overnight to log phase. A time course experiment was performed using high does of GA (10 μg/ml).

Figure 28. Hsp90 inhibition affects the stability of cAMP components after 18 hours of drug addition

Cells were treated for 18 h with an increased amount of GA (2 µg/ml, 5 µg/ml, 10 µg/ml). Equivalent amounts of total protein were analyzed by Western blotting. A wild type strain (MAP5) that expresses Git1-V5, Git2-Myc, and Hsp90-GFP was subcultured in YEL 3% glucose o.n. to log phase and then sub-cultured into a fresh YEL 3% glucose with the drug. After 16 h cells were harvested by TCA precipitation, and the western was performed. GA reduced Git1, Git2 and Gpa2 protein levels. As a control I used a Gpa2 deletion. Note the intensity of the nonspecific band above Gpa2 did not change with increase in GA doses.

Figure 28.

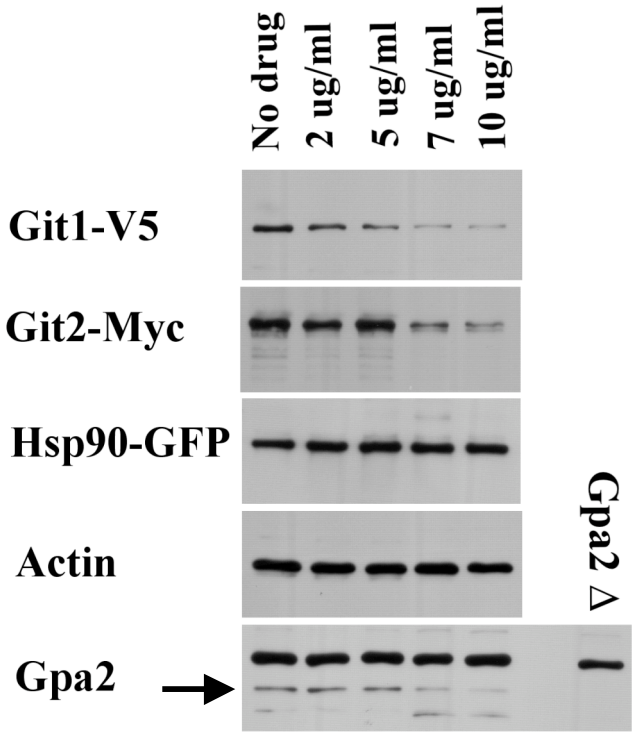
Gpa2
Actin
Hsp90-GFP
Git2-Myc
Git1-V5
No drug
2 ug/ml
5 ug/ml
7 ug/ml
10 ug/ml
Gpa2 Δ

Cells were collected before GA addition (0 time point) and after (15, 30, 60, and 90 minutes) GA addition; cells were kept on ice and then harvested, and proteins were extracted between time points. By conducting immunoblot analyses against the endogenous Git1-V5, Git2-Myc and Actin we determined if their protein levels were affected by GA treatment. Unlike the obvious decline in Git1 and Git2 levels after long GA exposure (18 h) (Figure 28), brief exposure to GA (2 h) fails to reduce Git1 or Git2 levels (Figure 29).

To examine if Hsp90 is a part of the cAMP core complex, I examined the possibility that GA treatment of cells could alter cAMP levels after a brief exposure. Seeing an effect shortly after drug treatment would be a likely consequence of the cAMP complex falling apart. To test this hypothesis, FWP72 strain was grown in EMM complete overnight to 8 $X10^{6}$ (cells/ml). The cultures were then treated with either a high dose of GA (10 μg/ml) or with an equivalent amount of DMSO as control. After two hours, cells were collected by filtration before, and 10 min after exposure to a final concentration of 100 mM glucose. Intracellular cAMP levels were immediately measured as previously described (BYRNE and HOFFMAN 1993) and by using a cAMP kit (Assay Designs).

Figure 29. The abundance of Git1 and Git2 was not affected by brief exposure of GA

MAP5 were grown in YEL 3% glucose medium o.n. to early log phase. A high dose of GA (10 μg/ml) was added and cells were collected before GA addition (0 time point) and after 15, 30, 60, and 90 min after GA addition. Cells were immediately placed on ice and proteins were extracted between time points. A western blot was then performed against the endogenous Git1-V5, Git2-Myc and Actin.

Figure 29.

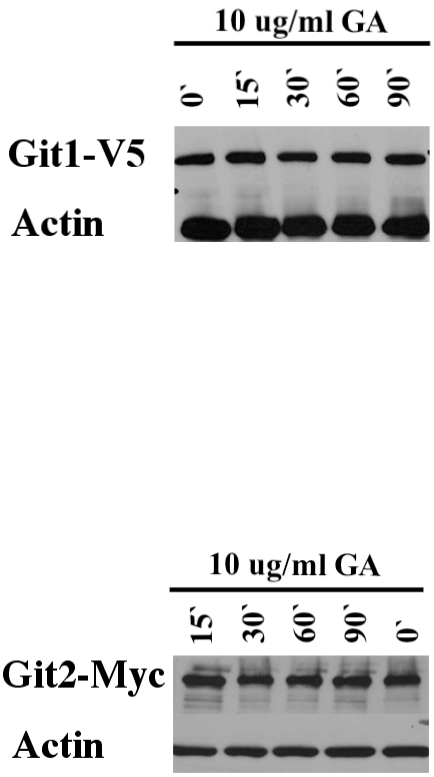
10 ug/ml GA
0`
15`
30`
60`
90`
Git1-V5
Actin
10 ug/ml GA
15`
30`
60`
90`
0`
Git2-Myc
Actin

The results showed that the glucose-triggered cAMP response in the presence of GA were similar to that observed for cells treated with DMSO; they both respond to glucose exposure with almost four-fold increase in cAMP levels (Figure 30). Considered side by side, the cAMP experiment and immunblot analysis indicate that GA treatment does not rapidly alter protein stability or function of the cAMP pathway.

Figure 30. Cyclic AMP response to glucose in the presence of GA

To examine the effect of brief exposure of GA treatment on cAMP signaling, we assayed the glucose-triggered cAMP response after incubating the culture with GA for two hours. Cells were cultured overnight in EMM complete to log phase. Then, cells were either treated with DMSO or with (10 μg/ml) of GA. cAMP levels were immediately measured as previously described (BYRNE and HOFFMAN 1993) and by using by a cAMP kit (Assay Design) prior to glucose addition to the cultures, as well as 10 min after glucose addition to cultures either grown in the presence of DMSO or GA for 2 h. Both display a similar-fold increase in cAMP levels after addition of glucose.

Figure 30.

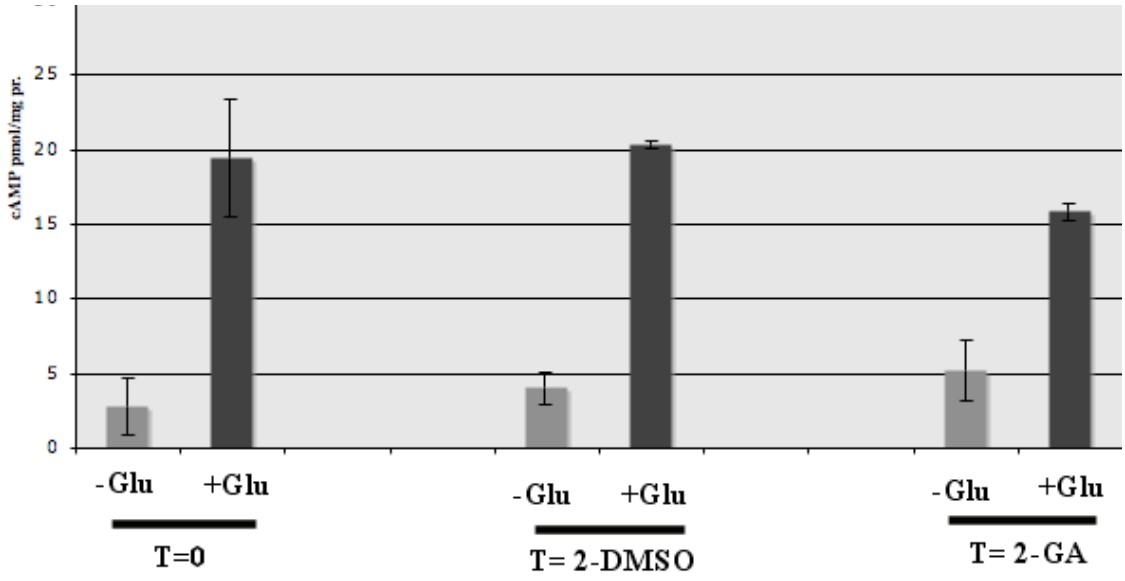
cAMP pmol/mg pr.
25
20
15
10
5
0
-Glu
+Glu
T=0
-Glu
+Glu
T= 2-DMSO
-Glu
+Glu
T= 2-GA

CHAPTER FIVE

SUMMARY AND FUTURE DIRECTIONS

SUMMARY AND FUTURE DIRECTIONS

From yeast to mammals, Hsp90 and Sgt1 family proteins (including Git7) are highly conserved proteins, which function together as chaperones. In *S. cerevisiae*, the Hsp90 and Sgt1 interaction is important for the formation of the CBF3 complex (LINGELBACH and KAPLAN 2004). In *Arabidopsis thaliana*, the Hsp90-Sgt1-RAR1 interaction is involved in forming the disease resistance complex (BOTER *et al.* 2007). This thesis is the first demonstration of Hsp90 and Git7 functioning together in *S. pombe* in the initial assembly of the cAMP signaling complex. In this section I will summarize and discuss findings from this thesis and propose a model for the role of Hsp90 and Git7 in cAMP pathway.

5.1. Git10 encodes an Hsp90 protein involved in the cAMP pathway

I have cloned *git10*, and shown that it encodes an Hsp90/Git10/Swo1 protein that acts in the *S. pombe* cAMP-signaling pathway. This pathway senses environmental glucose to repress transcription of genes involved in sexual development and gluconeogenesis, such as the *fbp1*$^{+}$ gene (HOFFMAN 2005a; HOFFMAN 2005b). I found that attenuating Hsp90 function either by mutation, pharmacological inhibition, or temperature stress impairs cAMP-mediated glucose signaling, consistent with a specific role for Hsp90 in the glucose/cAMP pathway.

Figure 31. Git10 in cAMP signaling pathway encodes an Hsp90 protein

A new member of the cAMP pathway (Git10) was identified as an Hsp90 protein. The Git3 receptor detects glucose and transfers the signal to the Gα subunit that in turn activates Git2 adenylate cyclase, which produces cAMP. Three other proteins Git7, Git10/Hsp90, and the Git1 are also required for the activation of Git2. Hsp90 interacts with Git7 (Sgt1 homolog) and has a critical role in the cAMP/glucose signaling.

Figure 31.

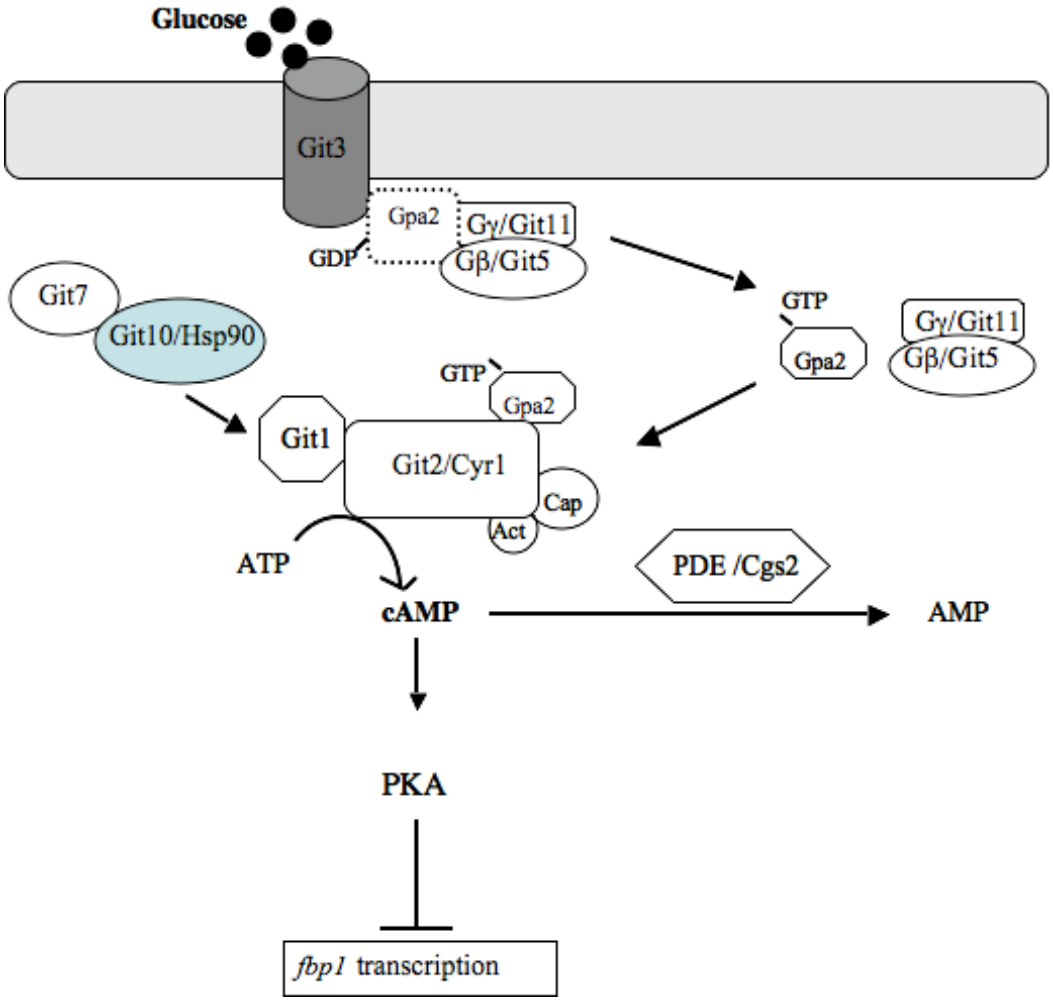
Glucose
Git3
Gpa2
Gγ/Git11
GDP
Gβ/Git5
Git7
Git10/Hsp90
GTP
Gpa2
Gγ/Git11
Gβ/Git5
GTP
Gpa2
Git1
Git2/Cyr1
Cap
Act
ATP
PDE /Cgs2
cAMP
AMP
PKA
fbp1 transcription

A defect in cAMP signaling in a *git10-201* mutant strain was previously demonstrated (BYRNE and HOFFMAN 1993), as was suppression of the *fbp1*$^{+}$ regulatory defect by cAMP addition to the growth medium or by overexpression of the *git2*$^{+}$/*cyr1*$^{+}$ adenylate cyclase gene (HOFFMAN and WINSTON 1991). Therefore, Hsp90 activity appears to be required for cells to detect glucose and activate adenylate cyclase.

The *hsp90*$^{+}$ is one of seven genes required for adenylate cyclase activation, which form at least two functionally-distinct groups as determined by the ability of mutations to be suppressed by the mutationally-activated Gpa2^{R176H} Gα or by overexpression of the wild type Gpa2^{+} protein (LANDRY and HOFFMAN 2001; WELTON and HOFFMAN 2000). Increasing Gpa2 function bypasses the loss of the Git3 GPCR or Git5-Git11 Gβ Gγ, but not mutations affecting the Git1 C2-domain protein (KAO *et al.* 2006), the Git7 Sgt1-family member protein (SCHADICK *et al.* 2002), or the Git10 Hsp90 protein.

The central domain of Hsp90 appears to be a major site for client protein interactions (FONTANA *et al.* 2002; MEYER *et al.* 2003; SATO *et al.* 2000). Recent findings revealed this domain could also play a role in distinguishing between different types of client proteins (HAWLE *et al.* 2006). Therefore, the *git10-201* L338P mutation in the central domain might impair client protein activity in the cAMP pathway specifically, whereas the temperature sensitive alleles *swo1-21* which affects the N-terminal ATP-binding domain and *swo1-26* which affects the C-terminal dimerization domain might cause a

universal impairment of Hsp90 function in the cell. Thus, *git10-201* represents a separation-of-function allele of *hsp90*$^{+}$, which confers a defect in cAMP signaling, but not other essential processes. A similar observation was reported in *C. elegans* in that loss of Hsp90/DAF-21 involved in cGMP signaling confers an early larval lethality; however, a missense mutation affecting a residue in the middle domain produces a viable adult with a chemosensory defect (BIRNBY *et al.* 2000). The *daf-21* mutation allows *C. elegans* to enter the dauer larval form in the absence of temperature or nutritional stress signals similar to the *S. pombe git10-201* mutation that allows mating and sporulation without the need of a starvation signal (Figure 13). Mapping of the residues altered by the *da-f21* mutation and by the *git10-201* mutation onto the crystal structure of the *S. cerevisiae* Hsc82p central domain reveals that these two residues are in close proximity to each other (Figure 20). Therefore, these two separation-of-function alleles may affect their individual cyclic nucleotide signaling pathways via the same mechanism.

5.2. A novel link between glucose and heat sensing appears to involve Hsp90

This thesis also revealed a new insight into heat stress in *S. pombe*. It has been long known that heat stress activates the Spc1/Sty1 SAPK pathway required for *fbp1*$^{+}$ transcription, presumably by regulating the activity of the Pyp1 tyrosine phosphatase (SAMEJIMA *et al*. 1997). Data from this thesis further indicate that in addition to activating the SAPK pathway, heat stress reduces PKA activity. Stresses such as nitrogen starvation and osmotic stress, which activate the SAPK pathway, do not derepress *fbp1*$^{+}$

transcription (DEVOTI *et al*. 1991; JANOO *et al*. 2001; STETTLER *et al*. 1996; STIEFEL *et al*. 2004; YANG *et al*. 2003), indicating that reduction of PKA activity is required for *fbp1*$^{+}$ derepression. Therefore, I have discovered a novel link between glucose and heat sensing that appears to involve Hsp90. Heat stress may redirect Hsp90 from acting in the cAMP pathway to acting upon targets that are critical to survival of heat stress (Figure 32). As a secondary effect, the ability of heat stress to reduce PKA activity and thus mimic glucose starvation may assist in producing a growth arrest that enhances cell survival at elevated temperatures. Greater insight into the relationship between heat stress and glucose signaling might be gained by studying glucose triggered cAMP signaling by assaying cAMP levels. Heat stress might alter the formation of the cAMP complex that is required for glucose repression. Comparing the cAMP complex composition (Git2-Git1 complex) purified under starvation conditions (nutrition stress) and purified under elevated temperature (heat stress) could also provide new insights. Another avenue of research would test whether Hsp90 is required for the localization of any of the cAMP complex proteins (Gpa2, Git1, and Git2) to either the plasma membrane or to punctate structures in the cytoplasm. This can be accomplished easily by immunofluorescence using geldanamycin or heat stress, which might induce the delocalization of these proteins.

Figure 32. Stress may redirect Hsp90 from acting in the cAMP pathway to acting upon targets that are critical to survival of heat stress.

(A) Hsp90 is involved in different processes in the cell including the cAMP signaling discovered in this thesis. **(B)** Heat stress might lead to accumulation of misfolded proteins might titer away Hsp90 from cAMP resulting in the release of *fbp1* transcription under repression conditions.

Figure 32.

A.

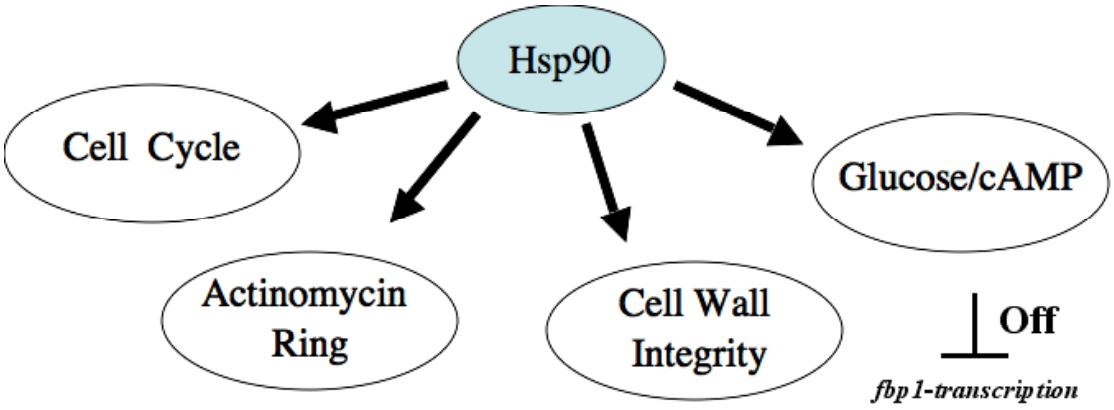
Hsp90
Cell Cycle
Glucose/cAMP
Actinomycin Ring
Cell Wall Integrity
Off
fbp1-transcription

B.

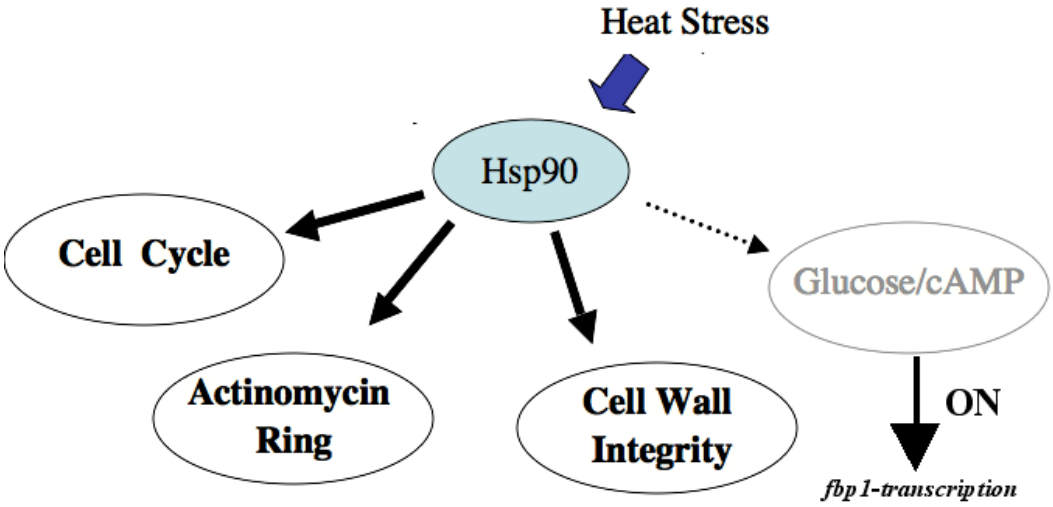
Heat Stress
Hsp90
Cell Cycle
Glucose/cAMP
Actinomycin Ring
Cell Wall Integrity
ON
fbp1-transcription

5.3. Hsp90 and Git7 transiently interact in *S. pombe*

Human, *S. cerevisiae*, and *Arabidopsis thaliana* Hsp90 proteins have been shown to interact with the Sgt1 protein (homologous to Git7), which appears to function as a co-chaperone to Hsp90. Sgt1 recruits specific clients to Hsp90 and aids in the transient assembly of protein complexes (CATLETT and KAPLAN 2006);(LINGELBACH and KAPLAN 2004; TAKAHASHI *et al.* 2003). In *S cerevisiae*, this interaction is essential for the formation of the CBF3 (LINGELBACH and KAPLAN 2004). In *Arabidopsis thaliana*, the Hsp90-Sgt1-RAR1 interaction is involved in forming the disease resistance complex (BOTER *et al.* 2007). Both Sgt1 and Hsp90 are highly conserved in eukaryotes; thus, this chaperone co-chaperone interaction might be conserved from yeast to humans.

Findings that Sgt1 interacts with Hsp90 in other systems and the demonstration that *git7* mutants are geldanamycin supersensitive (Chapter 4) led me test whether Git7 and Hsp90 form a co-chaperone complex in *S. pombe.* Experiments revealed an interaction between Git7 and Hsp90 in *S. pombe*. Surprisingly, mutations in both *git7* and *git10*/*swo1* act to strengthen this interaction (Figure 24). These mutations might change the conformation of the proteins, and therefore could stabilize a transient interaction. This result indicates that the Hsp90-Git7 interaction must remain transient for the complex to function properly.

Other research has also indicated that Hsp90 transient interactions can be stabilized by mutations in interacting proteins. A study by Piper *al et.* 2004 showed that many Hsp90 interactions with other proteins are transient, preventing an analysis of these associations by the two-hybrid system. However, they demonstrated that these Hsp90/Hsp82 interactions could be stabilized *in vivo* by using an Hsp90/Hsp82 mutation that inhibits the ATP hydrolysis step of the Hsp90 chaperone cycle (MILLSON *et al.* 2005). Similarly, the Sgt1 interaction with Hsp90 and Skp1 in *S. cerevisiae* is stabilized by a mutation affecting the C-terminus of Sgt1 designated as *sgt1-5*, disrupting CBF3 assembly and affecting cell growth (LINGELBACH and KAPLAN 2004). Thus, it is evident that the transient interaction between Hsp90 and its Sgt1/Git7 co-chaperone is critical to the function of this complex.

Observations in this thesis do not address whether the Git7-Hsp90 interaction is direct but could represent that they are in the same complex. Additional proteins might be required to mediate the Git7-Hsp90 interaction. This can be investigated by using yeast two-hybrid to test these interactions. Further studies are also needed to determine which domains in Git7 and Git10/Hsp90 are involved in the interaction. In addition, different conformational states of Hsp90 (Hsp90-ADP open structure /Hsp90-ATP closed structure) might have an effect on the nature of these interactions. This can be tested by performing Hsp90-Git7 co-immunoprecipitation in *wt* and different *git* mutants and *git10-201* in the presence of geldanamycin (to lock Hsp90 in the ADP–bound

conformation) or molybdate (to lock Hsp90 in the ATP–bound conformation) and assess the effect of these different conditions on Git1-Git2 interaction.

5.4. Git7 is an Hsp90 co-chaperone

As mentioned above, Sgt1 is involved in kinetochore assembly, cAMP signaling, and disease resistance in different organisms. Results from our lab revealed that although Git7 protein is essential, it does not appear to be involved in kinetochore function in *S. pombe*. Deletion of *git7* is lethal, thus indicating its involvement in cellular processes other than cAMP signaling, which is not essential for cell viability in *S. pombe* (SCHADICK *et al.* 2002). The presences of three *git7* glucose insensitive mutations (*git7-235, git7-27*, and *git7-93*) were informative in studying its function in *S. pombe* (Figure 33). The *git7-235* and *git7-27* mutations confer defects in cell wall integrity and septation as well cAMP signaling, but *git7-93* confers only a cAMP defect. Therefore, mutations affecting either the N-terminal (TPR domain) or in the highly conserved C-terminus (SGS domain) disrupt cAMP signaling. However, the N-terminus of Git7 serves another function in addition to a role in cAMP signaling. Figure 33 summarizes phenotypes associated with *git7* mutants in *S. pombe*.

After Git10 was identified as Hsp90, we significantly advanced our understanding of the function of Git7 in *S. pombe*. As discussed above, I was able to show that Hsp90 co-immunoprecipitates with the Git7 in *S. pombe*. However, these observations alone do not

demonstrate that Git7 is an Hsp90 co-chaperone.

Findings from other researchers indicating that Hsp90 and Sgt1 interact in various pathways in different organisms have assisted my exploration of Hsp90 function in *S. pombe*. A mutation in *git7* or in *hsp90* causes elevated levels of *fbp1* transcription (HOFFMAN and WINSTON 1990; HOFFMAN and WINSTON 1991). Hence, both Git7 and Hsp90 are important in proper cAMP signaling in *S. pombe.* Abrogating Hsp90 function using a pharmacological approach confirmed the genetic data. Furthermore I found that temperature-sensitive Git7 mutants (*git7-27* and *git7-235*) display GA super sensitivity at the permissive temperature. Schadick *et al.*2002 showed that that *git7* temperature-sensitive mutants develop cytokinetic defects when they are incubated at the restrictive temperature. Therefore, I used geldanamycin to test whether the previous cytokinetic defect observed in *git7* mutants at elevated temperature was specific to Hsp90 function with Git7. Consistent with Schadick *et al.*2002 findings, this analysis revealed that Geldanamycin-treated *git7* mutants (*git7-27* and *git7-235*) exhibit similar deleterious cytokinesis defects (Figure 25,33). Remarkably, *git7-93* and a *git2* deletion show no cytokinesis defect in the presence of geldanamycin although they both displayed severe defects in cAMP signaling, demonstrating that the cytokinesis is not due to the defect in cAMP signaling.

Figure 33. Schematic of Git7 protein structure

Schematic of the Git7 protein structure showing the three domains: TRP, CS, and SGS and the phenotypes associated with *git7* mutants in *S. pombe* presented in this thesis. A star represents a mutation.

Figure 33.

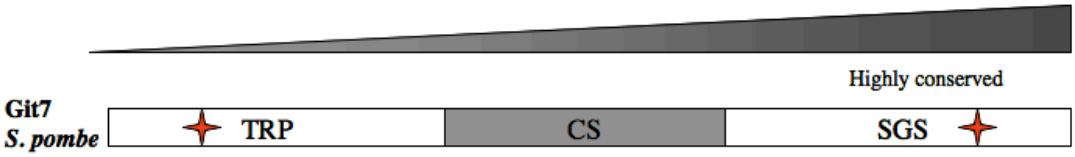

-Temperature sensitive

- Morphological defects
  In the presence of GA
  At permissive temperature

-cAMP defect

- GA supersensitive

-Not temperature sensitive

-Normal in the presence of
  GA and at elevated temperature

-cAMP defect

- Not GA sensitive

Recently, it was reported that Hsp90 has a role in assembling the myosin II complex, which is important for forming the actomyosin ring involved in cytokinesis (MISHRA *et al.* 2005). The *git7* mutants show phenotypic similarities to *hsp90*, *myo2*, and *rng3* mutants. The multinucleated phenotypes of the *S. pombe git7* alleles *git7-235* and *git7-27* suggest that the *git7* mutants might also be defective in actomyosin ring assembly as seen with *hsp90*, *myo2*, and *rng3* mutants. Therefore, Git7 in addition to Hsp90 and Rng3 might assist in proper Myo2p function in the fission yeast *S. pombe*.

Temperature, pharmacological, and western analyses in this thesis suggest that Hsp90 and Git7 function in tandem in *S. pombe*. Git7 with Hsp90 can help in forming at least two complexes. Given that *git7-27* and *git7-235* mutant alleles confer both morphological defects and cAMP signaling phenotypes similar to those of the *swo1*$^{-}$ mutant alleles, it suggests that Hsp90 and Git7 work in partnership in at least two different processes, cell division and in cAMP signaling. Furthermore, the presence of the separation-of-function alleles, *git7-93* and *git10-201*, implies that these proteins act on a specific client protein or on the assembly of a protein complex acting in the cAMP pathway and argues against a model in which mutations that impair Git7 and/or Hsp90 activity simply create a general stress that mimics a glucose-starvation signal. The focus should remain on investigating their roles in cAMP, not their role in other processes, which can be tempting. Focusing on *git7-93* and *gi10-201* alleles, both of which confer defects in cAMP but do not affect essential process, would be appropriate to restrict studies to

cAMP signaling. In addition, mutations in the *git7* middle domain would be worth investigating since little is known about this domain.

5.5. A model of the roles of Hsp90 and Git7 function in the cAMP pathway

Hsp90 and Sgt1/Git7 maintain the activity of a number of cellular proteins that are involved in signal transduction. It is proposed that Hsp90 and its co-chaperone Sgt1 act in signal transduction by assisting in complex formation. The downstream effector of Git7 and Hsp90 in the *S. pombe* cAMP signaling pathway is still unclear. In *S. cerevisiae*, Dubacq *et al.*2002 demonstrated that cAMP activity was affected by the *sgt1-5* mutation. In addition, they showed that Sgt1 physically interacts with adenylate cyclase (Cyr1/Cdc35) although this is only detected when the two proteins are over-expressed. In *S. pombe*, Hsp90 and Git7 are both required even in a strain carrying an activated *gpa2* allele. Therefore Hsp90 and Git7 may be required for stabilization of Gpa2 or adenylate cyclase, or for efficient coupling of Gpa2 to adenylate cyclase.

The Hsp90 machinery appears to regulate signaling pathways in cells by one of two mechanisms: in some cases it appears to stabilize client proteins; in others it functions in the assembly of protein complexes. In order to understand the role of Hsp90 in cAMP pathway, I tested three models (Figure 34). The first model suggests the involvement of Hsp90 in the stabilization of key players in cAMP pathway. The second model is that Hsp90 is a permanent structural component of the cAMP complex. Finally, the third

model is that Hsp90 is involved in the assembly of cAMP complex (Git2-Git1-Cap-Actin) (Figure 34).

To test the first model, I performed a time point experiment where brief exposure of GA to cells (2 h) demonstrated no change in Git1 and Git2 abundance (Figure 29). This indicates that Hsp90 does not stabilize Git1 or Git2 in the cAMP pathway.

To test the second model, I showed that cells treated with GA for 2 h were still able to produce cAMP signal in response to glucose addition (Figure 30). If Hsp90 is a permanent component of the cAMP pathway, I would have expected GA treatment to produce rapid loss in signaling. Therefore, my data indicate that Hsp90 is not part of the core Git1-Git2 cAMP complex.

To test the third model, I showed that GA treatment significantly reduced Git2, Git1, and Gpa2 protein levels after a long period of drug exposure (18 h) (Figure 28). This delay in cAMP defects suggests that Hsp90 is not a core component of the cAMP complex but is required for the complex assembly. These results might also imply that compromising Hsp90 function by GA only destabilized the newly synthesized Git2, Git1, Gpa2 (the free forms), but did not affect the pre-existing assembled complexes.

Figure 34. Three models proposed to test the function of Hsp90 in cAMP pathway

Geldanamycin (GA) is a drug that binds the N-terminal ATP-binding site of Hsp90 and will lock Hsp90 into the inactive form (ADP form). This will result in inhibiting Hsp90 normal function and subjecting its targets to degradation. Therefore, this drug has been used in this thesis to test the three proposed models to investigate Hsp90 role in cAMP signaling. **(A)** The first model suggests the involvement of Hsp90 in the stabilization of key players in cAMP pathway. **(B)** The second model suggests that Hsp90 is a permanent structural component of the cAMP complex. **(C)** The third model suggests that Hsp90 is involved in the assembly of the cAMP complex.

Figure 34.

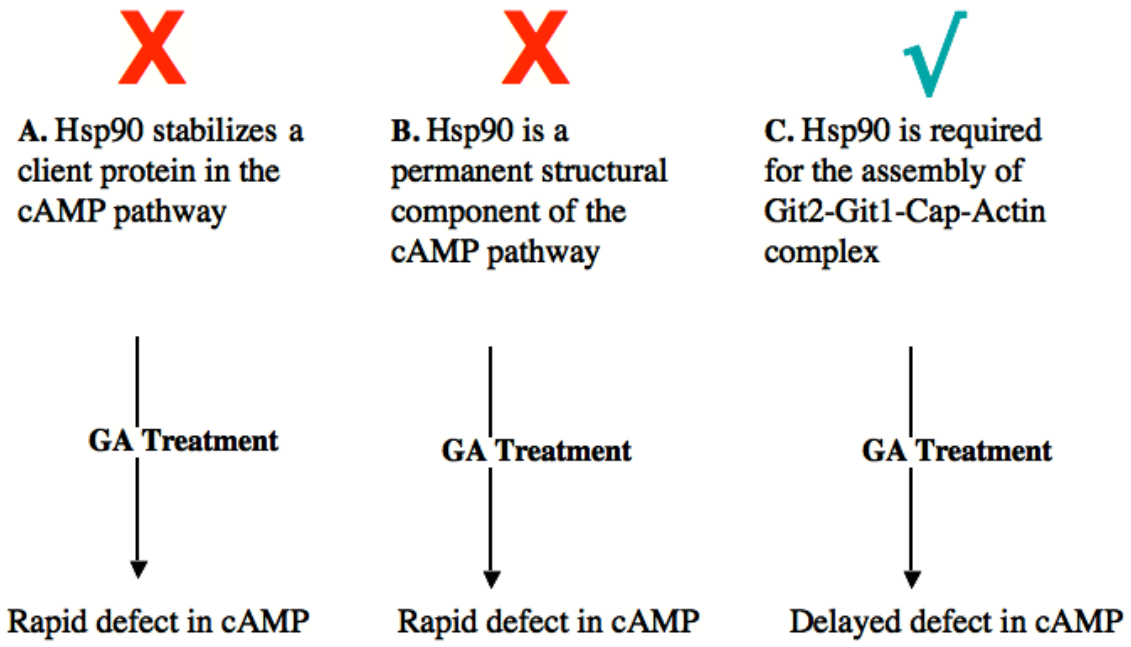
X
X
√
A. Hsp90 stabilizes a client protein in the cAMP pathway
B. Hsp90 is a permanent structural component of the cAMP pathway
C. Hsp90 is required for the assembly of Git2-Git1-Cap-Actin complex
GA Treatment
GA Treatment
GA Treatment
Rapid defect in cAMP
Rapid defect in cAMP
Delayed defect in cAMP

Previous findings in our lab have shown that adenylate cyclase (Git2) forms a complex with Git1 by co-immunoprecipitation (KAO *et al.* 2006) and that TAP tag purification (Wang ,unpublished data) of Git1 and Git2 in a wild type strain did not show the association of Git7 with Hsp90 (Figure 35A). However, it maybe that Hsp90 and Git7 work together in an initial step to aid in Git-Git2 complex formation and that this interaction is transient to detect in a TAP tag experiment. We hypothesized that if this were the case, we might observe loss of Git1-Git2 interaction in a Git7 or Hsp90 mutant background. To test this hypothesis I performed TAP purification in two mutant backgrounds: *git10-201* and *git7-235*. Git2-TAP tag purifications in these strains were not successful (data not shown). However, TAP tag purifications of Git2-TAP in strains carrying *git7-93* mutation and *git2-7* were successful (Wang, unpublished data). The Git1-Git2 interaction was lost in these mutants background and interestingly, Hsp90 was also found with Git2-TAP.

Findings from *git7-93* and *git2-7* Git2 TAP tag purifications suggest that Git7, an Hsp90 co-chaperone, is not a core component of the cAMP complex but a critical element for maintaining the Git1 and Git2 interaction, since the absence of functional Git7 protein resulted in a defect in complex assembly. Furthermore, Hsp90 detection with Git2-TAP in *git2* and *git7* mutant backgrounds supports the idea that Hsp90 is not a regular component of the active core complex but rather assists in assembly process. This abnormally stable interaction of Hsp90 with Git2 might prevent Git1 assembly with Git2

or might freeze the complex in an inactive state due to a defect in a component in the signaling pathway (Figure 35 B,C).

Consistent with this role for Hsp90-Git7, analyses of the cAMP response and of Git1, Git2, and Gpa2 levels after exposure to GA demonstrate that the effect of GA is not immediate loss of protein stability or cAMP signaling. In addition, unlike the core components of cAMP complex Git1 and Git2, Hsp90 and Git7 proteins levels are not regulated by glucose conditions; even though a mutation in either gene can result in *fbp1*-derepression. This further supports the idea that Hsp90 and Git7 are not core members of the cAMP complex but are required in the complex assembly.

Therefore, on the basis of the research performed for this thesis and other findings from our laboratory I propose a model where Git7 and Hsp90 form a co-chaperone complex and probably function together as an initial step to aid in Git1-Git2-Cap-Actin complex formation (Figure 31,35A).

Figure 35. Git7 and Git10/Hsp90 are required for the assembly of the cAMP complex

Schematic diagram showing the composition of the cAMP complex by using TAP and mass spectrometry analysis in different strain backgrounds. The Git2-Git1 interaction is lost in *git7-93* and *git2-7* mutants. Defective Git2-complexes contain Hsp90 in *git7-93* and *git2-7*. Incorporating the current findings from our lab in addition to the new data presented here support the idea that Git7 and Hsp90 are required for the assembly of the cAMP complex but are not permanent structural components of the active complex.

Figure 35.

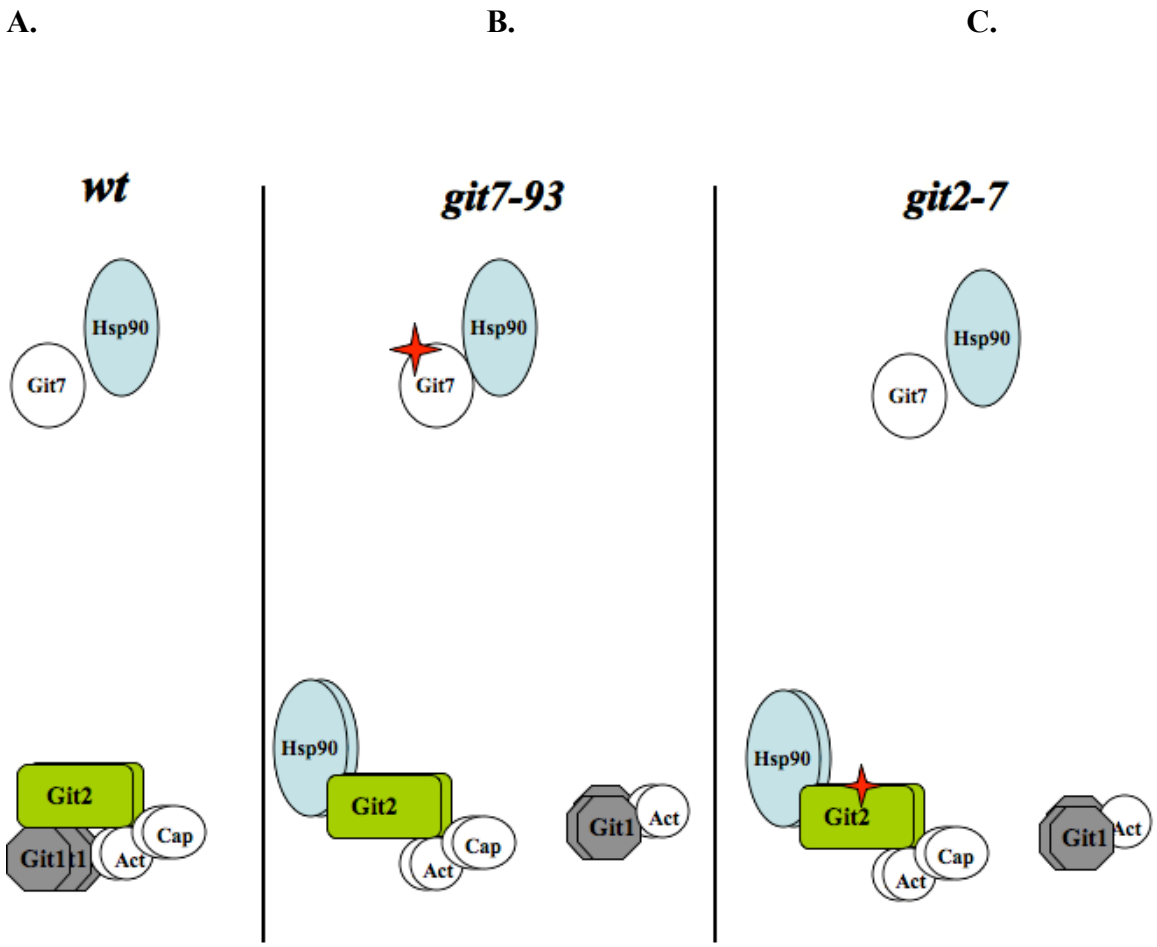
A.
B.
C.
wt
git7-93
git2-7
Hsp90
Git7
Hsp90
Git7
Hsp90
Git7
Hsp90
Git2
Cap
Act
Hsp90
Git2
Cap
Act
Git1
Act
Hsp90
Git2
Cap
Act
Git1
Act

To further understand the role of Hsp90-Git7 in cAMP complex formation, an immunoprecipitation and western analysis will be useful to check the presence of both Hsp90 and Git7 in Git2-Git1 complexes in different mutant backgrounds (*git7-235*, *git7-93*, *git7-27*, *git10-201, swo1-21, swo1-26, and git2-7*) and under different glucose conditions. Hsp90 and possibly Git7 might be also present in Git2 immunoprecipitates in some of these mutant backgrounds. These results might show that Hsp90 and Git7 bind to Git2 prior to complex assembly and that their presence with cyclase prevents Git1 from binding Git2. In addition, Hsp90 might be absent or reduced from the adenylate cyclase complex under conditions where the complex should be functional and active.

How does the co-chaperone complex (Hsp90-Git7) function to activate the Git1-Git2 complex in cAMP/glucose signaling pathway? Future studies could focus on the regions of Git1 and Git2 that interact with each other, as well with the Hsp90-Git7 complex. Findings from fission yeast will provide an additional regulatory mechanism of this co-chaperone complex that will contribute to a better understanding of their functions in other organisms.

APPENDIX ONE

THE DISCOVERY OF NOVEL HUMAN PDE7A INHIBITORS USING YEAST AS A CELL-BASED SYSTEM FOR HIGH THROUGHPUT SCREENING

1. INTRODUCTION

1.1. Cyclic AMP

Cyclic AMP is synthesized from adenosine triphosphate (ATP) by adenylate cyclase and is degraded by cAMP phosphodiesterase. Cyclic AMP activates protein kinase A (PKA), which consists of two catalytic and two regulatory subunits. It binds the regulatory subunits of a protein kinase, and this causes the dissociation of the regulatory and catalytic subunits resulting in the activation of the catalytic subunits. Concentration of cAMP in the cell is critical. Any change in this process can result in aberrant cell behavior. For example, impaired cAMP signaling may contribute to the pathophysiology of cardiovascular, neurological, metabolic and inflammatory disorders (CAI *et al.* 2001; MOORE and WILLOUGHBY 1995; MOVSESIAN and BRISTOW 2005).

1.2. Phosphodiesterases

Phosphodiesterases (PDEs) are enzymes that hydrolyze the cyclic nucleotide second messengers, cAMP and cGMP. There are 21 genes that encode 11 families of mammalian PDEs. There are PDEs which are cAMP-specific enzymes (PDE4, PDE7, PDE8), cGMP-specific (PDE5, PDE6, PDE9) and also PDEs, which can act on both cAMP and cGMP (PDE1, PDE2, PDE3, PDE10, and PDE11). Chemical inhibitors of PDEs are potential therapeutic compounds for the treatment of a variety of diseases including Alzheimer's Disease, Parkinson's Disease, Huntington's Disease, schizophrenia, asthma, pulmonary

disease, hypertension, stroke, rhinitis, chronic lymphocytic leukemia, prostate cancer, thyroid disease, cardiac disease, multiple sclerosis, rheumatoid arthritis, penile erectile dysfunction and depression. PDE enzymes are good targets for pharmacological inhibition due to their unique tissue distribution, structural and functional properties.

1.3. PDE7

PDE7 is a cAMP specific family. There are two PDE7 genes, PDE7A (has three splicing variants A1, A2, A3) and PDE7B (has three splicing variants B1, B2, B3). Both PDE7A and PDE 7B show 70% catalytic domain homology. PDE7 is sensitive to the nonselective PDE inhibitor IBMX (Figure 1) and resistant to rolipram, a PDE4 selective drug.

1.4. PDE7A

Expression of PDE7A1 RNA has been detected in pancreas, lung, spleen, testis, brain, B cells and in $CD4^+$ and $CD8^+$ T cells. It has been shown that PDE7A is upregulated in $CD4^+$ T cells, and that inhibition of PDE7A up-regulation with an antisense oligo leads to inhibition of cell proliferation, suggesting PDE7A involvement in the regulation of T cell proliferation (LI *et al.* 1999).

Figure 1. Human PDE7A binding to IBMX

PDE7A (1zkl) ribbon and surface structure showing the location of IBMX binding (Black color). The graphic image was created using Pymol (DeLano Scientific) and by MBT protein workshop (MORELAND *et al.* 2005) available on the PDB website. Human PDE7A crystal structure data was obtained from (WANG *et al.* 2005a).

Figure 1.

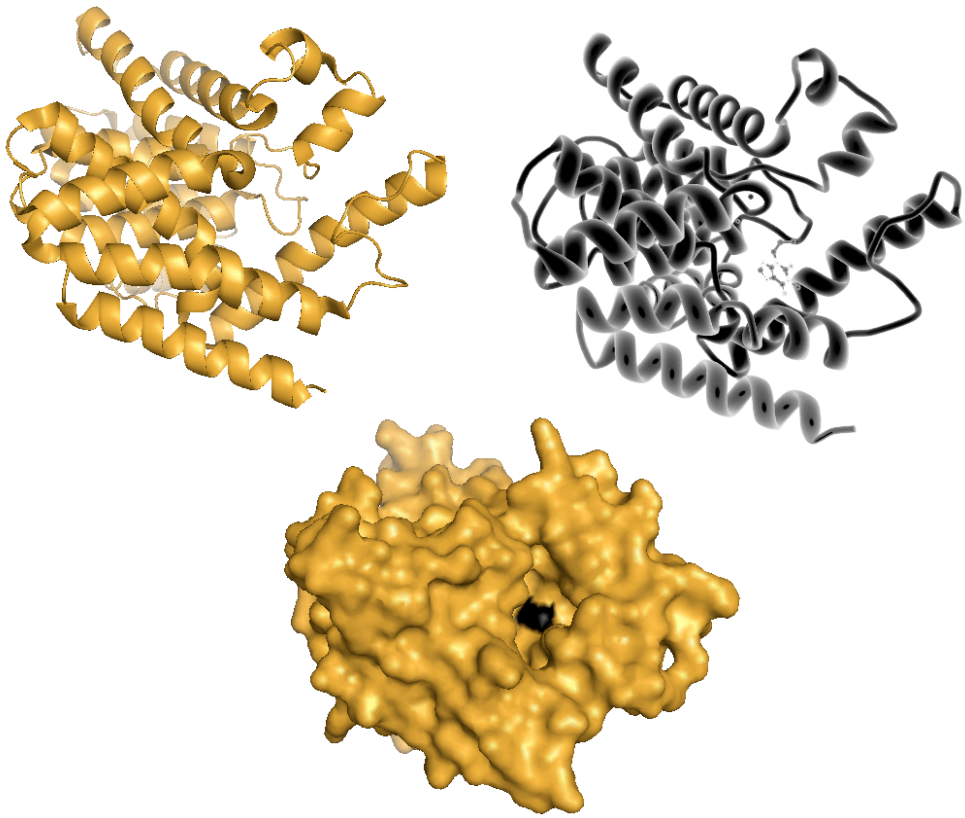

1.5. Using *Schizosaccharomyces pombe* to screen for PDE inhibitors

Since cAMP signaling is present in simpler single cell organisms such as fission yeast, these cells serve as a convenient model for studying these complex pathways. The fission yeast *Schizosaccharomyces pombe* monitors glucose to regulate a wide range of biological processes such as sexual development and metabolism.

Our lab (Hoffman lab, Boston College) has a history in studies regarding glucose – mediated transcriptional regulation identifying mutations in genes that confer constitutive *fbp1*$^{+}$ transcription, by using two reporters *fbp1-ura4* and *fbp1-lacZ* (VASSAROTTI and FRIESEN 1985); (HOFFMAN and WINSTON 1990). These genes are called the *g*lucose *i*nsensitive *t*ranscription (*git*) genes (HOFFMAN 2005b). One of the genes is *git2*$^{+}$/*cyr1*$^{+}$ which encodes adenylate cyclase (HOFFMAN and WINSTON 1991). The function of adenylate cyclase is to produce the second messenger cAMP from ATP in order to activate PKA. Additional *git* genes are required for adenylate cyclase activation. Four genes encode the Git3 G protein-coupled receptor (WELTON and HOFFMAN 2000) and its cognate heterotrimeric G protein composed of the Gpa2, Gα (ISSHIKI *et al.* 1992; NOCERO *et al.* 1994), the Git5 Gβ (LANDRY *et al.* 2000), and the Git11 Gγ (LANDRY and HOFFMAN 2001). Mutations in any of these genes result in the reduction of cAMP levels, and confer constitutive *fbp1*$^{+}$ transcription which will result in a Ura^{+} /5FOA^{s} phenotype (Figure 2A). Therefore, this system can be used to screen for PDE inhibitors, since a PDE

inhibitor should restore $5FOA^R$ growth by elevating cAMP levels to repress *fbp1-ura4* transcription (Figure 2B).

1.6. Focus of research

The recent identification of PDE7-specific inhibitor (BRL 50481) demonstrates the importance of PDE7 inhibition in the treatment of inflammatory illnesses. BRL 50481 was able to block TNF secretion and inhibit T cell proliferation in a dose-dependent manner (LERNER and EPSTEIN 2006; SMITH *et al.* 2004). Therefore the discovery of more PDE7A inhibitors is necessary to develop successful drugs that have the potential for treating anti-inflammatory disorders.

The power of this research is using *S. pombe* to develop *in vivo* assay to screen for inhibitors of Human PDE7A. This has been accomplished by replacing the *S. pombe* PDE with human PDE7A, in the presence of either the *git3* or *gpa2* mutation. This reduced cAMP levels, and consequently conferred a 5FOA-sensitive ($5FOA^S$) phenotype. In the presence of PDE7A inhibitor, cells should restore $5FOA^R$ growth by elevating cAMP levels to repress *fbp1-ura4* transcription. I will describe herein human PDE7A integration and the strain optimization process. Using it I was able to discover novel specific PDE7A inhibitors and show their direct effect on cAMP levels.

Figure 2. cAMP pathway in *S. pombe*

(A) Mutations in genes involved in glucose –mediated transcriptional regulation confer constitutive *fbp1*$^{+}$ transcription. These genes are called the *g*lucose *i*nsensitive *t*ranscription (*git*) genes. (AC) is *git2*$^{+}$/*cyr1*$^{+}$, which encodes adenylate cyclase that produces the second messenger cAMP from ATP to activate PKA. Additional *git* genes are required for (AC) activation. Four genes encode the Git3 G protein-coupled receptor and its cognate heterotrimeric G protein composed of the Gpa2 (Gα, Gitγ, Gβ). Mutations in any of these genes result in lowering cAMP levels, and confer constitutive *fbp1*$^{+}$ transcription which will result in a Ura $^{+}$/5FOA ^{s} phenotype.

(B) Phosphodiesterase (PDE) is the enzymes that hydrolyze the cyclic nucleotide second messengers, cAMP. In the presence of a PDE inhibitors cAMP levels should get elevated and repress *fbp1-ura4* transcription that will restore 5FOA^{R} growth.

Figure 2.

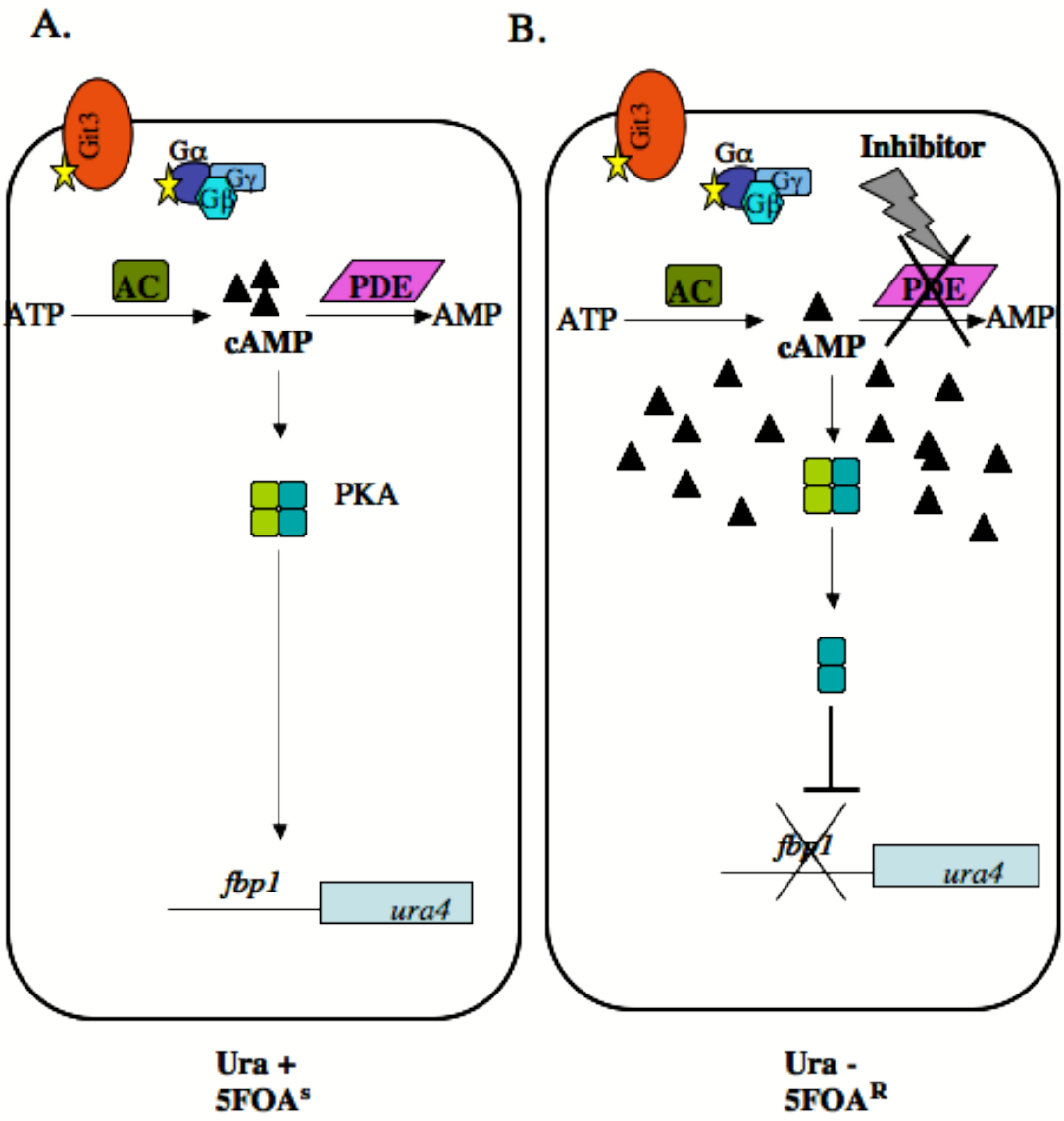
A.
B.
Git3
Gα
Gγ
Gβ
AC
ATP
cAMP
PDE
AMP
PKA
fbp1
ura4
Inhibitor
Ura +
5FOA^s
Ura -
5FOA^R

2. Materials and Methods

2.1. Growth Medium

Yeast were grown and maintained using several types of media. Yeast extract agar (YEA) for plates, yeast extract liquid YEL for gene transformation (GUTZ *et al.* 1974), defined medium EMM (Biochemicals) were supplemented with required nutrients at 75 mg/L, except for L-leucine, which was at 150 mg/liter, and 2.5 mM cAMP was used for pre-growth for screening purposes. SC liquid or solid medium containing 0.4 g/L 5-fluoro-orotic acid (5FOA) and 8% glucose were used for screening, as previously described (HOFFMAN and WINSTON 1990).

2.2. Yeast

Yeast strains used in this study are two strains carried the *fbp1::ura4*$^{+}$ and *ura4::fbp1-lacZ* reporters (Table 1). Both are translational fusions integrated at the *fbp1*$^{+}$ and *ura4*$^{+}$ loci, respectively, as described by Hoffman and Winston (HOFFMAN and WINSTON 1990). Strains were grown at 30°C unless indicated otherwise.

2.3. Strain mating and tetrad dissection

Mating was performed on malt-extract agar (MEA) for 24 to 48 h at 30°C. In the case of homothalic strains, they were pre-grown at 37°C prior to mating. Asci formed on MEA

were transferred using a dissection needle to a YEA 3% glucose rich plate. Zygotic asci that were selected were then incubated at 37°C for at least 2 h to facilitate the breakage of the cell wall and the release of the spores. Tetrads were then dissected and plates were subsequently incubated at 30°C for 3 days and then scored.

2.4. β-galactosidase assays of *fbp1-lacZ* expression

Cells were grown under repressing conditions (8% glucose) in yeast extract at the indicated temperatures (YEL). Subcultures were grown to exponential phase until reaching a density of 1 x 10^7 cells/ml. Soluble protein extracts were prepared by glass beads in breaking buffer (0.1 M Tris pH 8, 20% glycerol, 1 mM DTT) and PSMF (40 mM). The assay was performed using Z buffer, made as described in current protocol in molecular biology. Ortho-Nitrophenyl-β-galactoside (ONPG) was used to start the reaction and Na_2CO_3 (1 M) solution was used to stop the reaction when yellow color started to develop. Samples were read at OD_{420} for each sample. Total soluble protein was measured by BCA assay (Pierce Chemical Co).

2.5. PDE7A sequencing

PDE7A was PCR amplified from a plasmid clone obtained from the Beavo lab and the ends of the PCR product were sequenced using custom oligonucleotides (Integrated DNA

Technologies). DNA sequencing was performed using the CEQ DTCS-Quick Start kit (Beckman Coulter).

2.6. PCR

Human PDE7A was amplified using primers that were designed according to deduction by using the sequencing results. A high fidelity enzyme, Herculase, was used for amplification according to the manufacturer's instructions. Colony PCR was performed to screen for positive integrants by using Taq polymerase.

2.7. Cyclic AMP and protein extraction

Cells treated with a drug or DMSO were collected by air vacuum into a micropore glass filter (Fisher). Filters were then submerged into 1 ml of 1 M formic acid and vortexed for 30 s to break the cell walls. Filters were removed and the samples centrifuged for 10 min at 14000 x g. 400 ml of supernatant was lyophilized using a speed vacuum for 4 h (BYRNE and HOFFMAN 1993). Finally, the pellets were resuspended in 80 ml 0.1 HCl. Assay was performed using cAMP Direct kit (Assay Designs). Proteins from the same samples were extracted by resuspending the cells in 0.2 N NaOH with 0.4 g of glass beads. The tubes were then vortexed for 3 min to break the cells. The samples were boiled for 3 min followed by centrifugation for at 14,000 x g for 2 min to remove cell debris. Protein quantification was performed using a BCA kit.

2.8. PDE7A transformation and screen for positive integration

Cells were grown in YEL overnight to early log phase 5 x 10^6 cells/ml. Then cells were pelleted and washed twice with cold water and buffer (LiAc/TE). Pellets were resuspended in 100 ml LiAc/TE and mixed with 1 ml boiled salmon testes DNA and 10 ml of concentrated PDE7A DNA (8 samples were combined and ethanol precipitated then dissolved in 10 ml of dH_20). The samples were kept for 10 min at room temperature before adding 260 ml of (40% PEG, 100 mM LiOAc, 10 mM Tris-HCl pH 7.5) buffer. Samples were then incubated at 30˚ C for 1 h, then were heat shocked for 5 min at 42˚C after adding 43 ml of DMSO to each sample. The cells were grown in 3% YEL for 20 h for recovery. Finally, cells in different dilutions were plated on the 5FOA medium (BÄHLER *et al.* 1998). Colonies were screened for positives (PDE7A integrated colonies) after 6-8 d post gene transformation. Plates were inverted over iodine vapors for 5 min. Positive colonies that carry active PDE7A in them stain dark brown by iodine vapor. The amount of staining reflects the sporulation frequency. Sporulation was also confirmed microscopically. Positive colonies were streaked on fresh YEA medium and PCR analysis confirmed the presence of PDE7A in *S. pombe* (See Results).

2.9. Microscopy

The DIC Images of cells were captured using a Zeiss microscope with an Orca-ER CCD camera. The microscope – camera are connected to a computer that is equipped with Openlab software.

2.10. Screening process

High throughput drug screens were performed at the Broad Institute's Chemical Biology Program screening facility. Figure 3A summarizes the screening process. PDE7A cultures (CHP1189) were pre-grown in EMM complete medium, containing 2.5 mM cAMP for overnight growth. Cells were washed, mixed very well, then transferred to 384-well microtiter dishes into 5FOA medium at a final density 1 x 10^5 cells/ml and a final volume of 50 ml. 100 nl of compounds were pinned to the bottom of the wells at a final concentration of 20 μM. Control plates received 100 nl DMSO. Positive control plates had 5mM cAMP added in the 5FOA medium. Cultures were incubated for 48 h at 30ºC, and sealed in a container with moist paper towels to prevent evaporation. Optical density (OD_{600}) of cultures was measured after mixing the cells with a plate mixer. Positive Hits should show a high OD reading that can be even visible by eye, as seen in the case of one of the PDE7A inhibitors (Figure 3B).

2.11. Bioinformatics

Files from the Optical density (OD_{600}) readings were sent to the Bioinformatics team at the Broad institute in order to determine the CompositeZ scores. Hits were visualized and analyzed in the lab by using the Spotfire software (Spotfire, Inc., Somerville, MA).

Figure 3. PDE7A screening process

(A) This figure summarizes the screening process. 25ml of 5FOA medium was delivered to a 384-well microtiter plate. 100 nl of compounds were pinned into the wells to a final concentration of 20 mM. Control plates received 100 nl DMSO. (CHP1189) PDE7A expressing cells were then washed, mixed very well, and transferred to the prepared plates at a final density of 1 x 10^5 cells/ml and a final volume of 50 ml of 5FOA medium. Plates were stacked and incubated for 48 h at 30ºC, sealed in a container with moist paper towels to prevent evaporation. Optical density (OD_{600}) of cultures was measured after mixing the cells with a plate mixer. **(B)** "Hits" can be visible by eye as seen in the case of one of PDE7A inhibitors.

Figure 3.

A.

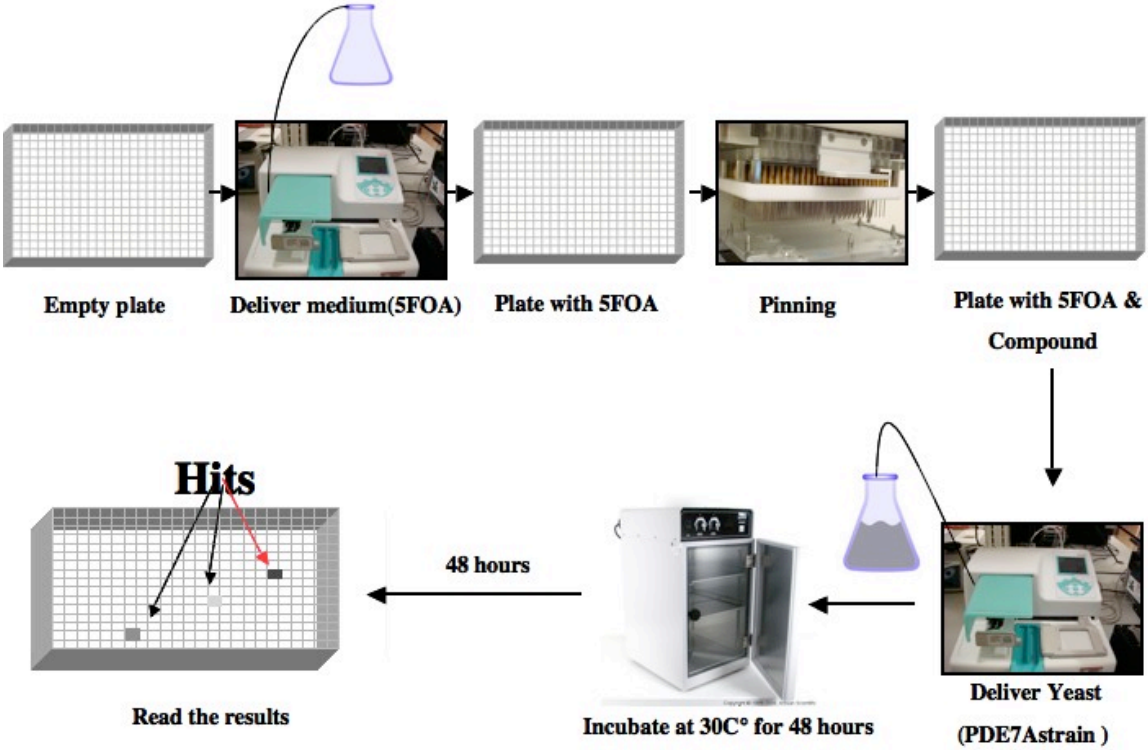
Empty plate
Deliver medium(5FOA)
Plate with 5FOA
Pinning
Plate with 5FOA &
Compound
Hits
48 hours
Read the results
Incubate at 30C° for 48 hours
Deliver Yeast
(PDE7Astrain)

B.

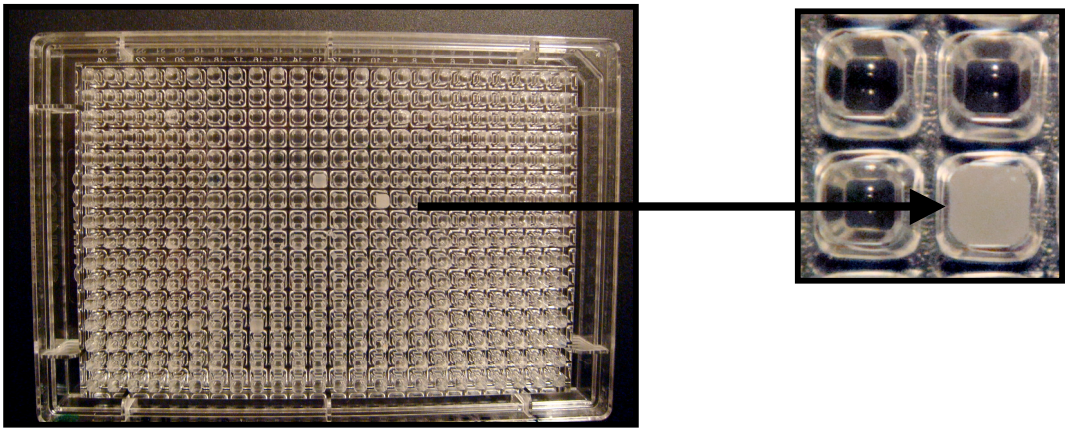

3. RESULTS

3.1. Construction of strains that express human PDE7A

I integrated human PDE7A in *S. pombe* by replacing the *cgs2*$^{+}$ gene (*S. pombe* PDE) with the PDE7A gene using homologous recombination. To accomplish this, PDE7A was amplified by PCR using primers that create product with PDE7A copies with flanking *cgs2* sequence for direct integration (Figure 4). The PCR product was then transformed into a *cgs*Δ::*ura4*$^{+}$ strain (JZ666), using a DMSO transformation protocol. Cells were grown in YEA3% glucose as a recovery period, then were plated on 5FOA (5FOA is being used for counter-selection) to identify and distinguish candidates that express the human PDE7A, from the *cgs2* locus.

A strain that carries an active PDE should be able to sporulate under starvation conditions, as seen in (Figure 5) with PDE7A integrants. Positive colonies were streaked onto fresh YEA medium and PCR analysis confirmed the presence of PDE7A in *S. pombe.* (See Materials and Methods for details in screening for positives).

Finally, crosses were performed to construct strains that contained the PDE7A construct with *fbp1-ura4* and *fbp1-lacz* reporters along with either the *gpa2* Gα subunit mutation or *git3* glucose receptor mutation, both of which are required for glucose detection, adenylate cyclase activation, and transcriptional repression of the *fbp1* gene.

Figure 4. Human PDE7A integration process to *S.pombe*

Human PDE7A integration into *S. pombe* by replacing the *cgs2*$^{+}$ gene (*S. pombe* PDE) with the PDE7A gene using homologous recombination. PDE7A was amplified by PCR using primers that create PDE7A copies with flanking *cgs2* sequence for direct integration.

Figure 4.

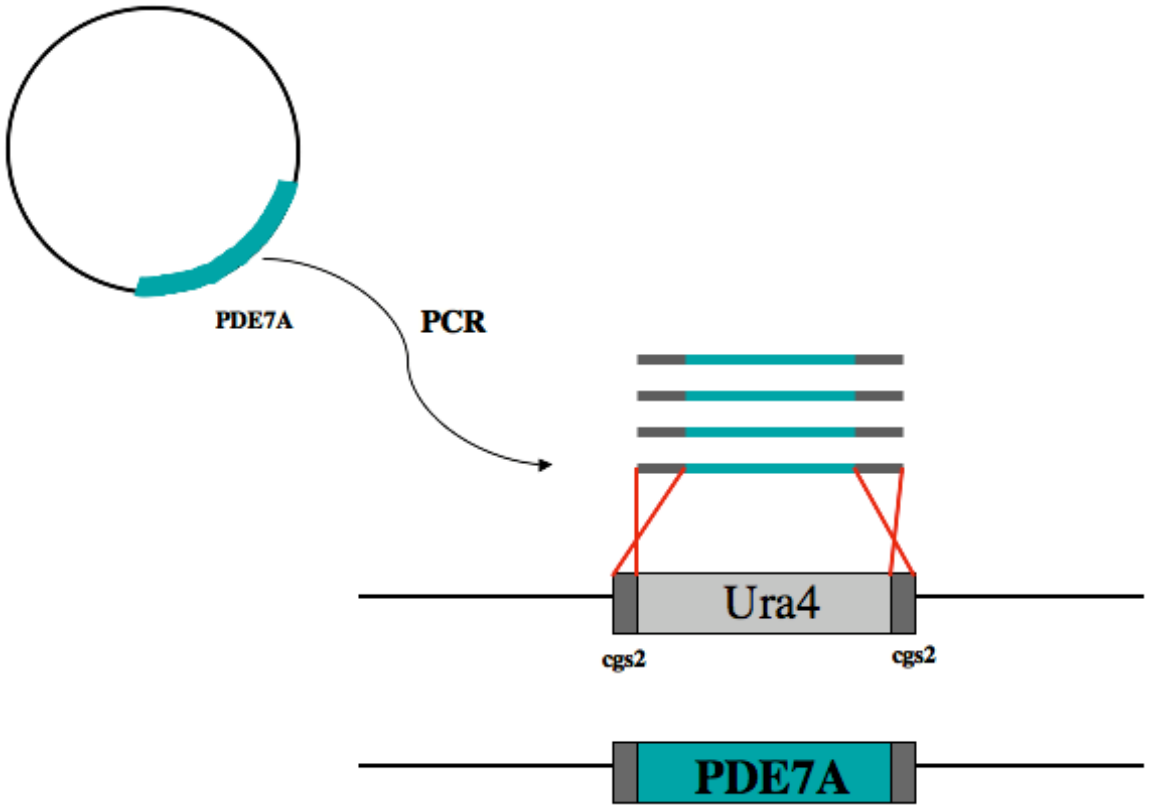

Figure 5. Human PDE7A integrants are able sporulate under starvation conditions

PDE7A integrants were able to sporulate under starvation a condition, which indicates the presence of an active PDE.

Figure 5.

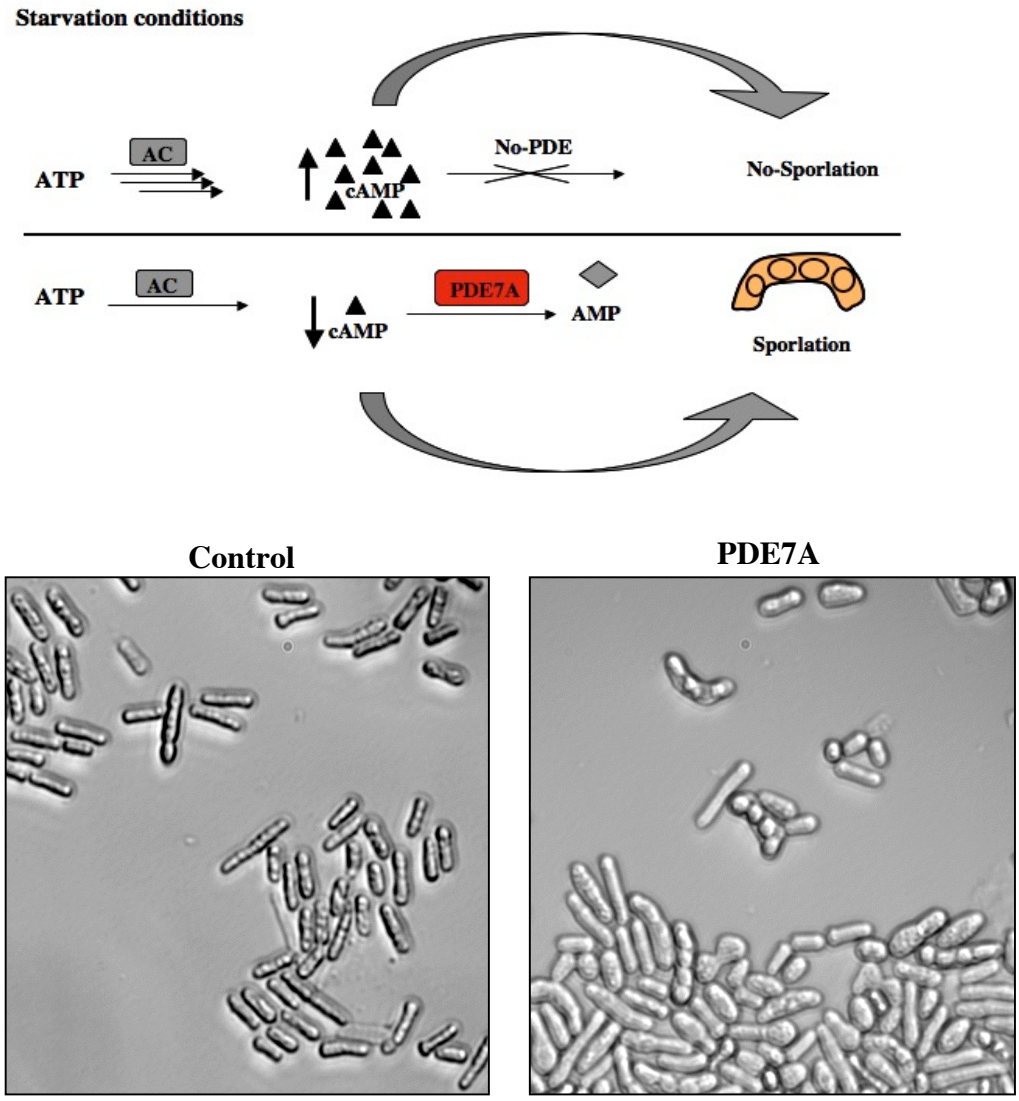
Starvation conditions
ATP
AC
cAMP
No-PDE
No-Sporlation
ATP
AC
cAMP
PDE7A
AMP
Sporlation
Control
PDE7A

The expression level of *ura4 and lacZ* reporters in these strains reflects the activity level of PDE7A. β-galactosidase activity in these strains, demonstrate PDE7A was active compared to a strain expressing defective truncated PDE (Cgs2-2) (data not shown).

Introducing a defect in cAMP (*git3*/*gpa2*) will confer 5FOA sensitive phenotype by reducing cAMP production. Therefore, this strain can be used to screen for PDE7A inhibitors. In the presence of an inhibitor, PDE7A activity will be reduced elevating cAMP levels. As a result, *fbp1- ura4* expression will be repressed, which will then result in 5FOA resistant growth (Figure 6).

3.2. PDE7A optimization

To determine the best conditions for high throughput drug screening, a number of factors need to be taken into consideration including the right genetic background, the right cAMP concentration for pre-growth conditions, and final cell densities, all important elements in the optimization process. As a first test, strain CHP1169 expressing PDE7A in the *git3* deletion background was pre-grown in EMM medium containing different concentrations (0, 0.5, 1, 1.5, 2.5) mM of cAMP and different final cell densities (0.5 x 10^5, 1 x 10^5, 4 x 10^5, then cultures were transferred to 5FOA in the presence or absence of 5 mM cAMP. The OD_{600} measurements were taken after 48 h of incubation at 30ºC (cells were grown in the presence of cAMP in order to repress the *fbp1-ura4* reporter prior to exposure to 5FOA medium).

Figure 6. PDE inhibitors screening concept

(A) *S. pombe* PDE replaced with human PDE7A, in the presence of either the *git3* or *gpa2* mutation, which will result in the reduction in cAMP levels, should confer a 5FOA-sensitive ($5FOA^S$) phenotype. **(B)** In the presence of a PDE7A inhibitor cells should restore $5FOA^R$ growth by elevating cAMP levels to repress *fbp1-ura4* transcription.

Figure 6.

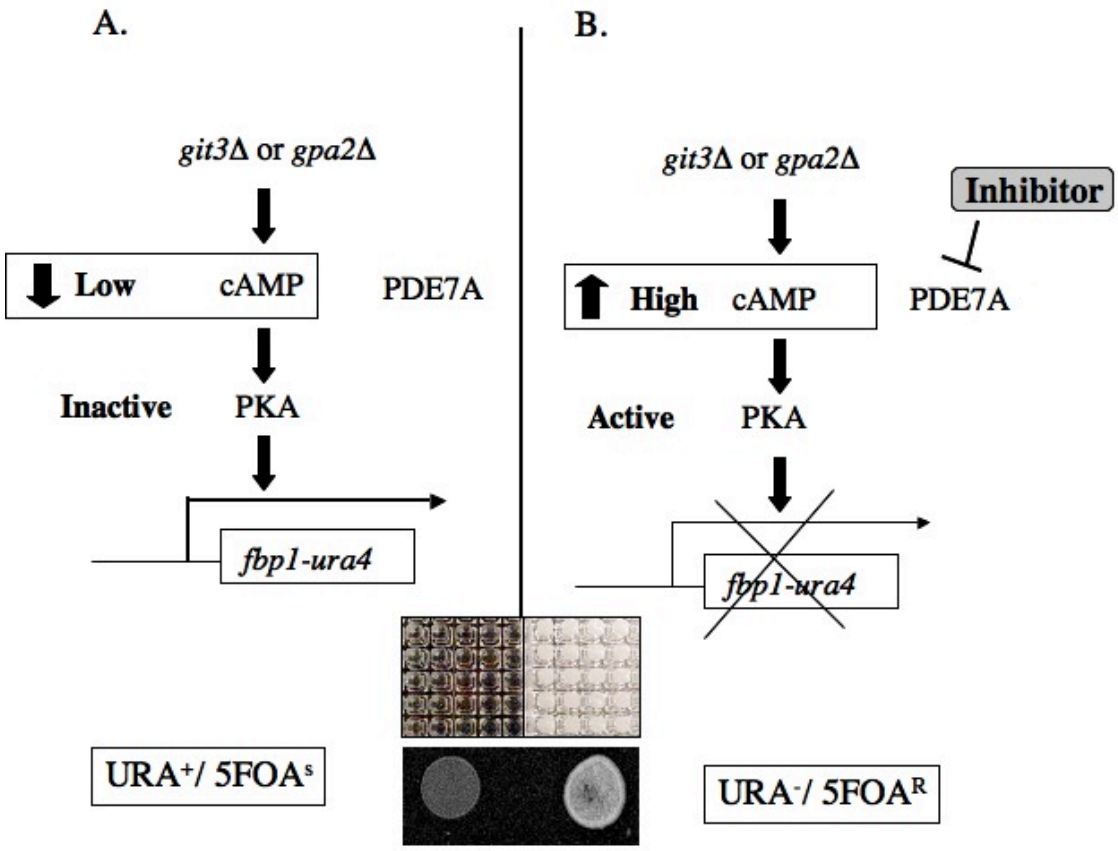
A.
B.
git3Δ or gpa2Δ
Low cAMP
PDE7A
Inactive PKA
fbp1-ura4
URA+/ 5FOAs
git3Δ or gpa2Δ
Inhibitor
High cAMP
PDE7A
Active PKA
fbp1-ura4
URA-/ 5FOAR

I found that the best conditions were when the strain was pre-grown in EMM with 2.5 mM of cAMP and by using 1 x 10^5 as final cell density when transferred to 5FOA. I also found that the PDE7A doubling time was 3.5 - 3.7 h. Testing the strain CHP1169 (PDE7A) in *git3* deletion background in the lab in a 96-well plate gave an OD_{600} of 0.93 +/- 0.05 in wells where cAMP was added to the cultures, while an OD_{600} of 0.07 +/- 0.01 was observed for wells where cAMP was not added (Figure 7).

To further test the best genetic background for high throughput drug screening, strains CHP1169 expressing PDE7A in a *git3* deletion background and the strain CHP1189 expressing PDE7A in a *gpa2* deletion background were pre-grown in EMM medium containing 2.5 mM cAMP and then transferred to 5FOA medium in 384-well microtiter plates in the presence 5mM of cAMP (representing the positives), or the absence of cAMP (representing the negatives). OD_{600} measurements were taken after 48 h of incubation at 30ºC. In each strain, the addition of cAMP restored $5FOA^R$ growth. In strain CHP1169, the OD_{600} of the cultures +cAMP was 1.45 +/- 0.074, while the OD_{600} of the cultures –cAMP was 0.61+/- 0.05 when the final density was $1x10^5$. When using strain CHP1189 , the OD_{600} of the cultures +cAMP was 1.31 +/- 0.03, while the OD_{600} of the –cAMP cultures was 0.060+/- 0.01 when the final density was $1x10^5$. The Z factors for these screens were 0.65 and 0.91, respectively. The Z factor is a statistical assessment of the quality of datasets used in high throughput screening. A strain should have a Z factor above the value 0.5 in order to qualify for screening (Figure 8).

Figure 7. Optimization conditions of strain CHP1169

The best conditions for strain CHP1169 PDE7A in the *git3* deletion background is to pre-grow the stain in EMM with 2.5 mM of cAMP and by using $1x10^5$ cells/ml as the final cell density in 5FOA. Results showed an OD_{600} of 0.93 +/- 0.05 in wells where cAMP was added to the cultures, and an OD_{600} of 0.07 +/- 0.01 in wells where cAMP was not added.

Figure 7.

cAMP	$0.5x10^5$ -				$0.5x10^5$ +				$1x10^5$ -				$1x10^5$ +				$4x10^5$ -				$4x10^5$ +			
0.0	0.04	0.04	0.05	0.04	0.04	0.04	0.05	0.04	0.06	0.06	0.06	0.06	0.07	0.05	0.06	0.06	0.18	0.19	0.21	0.26	0.37	0.54	0.27	0.30
	0.05	0.04	0.05	0.04	0.05	0.05	0.05	0.04	0.05	0.06	0.05	0.06	0.07	0.05	0.06	0.08	0.18	0.19	0.20	0.23	0.31	0.37	0.41	0.33
	0.04	0.04	0.05	0.05	0.05	0.05	0.05	0.04	0.06	0.06	0.06	0.06	0.06	0.52	0.53	0.07	0.19	0.20	0.27	0.20	0.47	0.51	0.59	0.38
0.5	0.07	0.06	0.06	0.06	0.35	0.37	0.37	0.41	0.26	0.24	0.31	0.38	1.04	1.03	1.07	1.15	0.73	0.40	0.50	0.45	1.09	1.04	1.05	0.92
	0.07	0.06	0.06	0.06	0.39	0.41	0.34	0.37	0.13	0.14	0.16	0.14	0.70	0.90	0.82	0.77	0.48	0.52	0.46	0.48	1.09	1.18	1.14	1.02
	0.06	0.06	0.06	0.06	0.36	0.32	0.31	0.35	0.14	0.14	0.16	0.13	0.84	0.85	0.79	0.84	0.53	0.51	0.53	0.52	1.09	1.10	1.11	1.03
1.0	0.06	0.05	0.05	0.05	0.41	0.40	0.32	0.39	0.26	0.26	0.23	0.40	1.21	1.20	1.19	1.19	0.56	0.58	0.60	0.57	1.22	1.21	1.21	1.19
	0.05	0.05	0.05	0.05	0.39	0.39	0.34	0.40	0.10	0.08	0.09	0.10	0.96	0.92	0.99	0.94	0.53	0.63	0.62	0.60	1.23	1.21	1.21	1.19
	0.05	0.05	0.07	0.05	0.41	0.44	0.29	0.32	0.10	0.09	0.10	0.10	0.87	0.91	0.85	0.95	0.61	0.62	0.57	0.60	1.23	1.22	1.22	1.19
1.5	0.05	0.04	0.04	0.05	0.34	0.29	0.27	0.35	0.06	0.07	0.06	0.06	0.86	0.82	0.84	0.89	0.24	0.25	0.24	0.24	1.21	1.21	1.20	1.18
	0.05	0.04	0.04	0.04	0.21	0.26	0.24	0.14	0.06	0.06	0.06	0.06	0.63	0.88	0.70	0.84	0.28	0.26	0.25	0.24	1.22	1.19	1.22	1.18
	0.05	0.04	0.04	0.04	0.15	0.27	0.26	0.25	0.05	0.06	0.06	0.06	0.75	0.78	0.67	0.76	0.30	0.22	0.26	0.25	1.20	1.22	1.19	1.19
2.5	0.05	0.05	0.05	0.05	0.47	0.45	0.37	0.36	0.06	0.08	0.07	0.06	0.88	0.95	0.97	0.91	0.39	0.32	0.30	0.30	1.24	1.24	1.24	1.21
	0.05	0.05	0.05	0.05	0.35	0.30	0.37	0.49	0.06	0.07	0.06	0.07	0.92	1.00	0.95	1.00	0.30	0.34	0.27	0.30	1.20	1.23	1.23	1.21
	0.05	0.05	0.05	0.05	0.26	0.39	0.34	0.42	0.07	0.06	0.07	0.08	0.87	0.89	0.98	0.91	0.21	0.33	0.28	0.28	1.20	1.25	1.21	1.21

Figure 8. Test different PDE7 genetic background

Strain CHP1189 behaves much better than strain CHP1169. Strain CHP1169 expressing PDE7A in a *git3* deletion background and the strain CHP1189 were pre-grown in EMM medium containing 2.5 mM cAMP, then transferred to 5FOA medium with 5mM of cAMP (positives = orange bars) or the absence of cAMP (negatives = brown bars). OD_{600} measurements were taken after 48 h of incubation at 30ºC. In strain CHP1169, the OD_{600} of the cultures +cAMP was 1.45 +/- 0.074, while the OD_{600} of the cultures –cAMP was 0.61+/- 0.05. In strain CHP1189 the OD_{600} of the cultures +cAMP was 1.31 +/- 0.03 and the OD_{600} of the –cAMP cultures was 0.060+/- 0.01. The Z factors for these screens were 0.65 and 0.91, respectively. **1X**=$1*10^5$, **2X**=$1.5*10^5$ final cell densities added to 5FOA medium.

Figure 8.

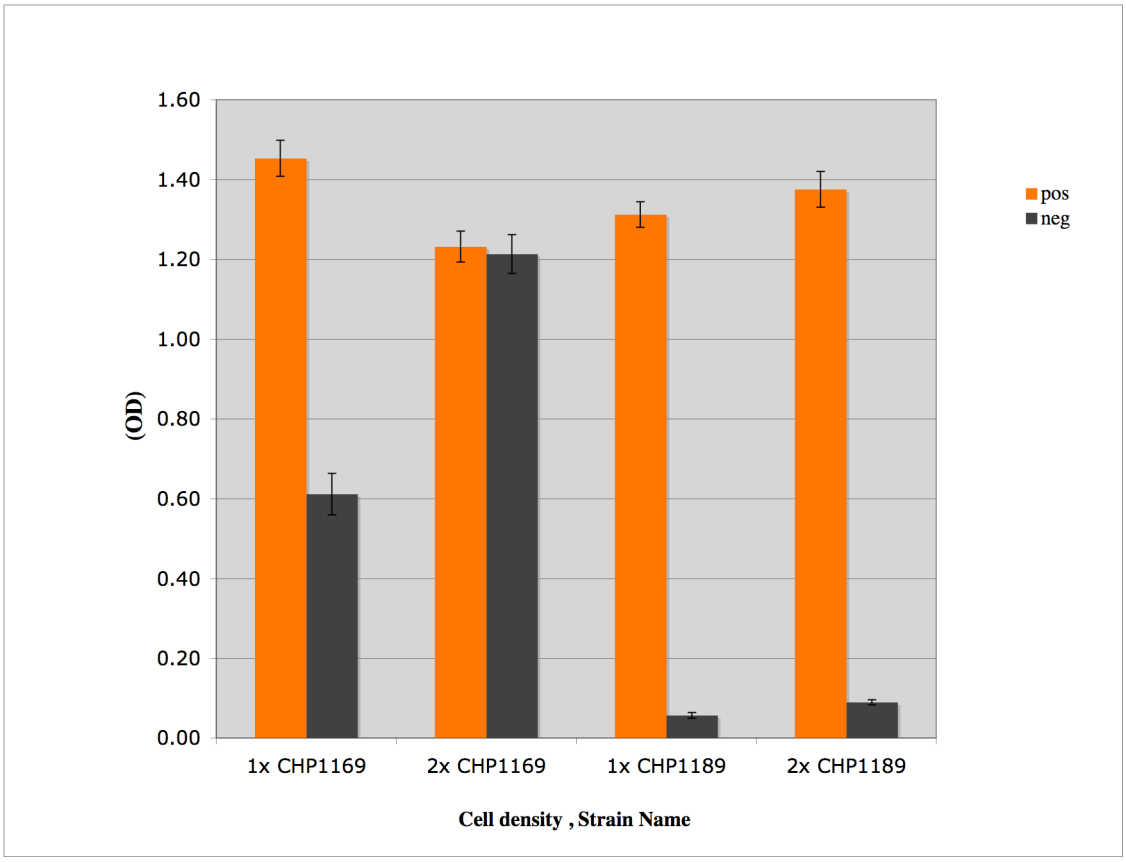
1.60
1.40
1.20
1.00
0.80
0.60
0.40
0.20
0.00
(OD)
1x CHP1169
2x CHP1169
1x CHP1189
2x CHP1189
Cell density , Strain Name
pos
neg

From these data, I identified the best genetic background for which PDE7A activity was able to show the 5-FOA growth sensitive phenotype. By testing strain CHP1189, a PDE7A in a *gpa2* deletion background, and, CHP1169 a PDE7A in a *git3* deletion background, I found that strain CHP1189 behaves much better than strain CHP1169 even though both confer the 5FOA sensitive phenotype, and had a Z factor above 0.5. Since loss of *gpa2* creates a greater defect in cAMP than the loss of *git3*, it displayed less background growth, represented by the negative values. Based on these results, I decided to use CHP1189 for high throughput screening.

3.3. Strain expressing PDE7A responds partially to IBMX but not to rolipram

Before performing high throughput screening, I wanted to further test the strains against commercially available drugs to validate the use of CHP1189 for screening. Thus, I tested the effects of a known PDE4 inhibitor (rolipram), and the nonselective PDE inhibitor (IBMX) on the expression of the *fbp1-lacZ* fusion in the human PDE7A expressing strain. As seen in Figure 9, rolipram did not reduce β-galactosidase activity, while IBMX partially reduces β-galactosidase activity expressed from the PDE7A strain (35 % reduction). These results support results reported from previous studies indicating that PDE7 is sensitive to the nonselective PDE inhibitor IBMX and resistant to rolipram a PDE4 selective drug.

Figure 9. The PDE7A is partially sensitive IBMX and resistant to rolipram

The PDE7 strain CHP1189 is sensitive to the nonselective PDE inhibitor IBMX and resistant to rolipram, a PDE4 selective drug. Rolipram did not reduce β-galactosidase activity in strain CHP1189. Whereas, the nonselective PDE inhibitor IBMX reduces β-galactosidase activity expressed from the PDE7A strain partially (35 % reduction).

Figure 9.

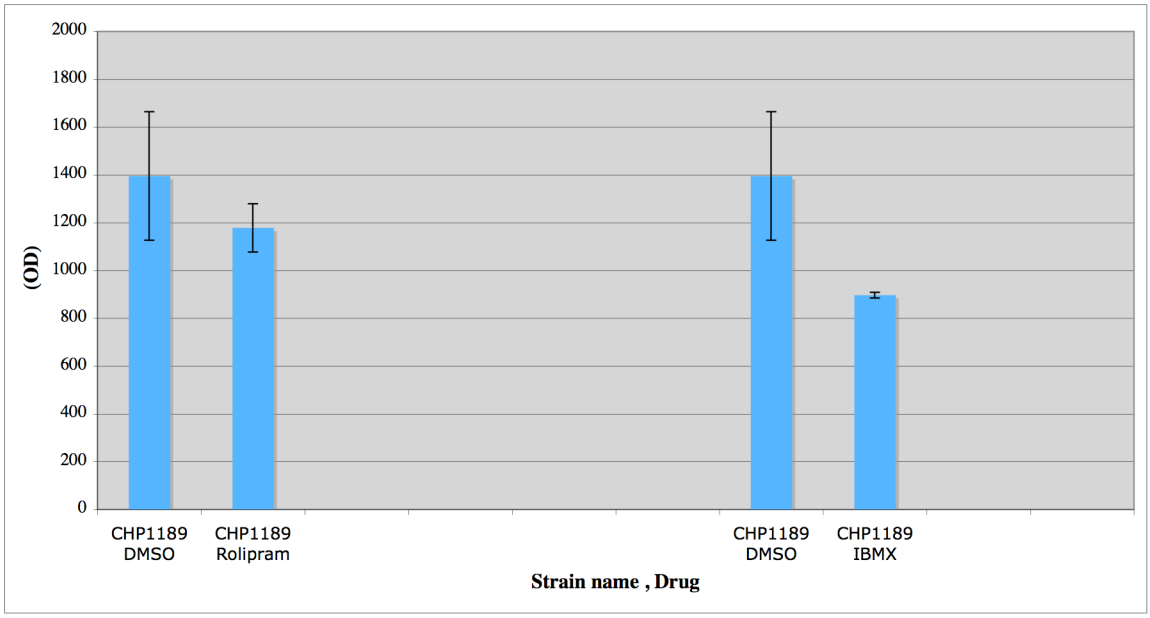
2000
1800
1600
1400
1200
1000
800
600
400
200
0
(OD)
CHP1189 DMSO
CHP1189 Rolipram
CHP1189 DMSO
CHP1189 IBMX
Strain name , Drug

3.4. Screening and Hits analysis

Using CHP1189 ($5FOA^s$ strain expressing PDE7A), I screened for compounds that would inhibit PDE7A to confer $5FOA^R$ growth. By performing five major experiments (1091.0126, 1091.0127, 1091.0128, 1091.0129, 1091.0130), I was able to screen all of the available libraries at the Broad Institute (Bioactive, PK04, Analyticon, Forma, Natural extracts, and Commercials compounds). All available libraries at that time represent screening of almost 50,000 compounds. Figure10A displays the results from these screens. In the Figure, yellow circles represent the positive controls (cells +cAMP) which show high Z scores as expected; Red circles represent the negative control (cells +DMSO) which display low Z scores; while the purple circles represent the 50,000 compounds that were screened. Also note the diagonal distribution of spots, which represents high data reproducibility of the screens, which were performed in duplicates.

Duplicate plates were screened and compounds that confer such growth with composite Z scores of ≥8.53 were identified as "Hits" which comprised almost 750 compounds (Figure 10B). Most of the hits that were identified were from the commercial libraries representing 40 % of the total hits (Figure 11).

Figure 10. PDE7A screening results

(A) Display of the results from the screen, yellow circles represent the positive controls (cells +cAMP) which show high Z scores as expected; Red circles represent the negative control (cells +DMSO) which display low Z scores, while the purple circles represent the all compounds that were screened.

(B) Compounds that confer such growth with composite Z scores of ≥8.53 were identified as "Hits" which comprised almost 750 compounds.

Figure10.

A.

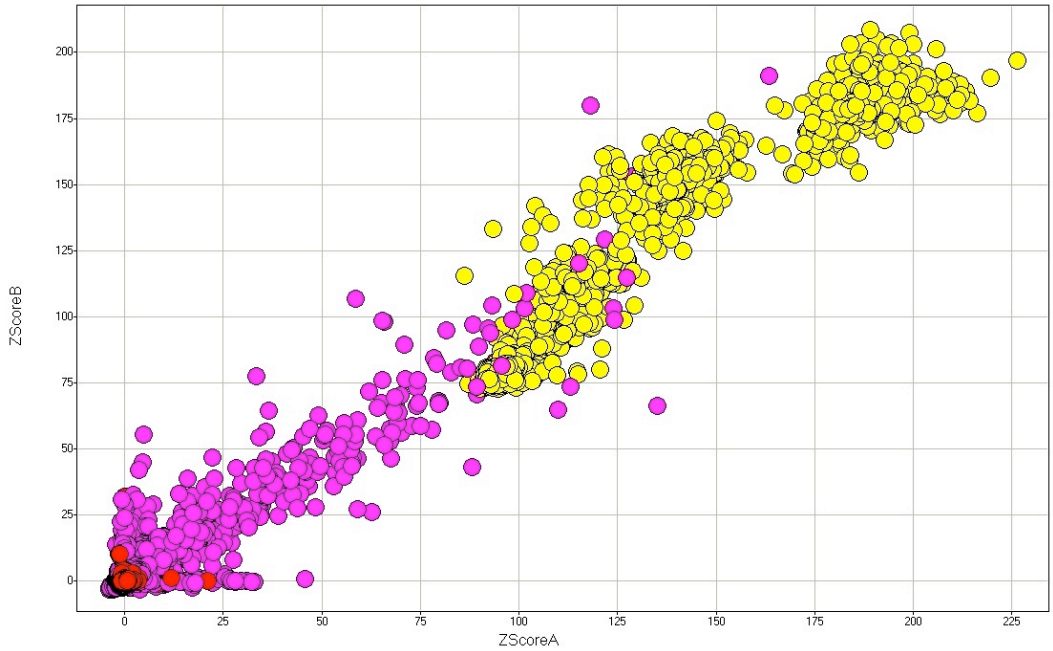
ZScoreB
ZScoreA
0
25
50
75
100
125
150
175
200
225

B.

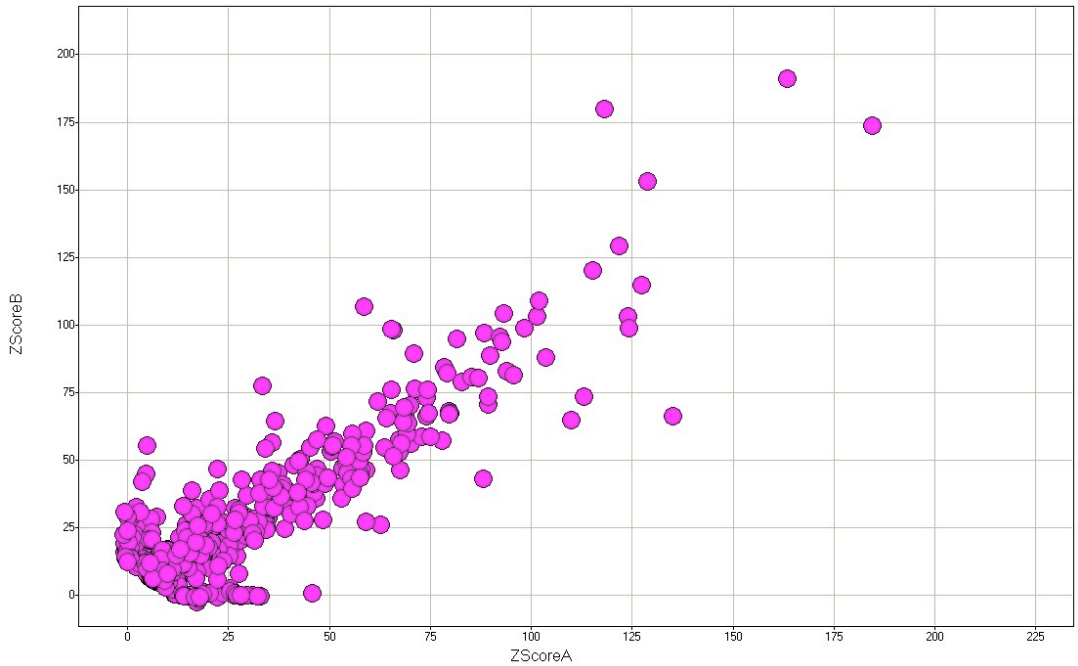
ZScoreB
ZScoreA
0
25
50
75
100
125
150
175
200
225

Figure 11. Most of PDE7A hits were identified from the commercial libraries

Most of the 750 hits that were identified were from the commercial libraries (experiment number 1091.0129-purple and 1091.0130-green) representing 40% of the total hits.

Figure 11.

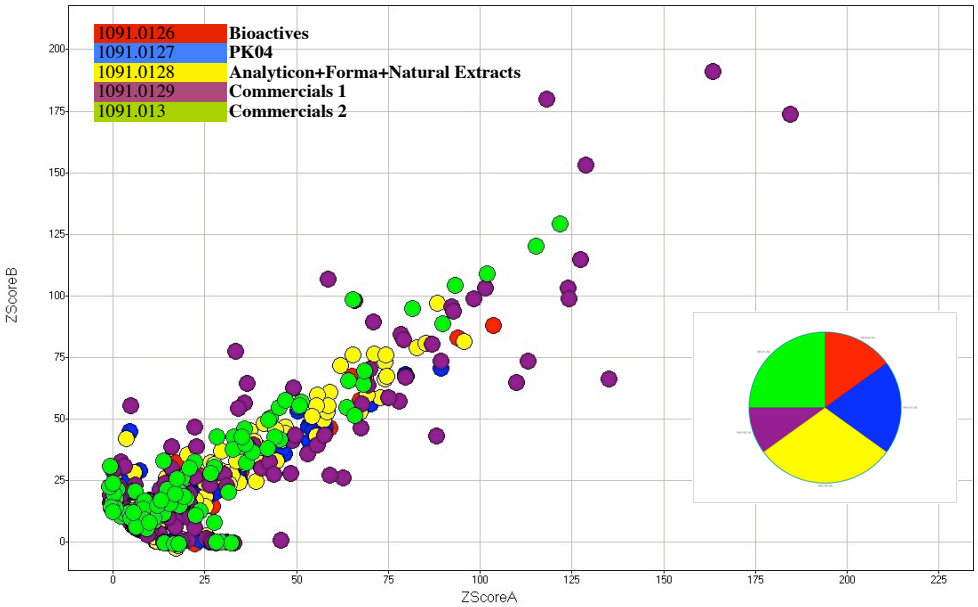
1091.0126 Bioactives
1091.0127 PK04
1091.0128 Analyticon+Forma+Natural Extracts
1091.0129 Commercials 1
1091.013 Commercials 2
ZScoreB
ZScoreA
0
25
50
75
100
125
150
175
200
225

These results were then compared with those from screens against other PDEs (PDE2A, PDE4A, PDE4B, and Cgs2) to identify PDE7A-specific inhibitors. This comparison resulted in 20 specific compounds with composite Z scores of ≥ 44.5, identified as "PDE7A specific Hits" (Figures 12). Four of these specific hits were picked for further analysis (compounds 11, 12, 13, 14).

3.5. PDE7A specific inhibitors restore 5FOA^R growth

I performed additional 5FOA assays to confirm "PDE7A specific hits", and to identify the ED50 (The dose of a compound that is pharmacologically effective to stimulate growth to 50% of the OD of a saturated culture) of compound (11, 12, 13, 14, 15, PAN). Compound 15 = BRL 50481, is the only specific PDE7 inhibitor commercially available whereas, PAN is a compound that stimulates the growth of most of the PDE-expressing strains. Compound number 15 and PAN were used as controls to validate our assays. Cells were subjected to 18 serially-diluted concentrations of each drug starting from 500mM and ending with 0.5 mM(2/3 serial dilutions).

In the presence of PDE7A inhibitors, cells should restore 5FOA^R growth by elevating cAMP levels to repress *fbp1-ura4* transcription. As seen in (Figures 13, 14) compound 11, 12, 14, 15, and PAN, all except drug 13, significantly exhibit compound -dependent growth. PDE7A was inhibited by less than 10 mM of compound 11, and 14.

Figure 12. PDE7 specific inhibitors

The 750 hits were compared with other PDE (PDE2A, PDE4A, PDE4B, and Cgs2) hits to identify PDE7A specific inhibitors. This resulted in 20 specific compounds with composite Z scores of ≥ 44.5, identified as "PDE7A specific Hits". Four of these specific hits were picked for further analysis (compound #11, #12, #13, #14).

Figure 12.

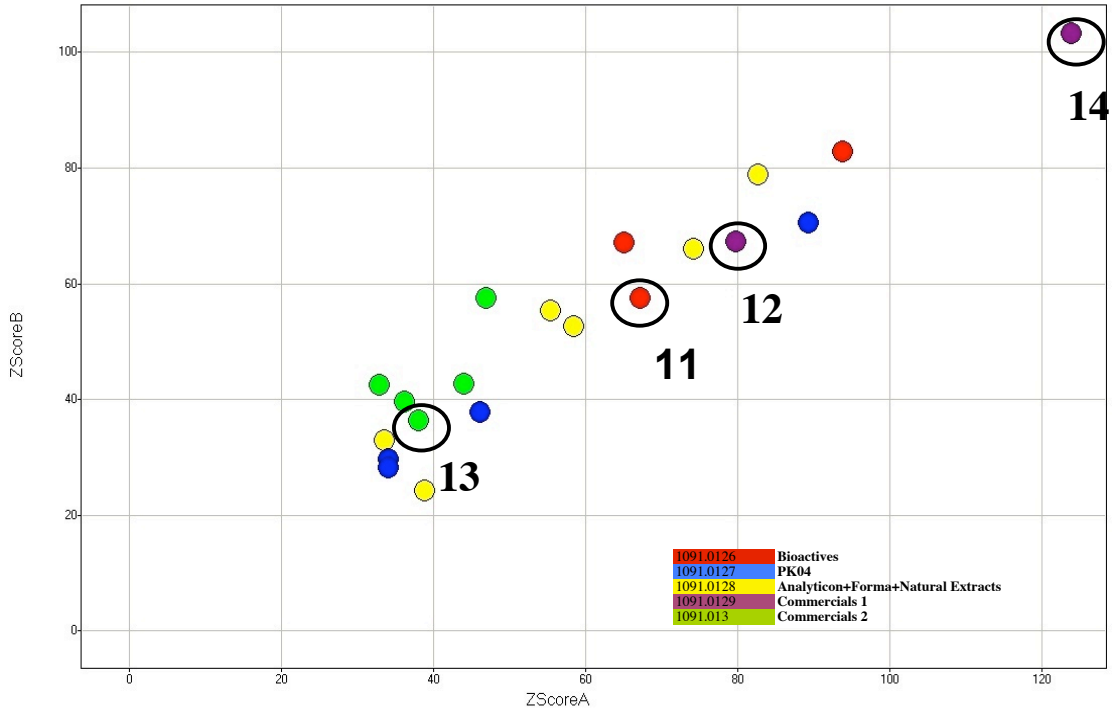

Expt Num	Comp Lab Num	PlateName	Well	Raw ValueA	Raw ValueB	ZScoreA	ZScoreB	Reproducibility	Composite Z
1091.0129	**14**	2005	B21	0.835	0.734	123.92	103.24	0.9959	160.6258
1091.0126	ND	2158	O06	1.144	1.145	93.86	82.88	0.9981	124.9724
1091.0127	ND	2181	N05	1.196	1.152	89.28	70.52	0.9932	112.997
1091.0128	ND	2055	G05	0.937	0.924	82.73	78.87	0.9997	114.2724
1091.0128	ND	2058	I14	0.845	0.785	74.17	66.11	0.9984	99.1982
1091.0129	**12**	2009	A18	0.556	0.498	79.81	67.29	0.9964	104.0182
1091.0126	ND	2159	B09	0.81	0.938	65.04	67.19	0.9999	93.4985
1091.0126	**11**	2160	G10	0.83	0.812	67.19	57.6	0.9971	88.2396
1091.0128	ND	2002	D09	0.684	0.64	58.41	52.63	0.9987	78.5153
1091.0128	ND	2057	G05	0.646	0.666	55.38	55.36	1	78.3038
1091.013	ND	2071	P12	0.442	0.493	46.97	57.56	0.9949	73.9171
1091.013	ND	2044	D16	0.417	0.38	43.96	42.75	0.9999	61.31
1091.0127	ND	2281	O07	0.653	0.65	46.17	37.78	0.995	59.3637
1091.013	ND	2073	D15	0.366	0.332	37.99	36.38	0.9998	52.5913
1091.013	ND	2074	J08	0.353	0.356	36.15	39.69	0.9989	53.6276
1091.013	**13**	2064	J21	0.326	0.381	32.88	42.64	0.9918	53.406
1091.0128	ND	2070	N01	0.435	0.431	33.54	32.93	1	47.0062
1091.0127	ND	2094	F23	0.495	0.521	34.06	29.63	0.9976	45.0371
1091.0127	ND	2093	B11	0.498	0.502	34.07	28.23	0.9956	44.0504
1091.0128	ND	2070	G18	0.491	0.338	38.86	24.35	0.9747	44.6967

Figure 13. PDE7A specific inhibitors restore 5FOA^R growth

In the presence of PDE7A inhibitors, cells should restore 5FOA^R growth by elevating cAMP levels to repress *fbp1-ura4* transcription. Drugs 11, 12, 14, 15, and PAN (the exception is drug 13) significantly exhibit drug dependent –growth.

Figure 13.

#11

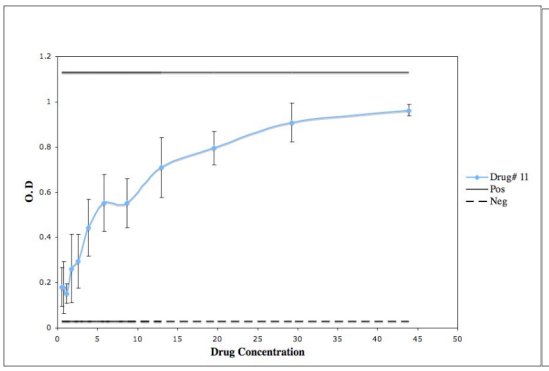

#12

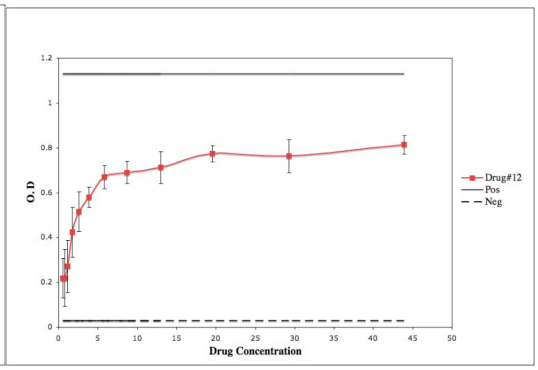

#13

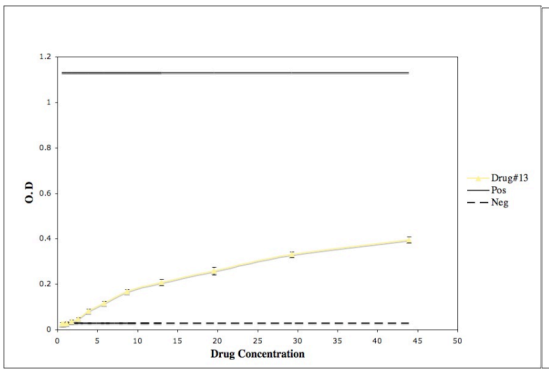

#14

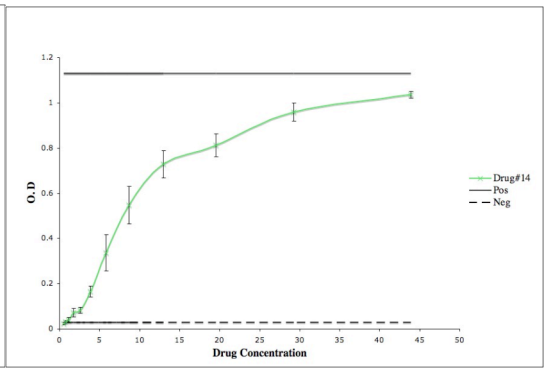

#15

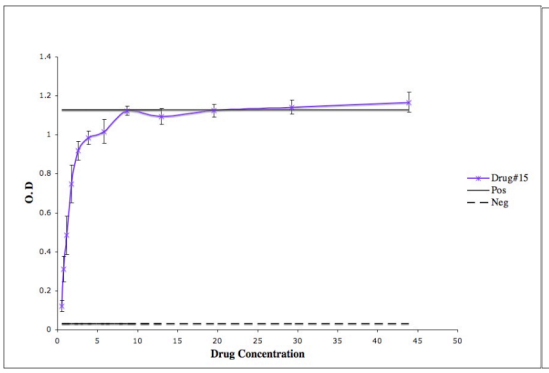

PAN

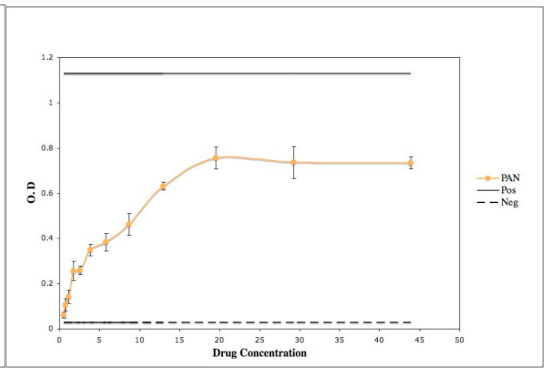

Figure 14. Comparing PDE7A specific inhibitors effect in 5FOA medium

Compound 11, 14 and 12 are potential PDE7 inhibitors. By comparing the compounds with each other, PDE7A was inhibited by < 10 mM of compound 11, and 14, whereas compound 12 and 15 inhibited PDE7A in a much lower concentration showing 3.9 and 1.5 ED50s, respectively. Compound 13 did not inhibit PDE7.

Figure 14.

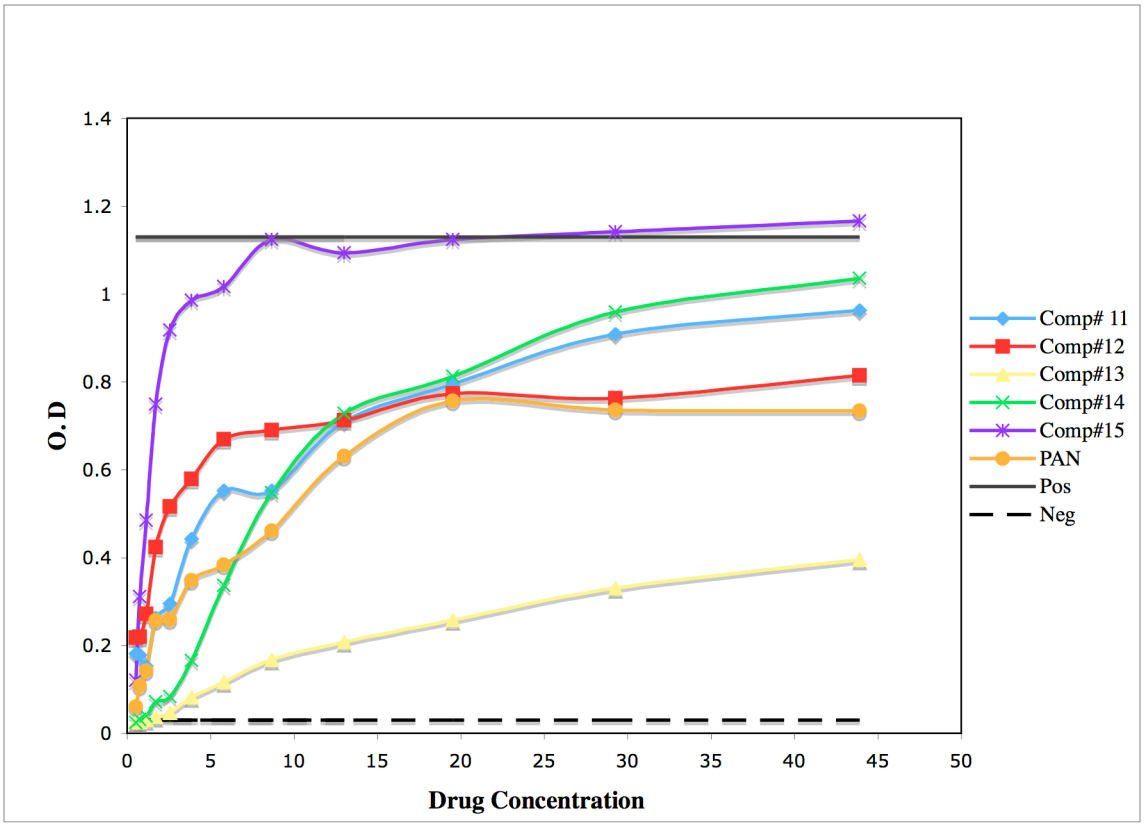

Comp	11	12	13	14	15	PAN
ED50	9.4	3.9	>50	9.4	1.4	11.7

3.6. PDE 7A specific inhibitor elevate cAMP levels

To determine if the effect of drugs 11, 12, 13, 14 and 15 is through PDE7A inhibition, I measured cAMP levels before and after drug treatment. As shown in Figure 15, cAMP levels increase within 1 h of exposure to 100 mM inhibitor in response to drug 11, 14, 15, and 13. Interestingly, drug 13 shows an increase in cAMP level even though showed the least stimulation of $5FOA^R$ growth. Drug 12 did not show significant increase in cAMP levels (See Summary and Discussion).

Figure 15. Comparing PDE7A specific inhibitors effect on cAMP levels

PDE 7A specific inhibitor elevates cAMP levels. cAMP levels were measured before (blue bars) and after (red bars) the compound treatment. cAMP levels increase in response to drugs 11, 14, 15, and 13, but, drug 12 did not show significant increase in cAMP levels.

Figure 15.

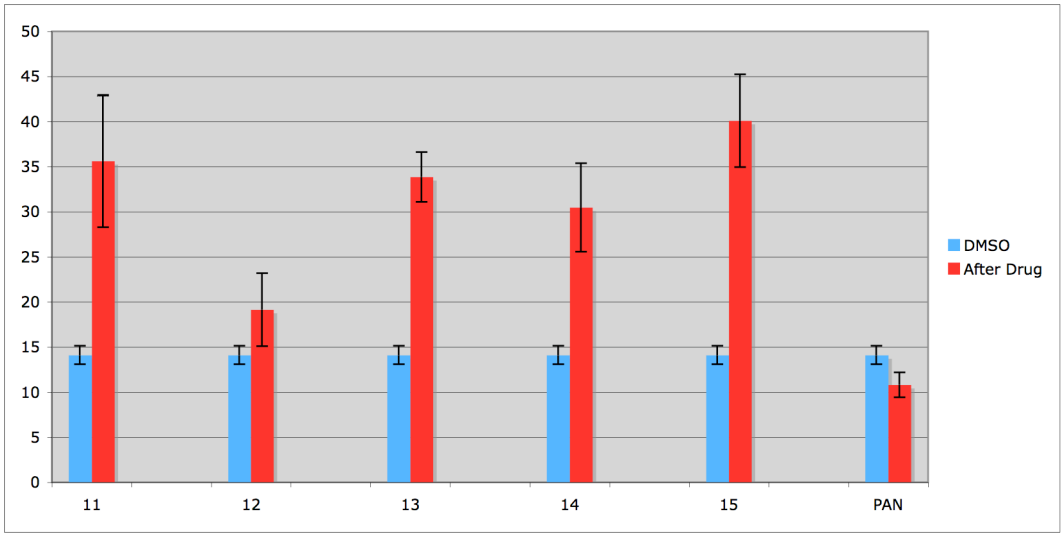

Compound 12 and 15 inhibited PDE7A in a much lower concentration showing 3.9 and 1.5 ED50s, respectively (See Discussion).

CONCLUSION

4.1. Summary

I have integrated human PDE7A into the *S. pombe* genome and identified a strain for use in a cell-based screening platform for finding PDE7A inhibitors. Using strain CHP1189, I have successfully screened 50,000 compounds and detected novel PDE7A inhibitors. High throughput screens performed against compound libraries identified almost 750 compounds that promote $5FOA^R$ growth. Comparing the results with other PDE hits from our lab identified at least 20 specific inhibitors with high Z scores.

The recently identified PDE7A specific inhibitor (BRL 50481) (LERNER and EPSTEIN 2006; SMITH *et al.* 2004) promotes PDE7A-expressed cells $5FOA^R$ growth and shows remarkable increases in cAMP levels upon cell treatment, supporting the validity of our assay and our hits.

Compound 11 and 14 were highly effective against PDE7A on cAMP and confer $5FOA^R$ growth. On the other hand, compound 13 promotes $5FOA^R$ growth poorly, but elevated cAMP level in 1 h of exposure. These data may suggest that compound 13 is less stable than other drugs, since we don't see any growth effect after 48 h of incubation. Therefore,

it is possible that drug 13 cannot maintain PDE7A inhibition for a long time, while we still can observe its effect on cAMP in 1 h after treatment. Another interesting finding is that a low dose of drug 12 was enough to confer $5FOA^R$, but growth plateaus at 6 μM of drug and display no elevated cAMP levels after 1 h of drug treatment.

4.2. Future directions

Results from this study suggest that compound 12 might function differently when inhibiting PDE7A. One reason for not seeing an effect on cAMP levels is that 1 h of exposure was not enough for drug 12 to inhibit PDE7A. Thus, it would be interesting to do a cAMP and 5FOA assay in a time course manner to determine when the cells plateau, and investigate if more than 1 h of treatment can increase cAMP levels. These experiments may uncover the mechanism of how drug 12 inhibits PDE7A. In addition, testing more drugs out of the "PDE7A specific collection" will help us understand the mode of action of these drugs, especially since some of the drugs share structural similarity (data not shown).

Little is known about PDE7 function and tools such as these inhibitors could help in the characterization of PDE7. Smith *et al* 2004 found that BRL 50481(SMITH *et al.* 2004) was able to block TNF secretion in a dose-dependent manner in aged monocytes and was more efficient when combined with the PDE4 inhibitor rolipram. In addition, T-2585 a dual PDE4/PDE7 inhibitor that suppresses the proliferation of T cells was more effective

than RP 73401 (piclamilast) a PDE4 selective inhibitor (LERNER and EPSTEIN 2006; SMITH *et al.* 2004). Therefore, finding and testing an inhibitor from our libraries that can target PDE7 and PDE4 can possibly be more effective as an anti-inflammatory drug.

APPENDIX TWO

SCREENING FOR HUMAN PDE7A ACTIVATORS USING A YEAST CELL-BASED SYSTEM

SCREENING FOR HUMAN PDE7A ACTIVATORS USING A YEAST CELL-BASED SYSTEM

1. INTRODUCTION

Finding new PDE7A activators can advance our understanding of the function of that enzyme. Thus it can potentially improve basic research and therapeutic approaches. I will describe herein an *in vivo* screen for identifying chemical activators of PDE7A using the same assay platform utilized for finding PDE7A inhibitors (APPENDIX I).

A potential PDE activator should confer growth in SC-ura or EMM medium to a strain that expresses high cAMP levels by reducing its cAMP levels, which will allow *fbp1-ura4* transcription. A suitable strain for screening must fail to grow in a SC- Ura /EMM-Ura medium in the absence of PDE7A stimulation.

2. SCREENING PROCESS

High throughput drug screens were performed at the Broad Institute's Chemical Biology Program screening facility. PDE7A cultures (CHP1171) were pre-grown in EMM complete medium overnight. Cells were then washed, mixed very well and transferred to 384-well microtiter dishes into EMM-Ura or SC-ura medium at a final density 1.5 x10^5 cells/ml and a final volume of 50 ml. 100 nl of compounds were pinned into the wells at a final concentration of 20 mM. Control plates received 100 nl DMSO. Cultures were incubated for 48 h at 30ºC, sealed in a container with moist paper towels to prevent

evaporation. Optical density (OD_{600}) of cultures was measured after mixing the cells with a plate mixer.

3. RESULTS

3.1. Strain optimization

To determine the best conditions for high throughput for chemical PDE7A activator screening, I used a PDE7A-strain that has an *fbp1-ura4* reporter that expresses high cAMP levels. This strain should not grow in SC- Ura /EMM-Ura medium in the absence of a PDE7A activator. Therefore, I performed an optimization experiment to determine the appropriate optimal cell densities that give low coefficient of variation (CV) value (The cut-off used by the Broad Institute's Chemical Biology Program requires a ≤15 % value). This is needed for screens for screens for which a positive control is not available as seen in Figure 1 by using $1.5x10^5$ cell density, I was able to lower the CV values using SC- Ura /EMM-Ura.

3.2. Strain Screening and Hit's

Using CHP1171, a strain expressing human PDE7A which express high basal cAMP levels, I screened for compounds that if activated, PDE7A should confer Ura^+ growth due to repression of *fbp1-ura4* expression. By performing two experiments (1091.0133) and (1091.0134) I screened the Bioactive, Natural extracts libraries and some additional

plates from Analyticon library. Experiment number (1091.0133) was performed in EMM -ura while screen number (1091.0134) was performed in SC -ura. Both experiments were incubated for 48 h. I also read experiment (1091.0134) plates after 67 h of incubation, and renamed the experiment number (changed to 1091.0135). Duplicate plates were screened and compounds that confer such growth with composite Z scores of ≥8.53 were identified as "Hits". One general finding in all of the activator screens is the presence of spots scattering away from the diagonal direction creating an "L" shape. This was due to problems with the reproducibility of the replicates.

Figure 1. Optimization of strain CHP1171

Optimization experiment of strain CHP1171 to determine the right cell densities that give lower coefficient of variation (CV) values (The cut-off used by the Broad Institute's Chemical Biology Program requires a ≤15 % value). Using $1.5x10^5$ cell densities gave the lowest the CV values using SC- Ura /EMM-Ura.

Figure 1.

1x=0.5*10^5
2x=1*10^5
3x=1.5*10^5

EMM-ura1x			**EMM-ura1x**		
	avg	0.04311719		avg	0.04141146
	stdev	0.01791278		stdev	0.0162791
	CV	41.544402		CV	39.3106177
EMM-ura2x			**EMM-ura2x**	avg	0.04595182
	avg	0.0506276		stdev	0.006449
	stdev	0.01655371		CV	14.0342623
	CV	32.6970106			
EMM-ura3x			**EMM-ura3x**		
	avg	0.06648307		avg	0.05430339
	stdev	0.01416313		stdev	0.00600003
	CV	21.3033617		CV	11.0490972
Sc-ura1x	avg	0.04129557	**Sc-ura1x**	avg	0.04057943
	stdev	0.01047079		stdev	0.00637989
	CV	25.3557183		CV	15.7219706
Sc-ura2x			**Sc-ura2x**		
	avg	0.0459349		avg	0.04480208
	stdev	0.01121758		stdev	0.01062898
	CV	24.4206048		CV	23.7242884
Sc-ura3x			**Sc-ura3x**		
	avg	0.05585286		avg	0.05167448
	stdev	0.01415367		stdev	0.00490837
	CV	25.3409958		CV	9.49863009

3.2.1. Experiment 1091.0133 Hits

Using CHP1171, a strain expressing human PDE7A for screening in EMM-Ura, I only obtained two hits from the Natural extract library, which were highly reproducible with a composite Z of 11 and 10.5, respectively, as seen in Figure 2.

3.2.2. Experiment 1091.0134 Hits

Using CHP1171, a strain expressing human PDE7A for screening in SC –Ura , I obtained 15 hits (Figure 3 A, B), three of them were DMSO, as seen in (Figure 3C) highlighted in gray. The plates of this experiment were read again after 67 h and renamed to experiment 1091.0135. Results from these experiments are shown in (Figure 4) were it is displayed shared hits between PDE7A and PDE8 and PDE2 (See Discussion).

Figure 2. Experiment 1091.0133 Hits

CHP1171 growth in EMM-Ura displayed only two hits, which were reproducible with a composite Z 11, and 10.5. Note the presence of spots scattering away from the diagonal direction creating an "L" shape due to low reproducibility of replicates. Red circles represent the negative control (cells+DMSO), while the blue circles represent compounds that were screened.

Figure 2.

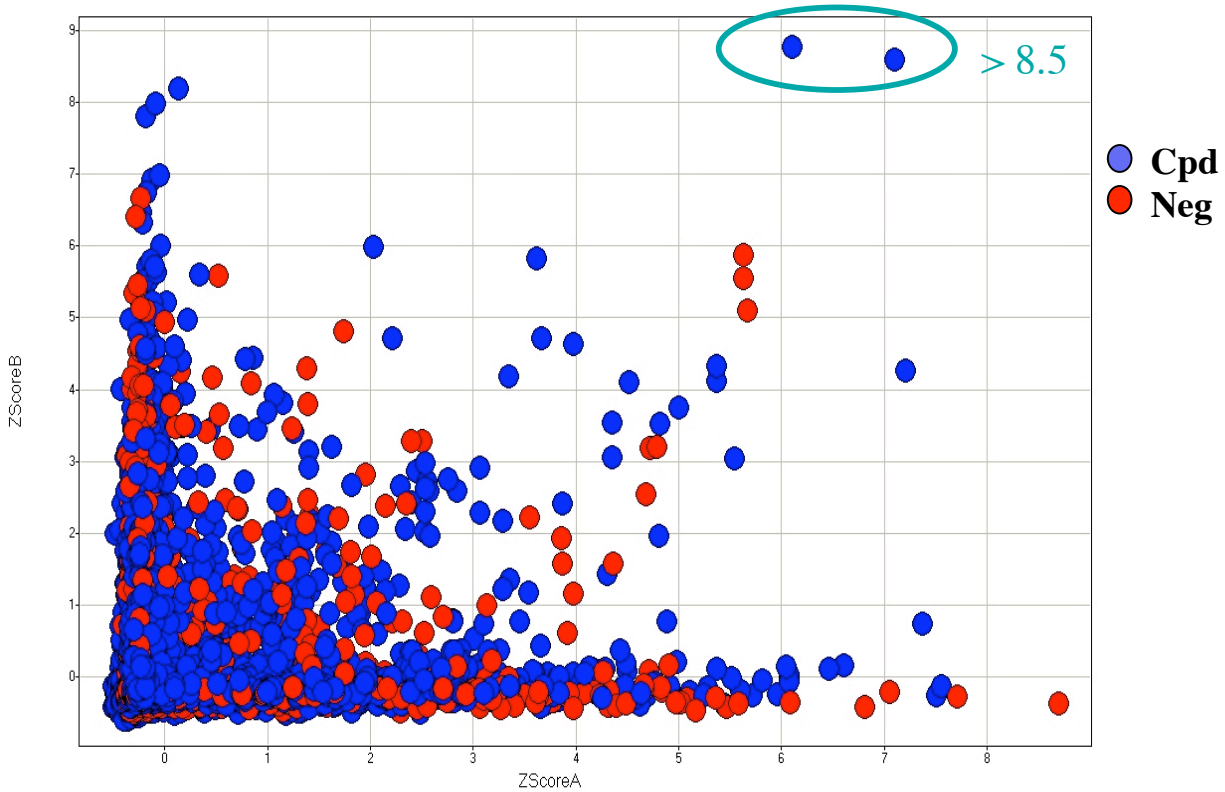

Plate	Type	Well	ZScoreA	ZScoreB	CompositeZ	Reproducibility	Compound Name
2091	Cpd	D19	7.1	8.6	11.1002	0.9955	LDV0794.217I.Frx2(5)
2144	Cpd	K04	6.1	8.78	10.5235	0.9842	86.3983V.35

Figure 3. Experiment 1091.0134 Hits

(A) Display of PDE7A screen results using CHP1171 strain in SC -Ura. **(B)** Display of 15 hits on the diagonal (green circle), although this indicates three DMSO negatives control wells (red circles highlighted in gray). Note the presence of spots scattering away from the diagonal direction creating an "L" shape due to low reproducibility of replicates. Red circles represent the negative control (cells +DMSO), while the blue circles represent compounds that were screened. **(C)** Table show 15 hits, three of them were DMSO highlighted in gray.

Figure 3.

A.

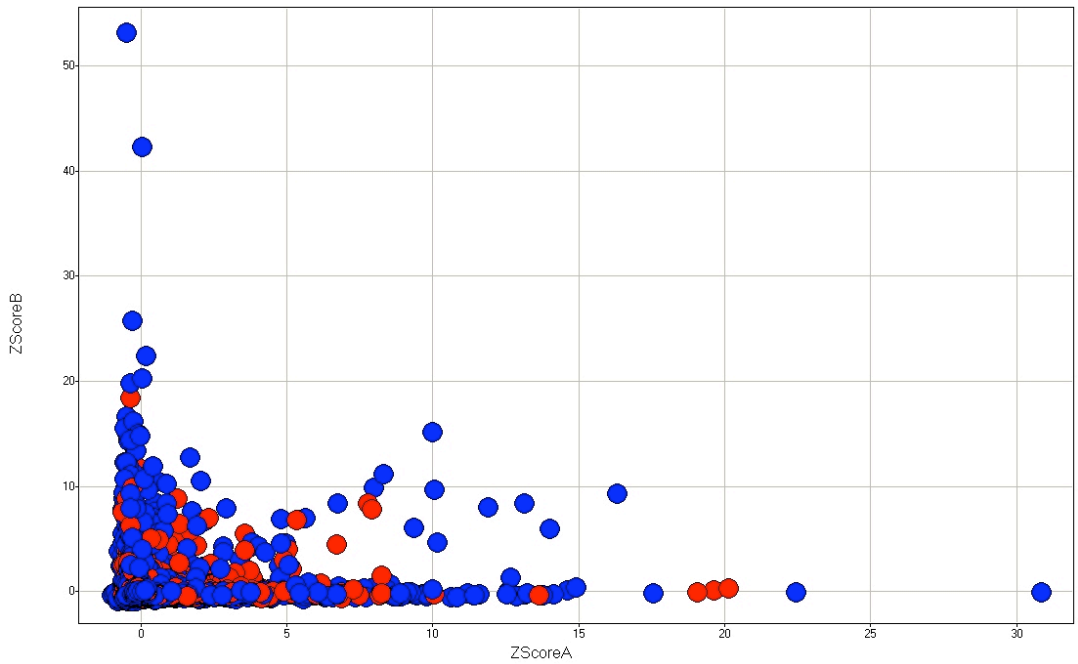
ZScoreB
ZScoreA
0
10
20
30
40
50
0
5
10
15
20
25
30

B.

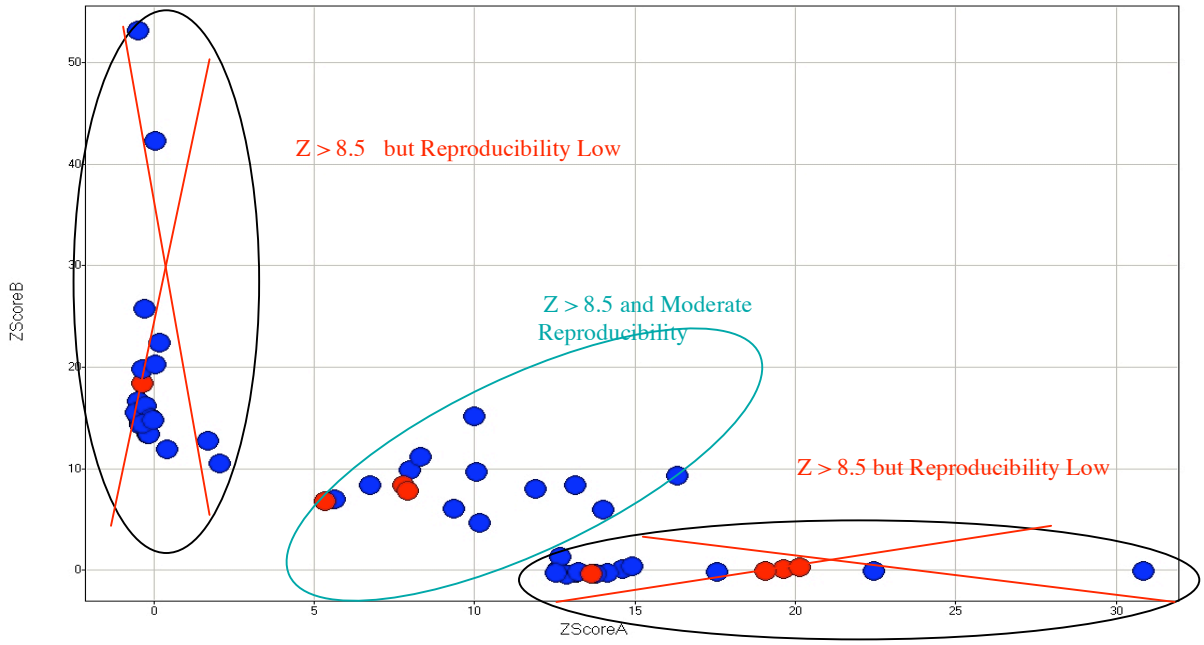
Z > 8.5 but Reproducibility Low
Z > 8.5 and Moderate Reproducibility
Z > 8.5 but Reproducibility Low
ZScoreB
ZScoreA
0
10
20
30
40
50
0
5
10
15
20
25
30

(C)

Plate	Well	ZScoreA	Type	ZScoreB	CompositeZ	Reproducibility	Compound Name
2099	C20	9.99	Cpd	15.18	17.7997	0.9795	malachite green carbinol base
2099	G17	5.63	Cpd	7.02	8.9429	0.994	thionin acetate
2099	I05	10.06	Cpd	9.66	13.9448	0.9998	mitoxantrone
2104	H08	14.01	Cpd	6	14.1506	0.9284	3,4-Dichloroisocoumarin
2160	F18	7.98	Cpd	9.84	12.604	0.9946	mitoxanthrone hydrochloride
2160	K03	11.9	Cpd	8.03	14.0906	0.9816	menthone
2160	L14	16.33	Cpd	9.31	18.1308	0.9645	tropicamide
2161	I18	8.33	Cpd	11.2	13.8141	0.9894	gentian violet
2162	L02	7.79	Con	8.39	11.4427	0.9993	DMSO
2163	K12	9.35	Cpd	6.02	10.8686	0.9774	isobutylmethylxanthine
2163	P05	13.13	Cpd	8.37	15.2029	0.9763	4-nonylphenol
2165	B08	10.14	Cpd	4.64	10.448	0.9372	Azathymine, 6
2166	H04	6.75	Cpd	8.39	10.708	0.9942	Butacaine
Base	K05	5.35	Con	6.82	8.6049	0.9928	DMSO
Base	L10	7.92	Con	7.8	11.1151	1	DMSO

Figure 4. Experiment 1091.0135 Hits

The plates of experiment 1091.0134 were read again after 67 h and renamed to experiment 1091.0135. (A) Display PDE7A screen results using (CHP1171) strain in SC –Ura after 67 h **(B)** Display hits on the diagonal (green check mark). Note the presence of spots scattering away from the diagonal direction creating an "L" shape due to low reproducibility of replicates. Red circles represent the negative control (cells +DMSO), while the blue circles represent compounds that were screened.

Figure 4.

A.

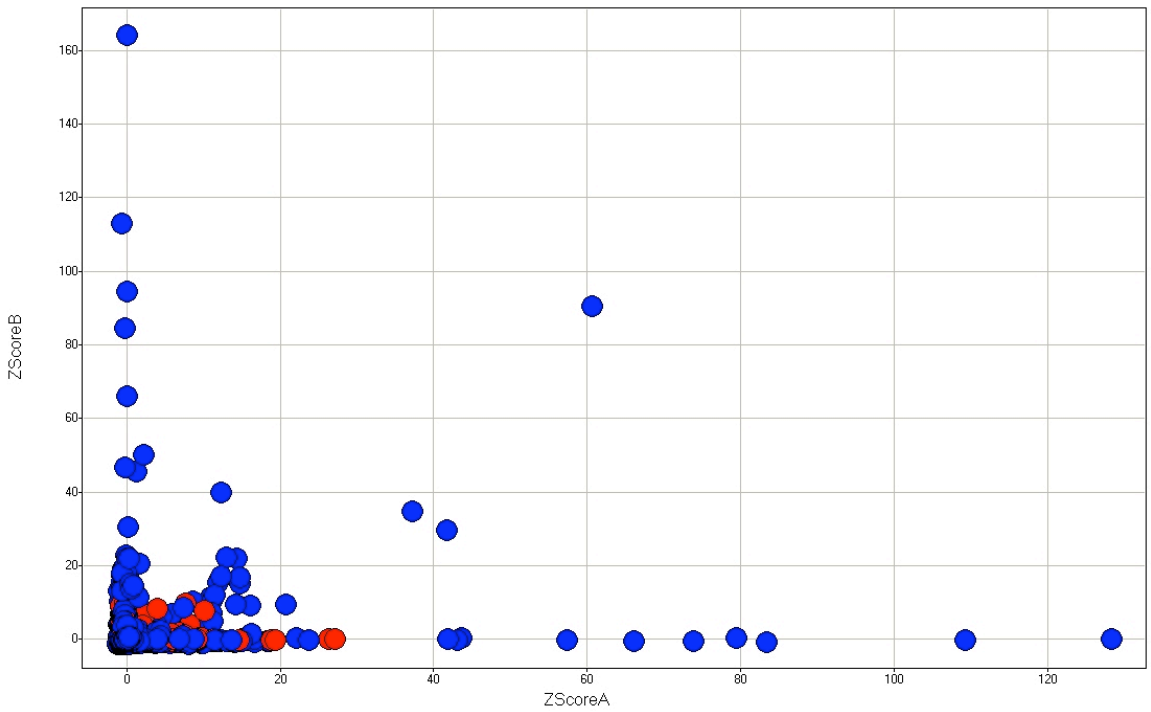
ZScoreB
ZScoreA
0
20
40
60
80
100
120
140
160

B.

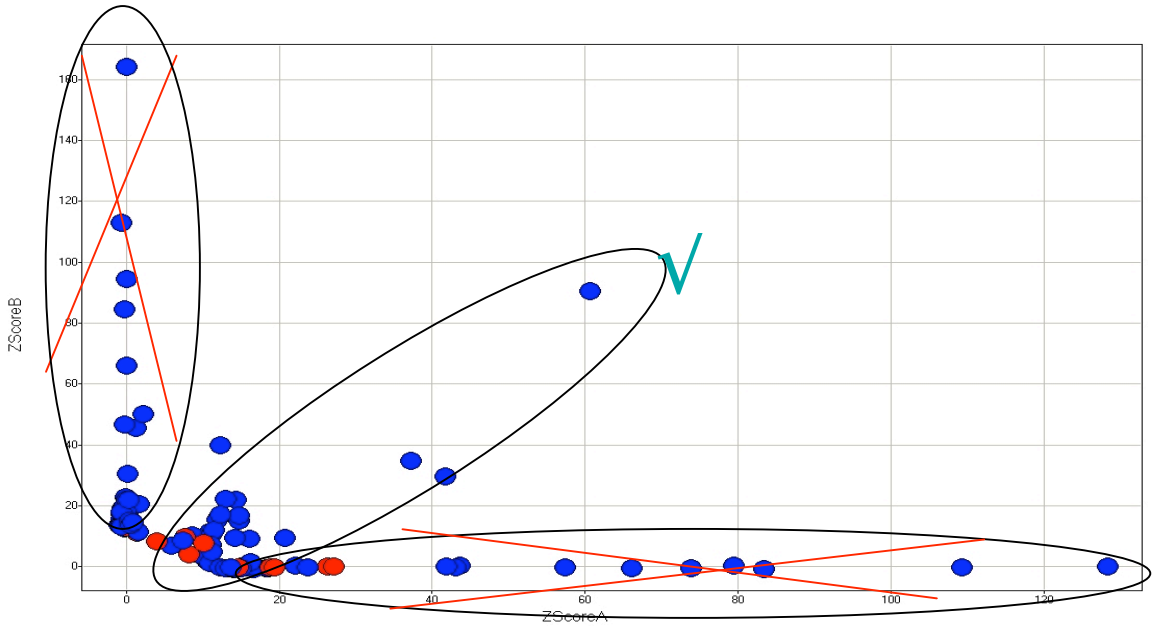
ZScoreB
ZScoreA
0
20
40
60
80
100
120
140
160

Table 1. Shared hits between (PDE7A, PDE8 and PDE2)

This table demonstrates the compounds that were shared hits among activators screens carried out against strains expressing PDE7A, PDE8 and PDE2. Yellow: PDE7A Hits (48 and 67 h). Green: PDE7A and PDE2 shared hits. Blue: PDE7, PDE8 and PDE2 shared hits. The presence of spots scattering away from the diagonal direction creating an "L" shape is due to low reproducibility of replicates.

Table 1.

Type	Plate	Well	ZScoreA	ZScoreB	CompositeZ	Reproducibility	Compound Name
Cpdm	2104	E07	60.59	90.6	106.904	0.9809	Oxindole I
Cpd	2105	L03	37.27	34.84	50.9863	0.9994	Ro-31-8425
Cpd	BioKin1	C11	41.65	29.6	50.3835	0.986	BiomolKI2_000016
Cpd	2099	C20	14.41	21.9	25.6722	0.9794	malachite green carbinol base
Cpd	2159	J11	13.03	22.13	24.8568	0.9681	uridine triphosphate trisodium
Cpd	2099	K06	14.69	16.69	22.1907	0.998	N,N-dimethyl-D-erythro-sphingosine
Cpd	2104	H08	20.77	9.33	21.2855	0.9347	3,4-Dichloroisocoumarin
Cpd	2099	I05	14.69	15.12	21.0774	0.9999	mitoxantrone
Cpd	2161	I18	12.26	17.23	20.8522	0.9861	gentian violet
Cpd	2160	F18	11.87	15.52	19.3698	0.9912	mitoxanthrone hydrochloride
Cpd	2160	K03	16.14	9.22	17.9328	0.9648	menthone
Cpd	2163	E20	14.26	9.29	16.649	0.9784	6-aminonicotinamide
Cpd	2160	L14	11.49	11.89	16.5325	0.9999	tropicamide
Cpd	2099	G06	10.99	11.48	15.8939	0.9998	N,N,N-trimethyl-D-erythro-sphingosine
Cpd	2099	L13	11.18	10.88	15.5998	0.9999	D-lactosyl-B1-1'-D-erythro-sphingosine
Cpdweak	2099	G17	8.62	10.27	13.3617	0.9962	thionin acetate
Cpd	2163	K12	11.13	7.23	12.9811	0.9781	isobutylmethylxanthine
Con	Base	L10	10.16	7.7	12.6346	0.9906	DMSO
Con	2162	L02	7.69	9.84	12.3963	0.9925	DMSO
Cpdm	2165	B08	11.24	4.91	11.4229	0.9312	Azathymine, 6
Cpdm	2166	H04	7.37	8.65	11.3345	0.9968	Butacaine
Cpd	2105	G02	9.68	3.71	9.4705	0.9133	Sphingosylphosphorylcholine
Cpd	2165	F11	5.93	6.73	8.9539	0.998	Chicago sky blue 6B;4-aminoantipyrine
Con	Base	K05	4	8.31	8.7058	0.9439	DMSO
Con	2160	G01	8.18	3.89	8.534	0.9424	DMSO

DISCUSSION

One challenge of doing this type of screen is problems with the reproducibility of replicates (including the DMSO, which in some cases were showing up as positives in one of the two replicates). Comparing this screen with other screens performed on PDE2A and PDE8 in EMM-Ura (Wang, Demirbas) all three screens identified compound 2099 C20 (malachite green carbinol base) as a modest hit. Whereas, PDE7A screens carried in SC-ura compared with PDE2A screen have 8 shared hits. Therefore, despite the reproducibility problem encountered doing this screen, finding shared suggest that the growth is not due to PDE stimulation.

APPENDIX THREE

OPTIMIZATION OF DIFFERENT STRAINS TO BE USED FOR HIGH THROUGHPUT SCREENING

OPTIMIZATION OF DIFFERENT STRAINS TO BE USED FOR HIGH THROUGHPUT SCREENING

1. INTRODUCTION

To determine the best conditions for high throughput drug screening, a number of factors need to be taken into consideration including the right genetic background, the right cAMP concentration for pre-growth conditions, and final cell densities, all important elements in the optimization process. Here, I will show the best cell densities that should be used for four strains CHP1156, CHP1156, CHP1132 and CHP1142 to perform high throughput screening, as shown in Table 1.

2. STRAIN OPTIMIZATION

2.1. Strain CHP1156 optimization

Strain CHP1156 expressing *Trypanosoma cruzi* PDE in *git3* deletion background was pre-grown in EMM medium containing concentration 5 mM of cAMP and different final cell densities ($2x10^5$, $2.5\ x10^5$) then cultures were transferred to 5FOA in the presence or absence 5mM cAMP. All plates received 100 nl DMSO. The OD_{600} measurements were taken after 48 h of incubation at 30ºC. Cells were grown in the presence of cAMP in order to repress the *fbp1-ura4* reporter prior to exposure to 5FOA medium. I found that the best cell densities for this strain was $2.5\ x10^5$ as final cell density when transferred to 5FOA (Figure 1).

2.2. Strain CHP1155 optimization

Strain CHP1155 expressing PDE4A in the *gpa2* deletion background was pre-grown in EMM medium containing 2.5 mM of cAMP and different final cell densities ($0.75x10^5$, $1x10^5$) then cultures were transferred to 5FOA in the presence or absence 5 mM cAMP. Rolipram was also used as positive control for this strain. All plates received of 100 nl DMSO. OD_{600} measurements were taken after 48 h of incubation at 30ºC. Cells were grown in the presence of cAMP in order to repress the *fbp1-ura4* reporter prior to exposure to 5FOA medium. I found that the best cell density for this strain was 1 $x10^5$ as the final cell density when transferred to 5FOA (Figure 2).

2.3. Strain CHP1132 and CHP1142 optimization

Strain CHP1132 and CHP1142 were expressing *S. pombe cgs2* in a *git32* deletion background with different mating types h^- and an h^+, respectively. Both were pre-grown in EMM medium containing 2.5 mM of cAMP and different final cell densities ($1.5x10^5$, $2x10^5$ cells/ml) then cultures were transferred to 5FOA in the presence or absence 5 mM cAMP. All plates received 100 nl of DMSO. OD_{600} measurements were taken after 48 h of incubation at 30ºC. Cells were grown in the presence of cAMP in order to repress the *fbp1-ura4* reporter prior to exposure to 5FOA medium. I found that the best cell density for both strains is 1.5 $x10^5$ cells/ml as the final cell density when transferred to 5FOA (Figure 1).

3. CONCLUSION

All of these strains are ready to go through high throughput screening (HTS) since I was able to obtain a Z factor higher than 0.5.

Figure 1. Strains optimizations with 1x cell density

Two experiments were performed on different days on strains CHP1132, CHP1142, CHP1155, CHP1156 using these cells densities 1x=$1.5x10^5$, 1.5 $x10^5$, 0.75 $x10^5$, $2x10^5$ cells/ml respectively. Z factors of all the strains were higher than the Broad institute cut off.

Figure 1.

First experiment

CHP 1132	POS	NEG	Z
avg	1.21	0.07	0.92
stdev	0.02	0.01	
CV	1.84	10.1	

CHP1142	POS	NEG	Z
avg	1.25	0.09	0.9
stdev	0.03	0	
CV	2.8	4.99	

CHP 1155	POS	NEG	Z
avg	1.27	0.05	0.88
stdev	0.04	0.01	
CV	3.37	14.6	

CHP 1155 Rolipram	POS	NEG	Z
avg	0.86	0.05	0.56
stdev	0.11	0.01	
CV	13.1	12.9	

CHP 1156	POS	NEG	Z
avg	1.27	0.1	0.86
stdev	0.03	0.02	
CV	2.74	18.9	

Second experiment

CHP 1132	POS	NEG	Z
avg	0.79	0.1	0.81
stdev	0.04	0.01	
CV	4.69	6.29	

CHP1142	POS	NEG	Z
avg	1.07	0.1	0.81
stdev	0.05	0.01	
CV	4.89	7.52	

CHP 1155	POS	NEG	Z
avg	1.21	0.05	0.9
stdev	0.04	0	
CV	3.04	6.63	

CHP 1155 Rolipram	POS	NEG	Z
avg	1.07	0.05	0.67
stdev	0.11	0	
CV	10.2	6.38	

CHP 1156	POS	NEG	Z
avg	1.06	0.35	0.6
stdev	0.06	0.04	
CV	5.33	11.4	

Figure 2. Strain optimizations with 2X cell density

Two experiments were performed on different days using higher cell densities than shown in Figure 1 on strains CHP1132, CHP1142, CHP1155, CHP1156. Cell densities used for theses strains were 2X= $2x10^5$, 2 $x10^5$, $1x10^5$, 2.5 $x10^5$, respectively. Z factors of all strains under these conditions were also higher than the Broad Institute cut off.

Figure 2.

First experiment

CHP 1132	POS	NEG	Z
avg	1.21	0.07	0.92
stdev	0.02	0.01	
CV	1.84	10.1	

CHP1142	POS	NEG	Z
avg	1.25	0.09	0.9
stdev	0.03	0	
CV	2.8	4.99	

CHP 1155	POS	NEG	Z
avg	1.27	0.05	0.88
stdev	0.04	0.01	
CV	3.37	14.6	

CHP 1155 Rolipram	POS	NEG	Z
avg	0.86	0.05	0.56
stdev	0.11	0.01	
CV	13.1	12.9	

CHP 1156	POS	NEG	Z
avg	1.27	0.1	0.86
stdev	0.03	0.02	
CV	2.74	18.9	

CHP 1169	POS	NEG	Z
avg	1.52	0.78	0.58
stdev	0.04	0.06	
CV	2.91	7.66	

Second experiment

CHP 1132	POS	NEG	Z
avg	0.79	0.1	0.81
stdev	0.04	0.01	
CV	4.69	6.29	

CHP1142	POS	NEG	Z
avg	1.07	0.1	0.81
stdev	0.05	0.01	
CV	4.89	7.52	

CHP 1155	POS	NEG	Z
avg	1.21	0.05	0.9
stdev	0.04	0	
CV	3.04	6.63	

CHP 1155 Rolipram	POS	NEG	Z
avg	1.07	0.05	0.67
stdev	0.11	0	
CV	10.2	6.38	

CHP 1156	POS	NEG	Z
avg	1.06	0.35	0.6
stdev	0.06	0.04	
CV	5.33	11.4	

CHP 1169	POS	NEG	Z
avg	1.39	0.44	0.71
stdev	0.05	0.04	
CV	3.29	9.97	

REFERENCES

ALAAMERY, M. A., and C. S. HOFFMAN, 2008 Schizosaccharomyces pombe Hsp90/Git10 Is Required for Glucose/cAMP Signaling. Genetics **178:** 1927-1936.

ALFA, C., P. FANTES, J. HYAMS, M. MCLEOD and E. WARBRICK, 1993 *Experiments with Fission Yeast*. Cold Spring Harbor Laboratory Press, Cold Spring Harbor, N.Y.

ALIGUE, R., H. AKHAVAN-NIAK and P. RUSSELL, 1994 A role for Hsp90 in cell cycle control: Wee1 tyrosine kinase activity requires interaction with Hsp90. EMBO J **13:** 6099-6106.

AZEVEDO, C., A. SADANANDOM, K. KITAGAWA, A. FREIALDENHOVEN, K. SHIRASU *et al.*, 2002 The RAR1 interactor SGT1, an essential component of R gene-triggered disease resistance. Science **295:** 2073-2076.

BAGATELL, R., and L. WHITESELL, 2004 Altered Hsp90 function in cancer: a unique therapeutic opportunity. Mol Cancer Ther **3:** 1021-1030.

BÄHLER, J., J. Q. WU, M. S. LONGTINE, N. G. SHAH, A. MCKENZIE, 3RD *et al.*, 1998 Heterologous modules for efficient and versatile PCR-based gene targeting in Schizosaccharomyces pombe. Yeast **14:** 943-951.

BANERJI, U., A. O'DONNELL, M. SCURR, S. PACEY, S. STAPLETON *et al.*, 2005 Phase I pharmacokinetic and pharmacodynamic study of 17-allylamino, 17-demethoxygeldanamycin in patients with advanced malignancies. J Clin Oncol **23:** 4152-4161.

BANSAL, P. K., R. ABDULLE and K. KITAGAWA, 2004 Sgt1 associates with Hsp90: an initial step of assembly of the core kinetochore complex. Mol Cell Biol **24:** 8069-8079.

BARDWELL, J. C., and E. A. CRAIG, 1987 Eukaryotic Mr 83,000 heat shock protein has a homologue in *Escherichia coli*. Proc Natl Acad Sci U S A **84:** 5177-5181.

BEEBE, S. J., 1994 The cAMP-dependent protein kinases and cAMP signal transduction. Semin Cancer Biol **5:** 285-294.

BIJLMAKERS, M. J., and M. MARSH, 2000 Hsp90 is essential for the synthesis and subsequent membrane association, but not the maintenance, of the Src-kinase p56(lck). Mol Biol Cell **11:** 1585-1595.

BIRNBY, D. A., E. M. LINK, J. J. VOWELS, H. TIAN, P. L. COLACURCIO *et al.*, 2000 A transmembrane guanylyl cyclase (DAF-11) and Hsp90 (DAF-21) regulate a common set of chemosensory behaviors in caenorhabditis elegans. Genetics **155:** 85-104.

BLATCH, G. L., and M. LASSLE, 1999 The tetratricopeptide repeat: a structural motif mediating protein-protein interactions. Bioessays **21:** 932-939.

BORKOVICH, K. A., F. W. FARRELLY, D. B. FINKELSTEIN, J. TAULIEN and S. LINDQUIST, 1989 hsp82 is an essential protein that is required in higher concentrations for growth of cells at higher temperatures. Mol Cell Biol **9:** 3919-3930.

BOTER, M., B. AMIGUES, J. PEART, C. BREUER, Y. KADOTA *et al.*, 2007 Structural and functional analysis of SGT1 reveals that its interaction with HSP90 is required for

the accumulation of Rx, an R protein involved in plant immunity. Plant Cell **19:** 3791-3804.

BUCHNER, J., 1999 Hsp90 & Co. - a holding for folding. Trends Biochem Sci **24:** 136-141.

BYRNE, S. M., and C. S. HOFFMAN, 1993a Six git genes encode a glucose-induced adenylate cyclase activation pathway in the fission yeast Schizosaccharomyces pombe. J Cell Sci **105 (Pt 4):** 1095-1100.

CAI, D., J. QIU, Z. CAO, M. MCATEE, B. S. BREGMAN *et al.*, 2001 Neuronal cyclic AMP controls the developmental loss in ability of axons to regenerate. J Neurosci **21:** 4731-4739.

CATLETT, M. G., and K. B. KAPLAN, 2006 Sgt1p is a unique co-chaperone that acts as a client adaptor to link Hsp90 to Skp1p. J Biol Chem **281:** 33739-33748.

CHARLTON, C., 2005 Characterization of immunological reagents for the study of Schizosaccharomyces pombe Git7 in the glucose triggered cAMP pathway Boston College Master of Science Dissertation.

CHIOSIS G, VILENCHIK M, KIM J and S. D., 2004 Hsp90: the vulnerable chaperone. Drug Discov Today **9:** 881-888.

CLAPHAM, D. E., 1995 Calcium signaling. Cell **80:** 259-268.

COLOMBO, S., P. MA, L. CAUWENBERG, J. WINDERICKX, M. CRAUWELS *et al.*, 1998 Involvement of distinct G-proteins, Gpa2 and Ras, in glucose- and intracellular

acidification-induced cAMP signalling in the yeast Saccharomyces cerevisiae. Embo J **17:** 3326-3341.

COPPE, D., and M. L. STEER, 1978 Cyclic AMP. Int J Oral Surg **7:** 52-61.

CSERMELY, P., J. KAJTAR, M. HOLLOSI, G. JALSOVSZKY, S. HOLLY *et al.*, 1993 ATP induces a conformational change of the 90-kDa heat shock protein (hsp90). J Biol Chem **268:** 1901-1907.

CSERMELY, P., T. SCHNAIDER, C. SOTI, Z. PROHASZKA and G. NARDAI, 1998 The 90-kDa molecular chaperone family: structure, function, and clinical applications. A comprehensive review. Pharmacol Ther **79:** 129-168.

CSERMELY, P., C. SOTI and G. L. BLATCH, 2007 Chaperones as parts of cellular networks. Adv Exp Med Biol **594:** 55-63.

DAL SANTO, P., B. BLANCHARD and C. S. HOFFMAN, 1996 The *Schizosaccharomyces pombe* pyp1 protein tyrosine phosphatase negatively regulates nutrient monitoring pathways. J Cell Sci **109:** 1919-1925.

DAS, R., V. ESPOSITO, M. ABU-ABED, G. S. ANAND, S. S. TAYLOR *et al.*, 2007 cAMP activation of PKA defines an ancient signaling mechanism. Proc Natl Acad Sci U S A **104:** 93-98.

DEBOER, C., P. A. MEULMAN, R. J. WNUK and D. H. PETERSON, 1970 Geldanamycin, a new antibiotic. J Antibiot (Tokyo) **23:** 442-447.

DEVOTI, J., G. SEYDOUX, D. BEACH and M. MCLEOD, 1991 Interaction between ran1+ protein kinase and cAMP dependent protein kinase as negative regulators of fission yeast meiosis. Embo J **10:** 3759-3768.

DIVECHA, N., and R. F. IRVINE, 1995 Phospholipid signaling. Cell **80:** 269-278.

DUBACQ, C., R. GUEROIS, R. COURBEYRETTE, K. KITAGAWA and C. MANN, 2002 Sgt1p contributes to cyclic AMP pathway activity and physically interacts with the adenylyl cyclase Cyr1p/Cdc35p in budding yeast. Eukaryot Cell **1:** 568-582.

EISEMAN, J. L., J. LAN, T. F. LAGATTUTA, D. R. HAMBURGER, E. JOSEPH *et al.*, 2005 Pharmacokinetics and pharmacodynamics of 17-demethoxy 17-[[(2-dimethylamino)ethyl]amino]geldanamycin (17DMAG, NSC 707545) in C.B-17 SCID mice bearing MDA-MB-231 human breast cancer xenografts. Cancer Chemother Pharmacol **55:** 21-32.

FALSONE, S. F., B. GESSLBAUER, F. TIRK, A. M. PICCININI and A. J. KUNGL, 2005 A proteomic snapshot of the human heat shock protein 90 interactome. FEBS Lett **579:** 6350-6354.

FAN, A. C., M. K. BHANGOO and J. C. YOUNG, 2006 Hsp90 functions in the targeting and outer membrane translocation steps of Tom70-mediated mitochondrial import. J Biol Chem **281:** 33313-33324.

FONTANA J, C. Y. FULTON D, FAIRCHILD TA, MCCABE TJ, FUJITA N *et al.*, 2002 Domain mapping studies reveal that the m domain of hsp90 serves as a molecular scaffold to regulate akt-dependent phosphorylation of endothelial nitric oxide synthase and NO release. Circ Res **90:** 866–873.

FONTANA, J., D. FULTON, Y. CHEN, T. A. FAIRCHILD, T. J. MCCABE *et al.*, 2002 Domain mapping studies reveal that the M domain of hsp90 serves as a molecular scaffold to regulate Akt-dependent phosphorylation of endothelial nitric oxide synthase and NO release. Circ Res **90:** 866-873.

FUKUI, Y., T. KOZASA, Y. KAZIRO, T. TAKEDA and M. YAMAMOTO, 1986 Role of a ras homolog in the life cycle of Schizosaccharomyces pombe. Cell **44:** 329-336.

GOETZ, M. P., D. O. TOFT, M. M. AMES and ERLICHMAN, 2003 The Hsp90 chaperone complex as a novel target for cancer therapy. Ann Oncol **14:** 1169-1176.

GRAMMATIKAKIS, N., A. VULTUR, C. V. RAMANA, A. SIGANOU, C. W. SCHWEINFEST *et al.*, 2002 The role of Hsp90N, a new member of the Hsp90 family, in signal transduction and neoplastic transformation. J Biol Chem **277:** 8312-8320.

GRANDY, M. R., 2004 Transcription level of most fission yeast cyclic AMP pathway signaling genes is regulated by glucose availability. Boston College Master of Science Dissertation.

GRENERT, J. P., W. P. SULLIVAN, P. FADDEN, T. A. HAYSTEAD, J. CLARK *et al.*, 1997 The amino-terminal domain of heat shock protein 90 (hsp90) that binds geldanamycin is an ATP/ADP switch domain that regulates hsp90 conformation. J Biol Chem **272:** 23843-23850.

GUTZ, H., H. HESLOT, U. LEUPOLD and N. LOPRIENO, 1974 *Schizosaccharomyces pombe* in *Handbook of Genetics*, edited by R. C. KING. Plenum Press, New York.

HAGAN, I. M., and J. S. HYAMS, 1988 The use of cell division cycle mutants to investigate the control of microtubule distribution in the fission yeast Schizosaccharomyces pombe. J. Cell Sci **89:** 343–357.

HAWLE, P., M. SIEPMANN, A. HARST, M. SIDERIUS, H. P. REUSCH *et al.*, 2006 The middle domain of Hsp90 acts as a discriminator between different types of client proteins. Mol Cell Biol **26:** 8385-8395.

HOFFMAN, C. S., 2005a Except in every detail: Comparing and contrasting G protein signaling in *Saccharomyces cerevisiae* and *Schizosaccharomyces pombe*. Eukaryotic Cell **4:** 495-503.

HOFFMAN, C. S., 2005b Glucose sensing via the protein kinase A pathway in Schizosaccharomyces pombe. Biochem Soc Trans **33:** 257-260.

HOFFMAN, C. S., and F. WINSTON, 1987 A ten-minute DNA preparation from yeast efficiently releases autonomous plasmids for transformation of *Escherichia coli*. Gene **57:** 267-272.

HOFFMAN, C. S., and F. WINSTON, 1990 Isolation and characterization of mutants constitutive for expression of the *fbp1* gene of *Schizosaccharomyces pombe*. Genetics **124:** 807-816.

HOFFMAN, C. S., and F. WINSTON, 1991 Glucose repression of transcription of the Schizosaccharomyces pombe fbp1 gene occurs by a cAMP signaling pathway. Genes Dev **5:** 561-571.

ISAACS, J. S., W. XU and L. NECKERS, 2003 Heat shock protein 90 as a molecular target for cancer therapeutics. Cancer Cell **3:** 213-217.

ISSHIKI, T., N. MOCHIZUKI, T. MAEDA and M. YAMAMOTO, 1992 Characterization of a fission yeast gene, gpa2, that encodes a G alpha subunit involved in the monitoring of nutrition. Genes Dev **6:** 2455-2462.

IVEY, F. D., and C. S. HOFFMAN, 2005 Direct activation of fission yeast adenylate cyclase by the Gpa2 Galpha of the glucose signaling pathway. Proc Natl Acad Sci U S A **102:** 6108-6113.

JACKSON, S. E., C. QUEITSCH and D. TOFT, 2004 Hsp90: from structure to phenotype. Nat Struct Mol Biol **11:** 1152-1155.

JANOO, R. T., L. A. NEELY, B. R. BRAUN, S. K. WHITEHALL and C. S. HOFFMAN, 2001 Transcriptional regulators of the Schizosaccharomyces pombe fbp1 gene include two redundant Tup1p-like corepressors and the CCAAT binding factor activation complex. Genetics **157:** 1205-1215.

JIN, M., M. FUJITA, B. M. CULLEY, E. APOLINARIO, M. YAMAMOTO *et al.*, 1995 *sck1*, a high copy number suppressor of defects in the cAMP-dependent protein kinase pathway in fission yeast, encodes a protein homologous to the *Saccharomyces cerevisiae* SCH9 kinase. Genetics **140:** 457-467.

KAMENETSKY, M., S. MIDDELHAUFE, E. M. BANK, L. R. LEVIN, J. BUCK *et al.*, 2006 Molecular details of cAMP generation in mammalian cells: a tale of two systems. J Mol Biol **362:** 623-639.

KAO, R. S., E. MORREALE, L. WANG, F. D. IVEY and C. S. HOFFMAN, 2006 Schizosaccharomyces pombe Git1 is a C2-domain protein required for glucose activation of adenylate cyclase. Genetics **173:** 49-61.

KELLERMAYER, M. S., and P. CSERMELY, 1995 ATP induces dissociation of the 90 kDa heat shock protein (hsp90) from F-actin: interference with the binding of heavy meromyosin. Biochem Biophys Res Commun **211:** 166-174.

KITAGAWA, K., D. SKOWYRA, S. J. ELLEDGE, J. W. HARPER and P. HIETER, 1999 SGT1 encodes an essential component of the yeast kinetochore assembly pathway and a novel subunit of the SCF ubiquitin ligase complex. Mol Cell **4:** 21-33.

KOCH, H., K. HOFMANN and N. BROSE, 2000 Definition of Munc13-homology-domains and characterization of a novel ubiquitously expressed Munc13 isoform. Biochem J **349:** 247-253.

KORCSMAROS, T., I. A. KOVACS, M. S. SZALAY and P. CSERMELY, 2007 Molecular chaperones: the modular evolution of cellular networks. J Biosci **32:** 441-446.

KORDES, E., L. SAVELYEVA, M. SCHWAB, J. ROMMELAERE, J. C. JAUNIAUX *et al.*, 1998 Isolation and characterization of human SGT and identification of homologues in Saccharomyces cerevisiae and Caenorhabditis elegans. Genomics **52:** 90-94.

LAMB, J. R., S. TUGENDREICH and P. HIETER, 1995 Tetratrico peptide repeat interactions: to TPR or not to TPR? Trends Biochem Sci **20:** 257-259.

LANDRY, S., and C. S. HOFFMAN, 2001a The git5 Gbeta and git11 Ggamma Form an Atypical Gbetagamma Dimer Acting in the Fission Yeast Glucose/cAMP Pathway. Genetics **157:** 1159-1168.

LANDRY, S., M. T. PETTIT, E. APOLINARIO and C. S. HOFFMAN, 2000 The fission yeast *git5* gene encodes a Gβ subunit required for glucose-triggered adenylate cyclase activation. Genetics **154:** 1463-1471.

LEE, Y. T., J. JACOB, W. MICHOWSKI, M. NOWOTNY, J. KUZNICKI *et al.*, 2004 Human Sgt1 binds HSP90 through the CHORD-Sgt1 domain and not the tetratricopeptide repeat domain. J Biol Chem **279:** 16511-16517.

LERNER, A., and P. M. EPSTEIN, 2006 Cyclic nucleotide phosphodiesterases as targets for treatment of haematological malignancies. Biochem J **393:** 21-41.

LINDQUIST, S., and E. A. CRAIG, 1988 THE HEAT-SHOCK PROTEINS Annu. Rev. Genet **22:** 631-677.

LINGELBACH, L. B., and K. B. KAPLAN, 2004 The interaction between Sgt1p and Skp1p is regulated by HSP90 chaperones and is required for proper CBF3 assembly. Mol Cell Biol **24:** 8938-8950.

LIU, Y., T. BURCH-SMITH, M. SCHIFF, S. FENG and S. P. DINESH-KUMAR, 2004 Molecular chaperone Hsp90 associates with resistance protein N and its signaling proteins SGT1 and Rar1 to modulate an innate immune response in plants. J Biol Chem **279:** 2101-2108.

LOUVION, J. F., R. WARTH and D. PICARD, 1996 Two eukaryote-specific regions of Hsp82 are dispensable for its viability and signal transduction functions in yeast. Proc Natl Acad Sci U S A **93:** 13937-13942.

MAEDA, T., N. MOCHIZUKI and M. YAMAMOTO, 1990 Adenylyl cyclase is dispensable for vegetative cell growth in the fission yeast Schizosaccharomyces pombe. Proc Natl Acad Sci U S A **87:** 7814-7818.

MALONEY A, and W. P., 2002 HSP90 as a new therapeutic target for cancer therapy: The story unfolds. Expert Opin Biol Ther **2:** 3–24.

MAYOR, A., F. MARTINON, T. DE SMEDT, V. PETRILLI and J. TSCHOPP, 2007 A crucial function of SGT1 and HSP90 in inflammasome activity links mammalian and plant innate immune responses. Nat Immunol **8:** 497-503.

MBONYI, K., M. BEULLENS, K. DETREMERIE, L. GEERTS and J. M. THEVELEIN, 1988 Requirement of one functional RAS gene and inability of an oncogenic ras variant to mediate the glucose-induced cyclic AMP signal in the yeast Saccharomyces cerevisiae. Mol Cell Biol **8:** 3051-3057.

MEYER, P., C. PRODROMOU, B. HU, C. VAUGHAN, S. M. ROE *et al.*, 2003 Structural and functional analysis of the middle segment of hsp90: implications for ATP hydrolysis and client protein and cochaperone interactions. Mol Cell **11:** 647-658.

MILLSON, S. H., A. W. TRUMAN, V. KING, C. PRODROMOU, L. H. PEARL *et al.*, 2005 A two-hybrid screen of the yeast proteome for Hsp90 interactors uncovers a novel Hsp90 chaperone requirement in the activity of a stress-activated mitogen-activated protein kinase, Slt2p (Mpk1p). Eukaryot Cell **4:** 849-860.

MINAMI, Y., Y. KIMURA, H. KAWASAKI, K. SUZUKI and I. YAHARA, 1994 The carboxy-terminal region of mammalian HSP90 is required for its dimerization and function in vivo. Mol Cell Biol **14:** 1459-1464.

MINTZER, K. A., and J. FIELD, 1994 Interactions between adenylyl cyclase, CAP and RAS from Saccharomyces cerevisiae. Cell Signal **6:** 681-694.

MISHRA, M., M. D'SOUZA V, K. C. CHANG, Y. HUANG and M. K. BALASUBRAMANIAN, 2005 Hsp90 protein in fission yeast Swo1p and UCS protein Rng3p facilitate myosin II assembly and function. Eukaryot Cell **4:** 567-576.

MITCHELL-OLDS, T., and C. A. KNIGHT, 2002 Evolution. Chaperones as buffering agents? Science **296:** 2348-2349.

MOORE, A. R., and D. A. WILLOUGHBY, 1995 The role of cAMP regulation in controlling inflammation. Clin Exp Immunol **101:** 387-389.

MORELAND, J. L., A. GRAMADA, O. V. BUZKO, Q. ZHANG and P. E. BOURNE, 2005 The Molecular Biology Toolkit (MBT): a modular platform for developing molecular visualization applications. BMC Bioinformatics **6:** 21.

MOVSESIAN, M. A., and M. R. BRISTOW, 2005 Alterations in cAMP-mediated signaling and their role in the pathophysiology of dilated cardiomyopathy. Curr Top Dev Biol **68:** 25-48.

NATHAN, D. F., and S. LINDQUIST, 1995 Mutational analysis of hsp90 function: interactions with a steroid receptor and a protein kinase. Mol. Cell. Biol. **15:** 3917-3925.

NECKERS, L., 2007 Heat shock protein 90: the cancer chaperone. J Biosci **32:** 517-530.

NEMOTO, T., T. MATSUSAKA, M. OTA, T. TAKAGI, D. B. COLLINGE *et al.*, 1996 Dimerization characteristics of the 94-kDa glucose-regulated protein. J Biochem (Tokyo) **120:** 249-256.

NOCERO, M., T. ISSHIKI, M. YAMAMOTO and C. S. HOFFMAN, 1994 Glucose repression of *fbp1* transcription of *Schizosaccharomyces pombe* is partially regulated by adenylate cyclase activation by a G protein α subunit encoded by *gpa2* (*git8*). Genetics **138:** 39-45.

NOLLEN, E. A., and R. I. MORIMOTO, 2002 Chaperoning signaling pathways: molecular chaperones as stress-sensing 'heat shock' proteins. J Cell Sci **115:** 2809-2816.

OBERMANN, W. M., H. SONDERMANN, A. A. RUSSO, N. P. PAVLETICH and F. U. HARTL, 1998 In vivo function of Hsp90 is dependent on ATP binding and ATP hydrolysis. J Cell Biol **143:** 901-910.

PAI, K. S., V. B. MAHAJAN, A. LAU and D. D. CUNNINGHAM, 2001 Thrombin receptor signaling to cytoskeleton requires Hsp90. J Biol Chem **276:** 32642-32647.

PEARL, L. H., and C. PRODROMOU, 2000 Structure and in vivo function of Hsp90. Curr Opin Struct Biol **10:** 46-51.

PEARL, L. H., and C. PRODROMOU, 2006 Structure and mechanism of the Hsp90 molecular chaperone machinery. Annu Rev Biochem **75:** 271-294.

PFISTER, C., 1989 [Signal transmission using second messengers]. Reprod Nutr Dev **29:** 639-651.

POWERS, M. V., and P. WORKMAN, 2006 Targeting of multiple signalling pathways by heat shock protein 90 molecular chaperone inhibitors. Endocr Relat Cancer **13 Suppl 1:** S125-135.

PRATT, W. B., and D. O. TOFT., 1997 Steroid receptor interactions with heat shock protein and immunophilin chaperones. Endocr. Rev **18:** 306-360.

PRODROMOU, C., B. PANARETOU, S. CHOHAN, G. SILIGARDI, R. O'BRIEN *et al.*, 2000 The ATPase cycle of Hsp90 drives a molecular 'clamp' via transient dimerization of the N-terminal domains. EMBO J **19:** 4383-4392.

PRODROMOU, C., S. M. ROE, R. O'BRIEN, J. E. LADBURY, P. W. PIPER *et al.*, 1997 Identification and structural characterization of the ATP/ADP-binding site in the Hsp90 molecular chaperone. Cell **90:** 65-75.

RICHTER, K., and J. BUCHNER, 2001 Hsp90: chaperoning signal transduction. J Cell Physiol **188:** 281-290.

RICHTER, K., and J. BUCHNER, 2006 hsp90: twist and fold. Cell **127:** 251-253.

RICHTER, K., J. REINSTEIN and J. BUCHNER, 2002 N-terminal residues regulate the catalytic efficiency of the Hsp90 ATPase cycle. J Biol Chem **277:** 44905-44910.

RUTHERFORD, S. L., 2003 Between genotype and phenotype: protein chaperones and evolvability. Nat Rev Genet **4:** 263-274.

RUTHERFORD, S. L., and S. LINDQUIST, 1998 Hsp90 as a capacitor for morphological evolution. Nature **396:** 336-342.

SAKISAKA, T., T. MEERLO, J. MATTESON, H. PLUTNER and W. E. BALCH, 2002 Rab-alphaGDI activity is regulated by a Hsp90 chaperone complex. EMBO J **21:** 6125-6135.

SAMEJIMA, I., S. MACKIE and P. A. FANTES, 1997 Multiple modes of activation of the stress-responsive MAP kinase pathway in fission yeast. Embo J **16:** 6162-6170.

SANDS, W. A., and T. M. PALMER, 2008 Regulating gene transcription in response to cyclic AMP elevation. Cell Signal **20:** 460-466.

SATHIYAA, R., T. CAMPBELL and M. M. VIJAYAN, 2001 Cortisol modulates HSP90 mRNA expression in primary cultures of trout hepatocytes. Comp Biochem Physiol B Biochem Mol Biol **129:** 679-685.

SATO, S., N. FUJITA and T. TSURUO, 2000 Modulation of Akt kinase activity by binding to Hsp90. Proc Natl Acad Sci U S A **97:** 10832-10837.

SCHADICK, K., H. M. FOURCADE, P. BOUMENOT, J. J. SEITZ, J. L. MORRELL *et al.*, 2002 Schizosaccharomyces pombe Git7p, a member of the Saccharomyces cerevisiae Sgtlp family, is required for glucose and cyclic AMP signaling, cell wall integrity, and septation. Eukaryot Cell **1:** 558-567.

SCHNEIDER, C., L. SEPP-LORENZINO, E. NIMMESGERN, O. OUERFELLI, S. DANISHEFSKY *et al.*, 1996 Pharmacologic shifting of a balance between protein refolding and degradation mediated by Hsp90. Proc Natl Acad Sci U S A **93:** 14536-14541.

SCHULTE, T. W., S. AKINAGA, T. MURAKATA, T. AGATSUMA, S. SUGIMOTO *et al.*, 1999 Interaction of radicicol with members of the heat shock protein 90 family of molecular chaperones. Mol Endocrinol **13:** 1435-1448.

SMITH, S. J., L. B. CIESLINSKI, R. NEWTON, L. E. DONNELLY, P. S. FENWICK *et al.*, 2004 Discovery of BRL 50481 [3-(N,N-dimethylsulfonamido)-4-methyl-nitrobenzene], a selective inhibitor of phosphodiesterase 7: in vitro studies in human monocytes, lung macrophages, and CD8+ T-lymphocytes. Mol Pharmacol **66:** 1679-1689.

SNYDER, M. J., E. GIRVETZ and E. P. MULDER, 2001 Induction of marine mollusc stress proteins by chemical or physical stress. Arch Environ Contam Toxicol **41:** 22-29.

SOGA, S., Y. SHIOTSU, S. AKINAGA and S. V. SHARMA, 2003 Development of radicicol analogues. Curr Cancer Drug Targets **3:** 359-369.

SOUTHERN, J. A., D. F. YOUNG, F. HEANEY, W. K. BAUMGARTNER and R. E. RANDALL, 1991 Identification of an epitope on the P and V proteins of simian virus 5 that distinguishes between two isolates with different biological characteristics. J Gen Virol **72:** 1551-1557.

SPEES, J. L., S. A. CHANG, M. J. SNYDER and E. S. CHANG, 2002 Osmotic induction of stress-responsive gene expression in the lobster Homarus americanus. Biol Bull **203:** 331-337.

SPENCE, J., and C. GEORGOPOULOS, 1989a Purification and properties of the Escherichia coli heat shock protein, HtpG. J. Biol. Chem **264:** 4398-4403.

STEBBINS, C. E., A. A. RUSSO, C. SCHNEIDER, N. ROSEN, F. U. HARTL *et al.*, 1997 Crystal structure of an Hsp90-geldanamycin complex: targeting of a protein chaperone by an antitumor agent. Cell **89:** 239-250.

STEENSGAARD, P., M. GARRE, I. MURADORE, P. TRANSIDICO, E. A. NIGG *et al.*, 2004 Sgt1 is required for human kinetochore assembly. EMBO Rep **5:** 626-631.

STETTLER, S., E. WARBRICK, S. PROCHNIK, S. MACKIE and P. FANTES, 1996 The wis1 signal transduction pathway is required for expression of cAMP- repressed genes in fission yeast. J Cell Sci **109:** 1927-1935.

STIEFEL, J., L. WANG, D. A. KELLY, R. T. K. JANOO, J. SEITZ *et al.*, 2004 Suppressors of an adenylate cyclase deletion in the fission yeast *Schizosaccharomyces pombe*. Eukaryotic Cell **3:** 610-619.

SULLIVAN, W., B. STENSGARD, G. CAUCUTT, B. BARTHA, N. MCMAHON *et al.*, 1997 Nucleotides and two functional states of hsp90. J Biol Chem **272:** 8007-8012.

TAKAHASHI, A., C. CASAIS, K. ICHIMURA and K. SHIRASU, 2003 HSP90 interacts with RAR1 and SGT1 and is essential for RPS2-mediated disease resistance in Arabidopsis. Proc Natl Acad Sci U S A **100:** 11777-11782.

TERASAWA, K., M. MINAMI and Y. MINAMI, 2005 Constantly updated knowledge of Hsp90. J Biochem (Tokyo) **137:** 443-447.

THAO, N. P., L. CHEN, A. NAKASHIMA, S. HARA, K. UMEMURA *et al.*, 2007 RAR1 and HSP90 Form a Complex with Rac/Rop GTPase and Function in Innate-Immune Responses in Rice. Plant Cell **19:** 4035-4045.

THOMPSON, J. D., D. G. HIGGINS and T. J. GIBSON, 1994 CLUSTAL W: improving the sensitivity of progressive multiple sequence alignment through sequence weighting, position-specific gap penalties and weight matrix choice. Nucleic Acids Res **22:** 4673-4680.

VASSAROTTI, A., and J. D. FRIESEN, 1985 Isolation of the fructose-1,6-bisphosphatase gene of the yeast Schizosaccharomyces pombe. Evidence for transcriptional regulation. J Biol Chem **260:** 6348-6353.

VILENCHIK, M., D. SOLIT, A. BASSO, H. HUEZO, B. LUCAS *et al.*, 2004 Targeting wide-range oncogenic transformation via PU24FCl, a specific inhibitor of tumor Hsp90. Chem Biol **11:** 787-797.

VINCZE, T., J. POSFAI and R. J. ROBERTS, 2003 NEBcutter: A program to cleave DNA with restriction enzymes. Nucleic Acids Res **31:** 3688-3691.

VOLLAND, C., D. URBAN-GRIMAL, G. GERAUD and R. HAGUENAUER-TSAPIS, 1994 Endocytosis and degradation of the yeast uracil permease under adverse conditions. J Biol Chem **269:** 9833-9841.

WANG, H., Y. LIU, Y. CHEN, H. ROBINSON and H. KE, 2005a Multiple elements jointly determine inhibitor selectivity of cyclic nucleotide phosphodiesterases 4 and 7. J Biol Chem **280:** 30949-30955.

WANG, L., K. GRIFFITHS, JR., Y. H. ZHANG, F. D. IVEY and C. S. HOFFMAN, 2005b *Schizosaccharomyces pombe* adenylate cyclase suppressor mutations suggest a role for cAMP phosphodiesterase regulation in feedback control of glucose/cAMP signaling. Genetics **171:** 1523-1533.

WELTON, R. M., and C. S. HOFFMAN, 2000 Glucose monitoring in fission yeast via the gpa2 Gα, the git5 Gβ, and the git3 putative glucose receptor. Genetics **156:** 513-521.

WHITESELL, L., and S. L. LINDQUIST, 2005 HSP90 and the chaperoning of cancer. Nat Rev Cancer **5:** 761-772.

WHITESELL, L., E. G. MIMNAUGH, B. DE COSTA, C. E. MYERS and L. M. NECKERS, 1994 Inhibition of heat shock protein HSP90-pp60v-src heteroprotein complex formation by benzoquinone ansamycins: essential role for stress proteins in oncogenic transformation. Proc Natl Acad Sci U S A **91:** 8324-8328.

WIEGANT, F. A., N. SPIEKER and R. VAN WIJK, 1998 Stressor-specific enhancement of hsp induction by low doses of stressors in conditions of self- and cross-sensitization. Toxicology **127:** 107-119.

WILLOUGHBY, D., and D. M. COOPER, 2008 Live-cell imaging of cAMP dynamics. Nat Methods **5:** 29-36.

WOOD, V., R. GWILLIAM, M. A. RAJANDREAM, M. LYNE, R. LYNE *et al.*, 2002 The genome sequence of Schizosaccharomyces pombe. Nature **415:** 871-880.

XU, L., J. L. EISEMAN, M. J. EGORIN and D. Z. D'ARGENIO, 2003 Physiologically-based pharmacokinetics and molecular pharmacodynamics of 17-(allylamino)-17-demethoxygeldanamycin and its active metabolite in tumor-bearing mice. J Pharmacokinet Pharmacodyn **30:** 185-219.

YAMAWAKI-KATAOKA, Y., T. TAMAOKI, H. R. CHOE, H. TANAKA and T. KATAOKA, 1989 Adenylate cyclases in yeast: a comparison of the genes from Schizosaccharomyces pombe and Saccharomyces cerevisiae. Proc Natl Acad Sci U S A **86:** 5693-5697.

YANG, P., H. DU, C. S. HOFFMAN and S. MARCUS, 2003 The phospholipase B homolog Plb1 is a mediator of osmotic stress response and of nutrient-dependent repression of sexual differentiation in the fission yeast Schizosaccharomyces pombe. Mol Genet Genomics **269:** 116-125.

YOUNG, D., M. RIGGS, J. FIELD, A. VOJTEK, D. BROEK *et al.*, 1989 The adenylyl cyclase gene from Schizosaccharomyces pombe. Proc Natl Acad Sci U S A **86:** 7989-7993.

YOUNG, J. C., I. MOAREFI and F. U. HARTL, 2001 Hsp90: a specialized but essential protein-folding tool. J Cell Biol **154:** 267-273.

YU, G., J. LI and D. YOUNG, 1994 The Schizosaccharomyces pombe pka1 gene, encoding a homolog of cAMP-dependent protein kinase. Gene **151:** 215-220.

ZHANG, H., and F. BURROWS, 2004 Targeting multiple signal transduction pathways through inhibition of Hsp90. J Mol Med **82:** 488-499.

ZHAO, R., M. DAVEY, Y. C. HSU, P. KAPLANEK, A. TONG *et al.*, 2005 Navigating the chaperone network: an integrative map of physical and genetic interactions mediated by the hsp90 chaperone. Cell **120:** 715-727.

ZHAO, R., and W. A. HOURY, 2005 Hsp90: a chaperone for protein folding and gene regulation. Biochem Cell Biol **83:** 703-710.

ZHAO, R., and W. A. HOURY, 2007 Molecular interaction network of the Hsp90 chaperone system. Adv Exp Med Biol **594:** 27-36.